

**Development of organic-inorganic hybrids through deposition
of hydroxyapatite on organic substrates under a biomimetic
condition**

Takahiro Kawai

2005

**Graduate School of Materials Science
Nara Institute of Science and Technology**

CONTENTS

GENERAL INTRODUCTION	(1)
Chapter 1: Coating of a hydroxyapatite layer on polyamide films containing sulfonic groups	(27)
Chapter 2: Coating of a hydroxyapatite layer on polyamide films containing silanol groups	(55)
Chapter 3: Comparative study of induction of nucleation, crystal growth and adhesive strength of hydroxyapatite formed on polyamide films with different functional groups	(79)
Chapter 4: Adsorption of formaldehyde onto hydroxyapatite deposited polyamide film	(99)
GENERAL CONCLUSION	(125)
LIST OF PUBLICATIONS	(129)
ACKNOWLEDGEMENTS	(133)

GENERAL INTRODUCTION

Bone is an important organ that supports our body and enables exercises. Bone also fills roles on protection of our brain and viscera from damage, and on storage of calcium and phosphate ions required for metabolism. When bone is lost due to diseases or injuries, it would recover by itself through regeneration with appropriate rest and nutrition if the lost part would be small. However, when the amount of lost bone is too large to recover by self-regeneration, a substitute material is required to fill the defect. Although autologous or allogenic transplantation is commonly applied, there are a lot of problems such as the limitation and the risk of infections. Therefore, an artificial material is used for substitution of bone. But it is a well-known problem that artificial materials are generally encapsulated by a fibrous tissue and isolated from surrounding bones when they are implanted into the bony defects [1]. One may notify that specific type of ceramic materials can make a direct contact to living bone without any intervening layer of fibrous tissues after implantation in a bony defect. Such a unique ceramic is defined as a bioactive material. Namely bioactive materials can show specific biological activity against living bone, so-called bone-bonding property. The first discovered material showing bone-bonding property is a certain type of glass in the system $\text{Na}_2\text{O-CaO-SiO}_2\text{-P}_2\text{O}_5$, after Hench *et al.* in early 1970's [2-4]. The glass was named Bioglass[®]. Since then, some kinds of ceramic materials have been reported as bioactive materials showing bone-bonding property. Typical materials showing the bone-bonding property, i.e. bioactivity, are given in Table 1. Bioactive ceramics imply glass-ceramic Ceravital[®] [5], sintered hydroxyapatite ($\text{Ca}_{10}(\text{PO}_4)_6(\text{OH})_2$) [6,7], glass-ceramic A-W [8,9], glass-ceramic Bioverit[®] [10], $\text{MgO-CaO-SiO}_2\text{-P}_2\text{O}_5$ glasses [11] and CaO-SiO_2 glasses [12]. Some of these materials have already been used clinically as important bone substitutes such as artificial iliac crests, artificial vertebrae, artificial intervertebral discs, bone fillers [13-19]. Although these materials have great

advantage in biological affinity to living bone, their applications are still limited due to their mechanical performance, that is, lower fracture toughness than those of human cortical bone [20]. One may expect development of a novel bone substitute with bioactivity and high fracture toughness. Recently, titanium, titanium alloy and tantalum are provided with bioactivity through chemical treatment with sodium hydroxide (NaOH) solution, followed by heat treatment [21-29] or with hydrogen peroxide containing various kinds of metals [30]. These metallic materials show bioactivity, i.e. bone-bonding property, as well as higher fracture toughness than conventional bioactive ceramics. These metallic materials have high fracture toughness, but their elastic moduli are higher than that of cortical bone. It may cause resorption of the surrounding bone because of their stress shielding effects.

Mechanical properties of the bone are derived from their unique structure of the extracellular matrix of bone. The extracellular matrix of bone is regarded as an organic-inorganic composite that is constructed three-dimensionally with nano-sized crystals of hydroxyapatite and collagen fiber (Figure 1) [31]. This structure provides the characteristics of high fracture toughness and moderate flexibility. This means that such composites appear both characteristics from organic and inorganic materials, and hence it is better to regard such composites as “organic-inorganic hybrid”. The word “Hybrid” is defined as a composite combining more than two reinforcements, or as a composite consisting of multi-elements in its structure to carry out several functional capabilities [32,33]. Hydroxyapatite-organic polymer hybrids therefore provide a potential novel bone substitute material having both bone-bonding ability and mechanical properties analogous to natural bone.

Several methods have been reported for fabrication of organic-inorganic hybrids consisting of hydroxyapatite and organic polymer [34-45]. The methods are summarized in Table 2. Bonfield *et al.* developed composites of hydroxyapatite granules and high density polyethylene by mechanical mixing [34]. The composites showed high

deformability only when hydroxyapatite content was less than 40 vol%, whereas they showed low or no bioactivity at low hydroxyapatite content [3]. Kikuchi *et al.* reported fabrication of hydroxyapatite-collagen composite through a reaction of calcium hydroxide and phosphoric acid under coexistence of collagen at the pH range between 8 and 9 [35]. Interaction between hydroxyapatite and collagen produced self-organized structure in the hydroxyapatite-collagen hybrid. The hydroxyapatite-collagen hybrid shows unique characteristics on mechanical properties for bone substitutes. Coating of hydroxyapatite on organic polymer also provides a material with hydroxyapatite-polymer hybrid. Kokubo *et al.* proposed biomimetic coating of hydroxyapatite on organic polymer substrates. Such a method has been paid much attention because it allows a coating of so-called bone-like apatite, that is calcium-deficient and carbonate-containing nano-sized hydroxyapatite, which shows low crystallinity and defective structure [46]. Bone-like apatite is expected to show high biological affinity to living bone [47,48]. On the other hand, Taguchi *et al.* developed the alternate soaking process where hydroxyapatite was formed on/in organic polymer hydrogel matrices by soaking the substrates in a solution containing calcium ions and a solution containing phosphate ions alternatively [36].

In Kokubo's processing for coating of the hydroxyapatite on a substrate, the substrate was first placed in vicinity of bioactive glass particles composed mainly of CaO and SiO₂ in a simulated body fluid (SBF) [37-45] to result in a nucleation of apatite on the substrate. Thus formed nuclei on the substrates grow to a layer of hydroxyapatite in 1.5SBF that has 1.5 times ion concentrations to those of SBF [37-45,49]. It has been reported in several literatures that bioactive materials bond to living bone through a hydroxyapatite layer that is formed on their surface in the body circumstance [3,9,11,12,28,50-53]. The bone-like apatite layer coated on polymer substrates through biomimetic processing is expected to show bioactivity in bony defects. As the biomimetic coating does not require heat-treatment at high temperatures,

it can be applied to coating of hydroxyapatite on organic substrates. The organic polymer coated with bone-like apatite is regarded as a fundamentally structural unit of hydroxyapatite-organic polymer hybrid for bone substitutes. Namely, coating of a hydroxyapatite layer on polymer substrate with biomimetic process gives attractive solutions to fabricate devices in various shapes without losing the activity of hydroxyapatite (Figure 2). In addition, this type of film has been received an attention as a filter material because hydroxyapatite shows unique properties such as adsorption of proteins and virus [54-59], and has possibility of exchange of ionic species in its crystal lattice [60-63].

The biomimetic process utilizing SBF and 1.5SBF implies three steps; i) increase in degree of supersaturation with respect to apatite, ii) heterogenous nucleation of apatite on the substrates and iii) crystal growth of apatite nuclei. Among these steps, the process of heterogeneous nucleation of apatite on the substrates is the most important because it allows growth of hydroxyapatite especially on the polymer substrate. Ohtsuki *et al.* reported that -SiOH groups are effective to induce heterogeneous nucleation on the bioactive glass in SBF according to the research on the process of hydroxyapatite formation on the glasses in the system CaO-SiO₂-P₂O₅ [48,64]. They also confirmed that -SiOH groups on hydrated pure silica gel induce heterogeneous nucleation of apatite on its surface after exposure to SBF [65-67].

It has been reported that some functional groups other than -SiOH group also induce heterogeneous nucleation of apatite. -TiOH [68-70], -ZrOH [71], -TaOH [72], and -NbOH [73] groups on metal oxide gels are effective for induction of apatite deposition in SBF. It should be noted that carboxyl (-COOH) and phosphate (-OPO₃H₂) [74] groups of self-assembled monolayers on gold were also reported to have a potential to induce apatite formation, because such functional groups can be easily incorporated into organic polymer. On the basis of these findings concerning formation of the bone-like hydroxyapatite layer consisting of nano-sized particles, Miyazaki *et al.*

successfully fabricated a film composed of bone-like apatite and aromatic polyamide through a simple immersion of organic films in 1.5SBF [75]. In their process, polyamide film containing 50 mol% of carboxyl groups in this structure effectively induced heterogeneous nucleation of apatite in 1.5SBF when the polymer was incorporated with 40 mass% of calcium chloride (CaCl_2). CaCl_2 dissolves into surrounding solution after the film is immersed in 1.5SBF. Release of calcium ions from the examined polyamide films increases the degree of the supersaturation with respect to the apatite in an especially local area around the polymer surface, and enhances the nucleation. Once nuclei of apatite are formed on the substrates, they can grow spontaneously by consuming calcium and phosphate ions from the surrounding body fluid. The supposed process is schematically illustrated on Figure 3. However, the reason why specific functional groups are effective for induction of heterogeneous nucleation of apatite in a solution mimicking body fluid has not been clarified. In this study, the role of functional groups on the nucleation process, crystal growth process and adhesion performance of hydroxyapatite is focused on in view of electrostatic interaction, complex formation, and dipole interaction, to understand the fundamental principle for fabrication of hydroxyapatite coating on organic substrate through the biomimetic processing. Furthermore, a potential application on adsorption of formaldehyde was also evaluated for the specimens of hydroxyapatite-polymer hybrids.

Surface charges of the related oxide gels and their apatite-forming ability are listed in Table 3 [76]. Among these oxide gels, it was reported that $-\text{AlOH}$ group doesn't initiate apatite generation after immersion in SBF. This suggests that negatively charged surface provides sites for induction of apatite nuclei. Takadama *et al.* proposed that the nucleation of apatite was initiated by formation of calcium complex with surface functional groups such as $-\text{SiOCa}^+$, $(-\text{SiO})_2\text{Ca}$ [77]. Table 4 gives substances having typical functional groups whose surfaces are speculated to have negative charges in biomimetic conditions, and their negative of the logarithm of the dissociation constants

(pK_a) [78]. In comparison with the pK_a of their initial acid dissociation, Ph-SO₃H and SiO₄H₄ show the lowest and the highest among them, respectively. Degree of ease for formation of ion pairs and complexation between calcium ions and functional groups can be proposed as the other factors effective on hydroxyapatite formation and adhesive strength. The equilibrium constants for formation of ion pair and complexes of calcium ion with typical anions in aqueous solution are listed in Table 5 [79] and 6 [80], respectively. It is noted that effects of -SO₃H groups on induction of heterogeneous nucleation of apatite have not been clarified, although the sulfonic (-SO₃H) group is a typical functional group that has a high dissociation constant to possess negative charges under biomimetic conditions. In contrast, although -SiOH groups hardly dissociate in biomimetic condition, it is reported that -SiOH groups induce nucleation of apatite. It is interesting to compare the differences of ability to form hydroxyapatite between these functional groups.

In Chapter 1, behavior of hydroxyapatite deposition on aromatic polyamide containing -SO₃H groups was investigated in 1.5SBF, to reveal possibility of -SO₃H groups on induction of heterogeneous nucleation of apatite. The results were discussed in terms of the contents of -SO₃H group and CaCl₂.

In Chapter 2, modification with silanol (-SiOH) groups was applied on the aromatic polyamide film containing -COOH groups, since -SiOH groups were well known to show induction of apatite nucleation. However, the dissociation constant of -SiOH group is quite lower than -COOH. Therefore, it is worth investigating hydroxyapatite-forming ability on the modified films with different amounts of -SiOH groups in 1.5SBF, to discuss effects of modification of aromatic polyamide with the groups.

As adhesive strength of the hydroxyapatite with polymer substrate containing -COOH and -SO₃H groups was distinctly higher than that with polyamide films containing -SiOH groups, in Chapter 3, the differences of the hydroxyapatite formation

were compared in the detail between the polyamides containing $-\text{SO}_3\text{H}$ and $-\text{COOH}$ groups. The induction period of nucleation of apatite, the rate of crystal growth and adhesion performance between substrates and hydroxyapatite formed on it were examined by soaking in 1.5SBF. to discuss with comparison between the functional groups.

It is expected that the hydroxyapatite formed in such a biomimetic condition would show specific functionalities in comparison with a hydroxyapatite prepared by a conventional method such as homogeneous precipitation methods and hydrothermal methods [7]. To evaluate the characteristics of the hydroxyapatite prepared biomimetically, in Chapter 4, the ability to adsorb formaldehyde of hydroxyapatite formed on the polyamide film by soaking in 1.5SBF was examined as one of the evaluations of characteristics of hydroxyapatite. Potential functionality of adsorption of biomimetically deposited hydroxyapatite on polymer films has not been revealed, while many researches have conducted studies about adsorption of organic substances on synthesized hydroxyapatite with stoichiometric composition after heat-treatment [54-59]. Advantageous characters of the layer consisting of bone-like apatite formed through biomimetic processing were discussed with comparison to that of conventional hydroxyapatite powders and activated charcoal.

Finally, the whole results and discussions in the above chapters are summarized, and the future perspectives are described.

References

1. Hulbert SF. The use of alumina and zirconia in surgical implants. In: Hench LL, Wilson J, editors. An introduction to bioceramics. Singapore: World Scientific; 1993. p. 25-40.
2. Hench LL, Splinter RJ, Allen WC. Bonding mechanism at the interface of ceramic prosthetic Materials. *J Biomed Mater Res Symp.* 1971;2:117-141.
3. Hench LL. Bioceramics: From concept to clinic. *J Am Ceram Soc* 1991;74:1487-1510.
4. Hench LL, Andersson Ö. Bioactive Glasses. In: Hench LL, Wilson J, editors. An introduction to bioceramics. Singapore: World Scientific; 1993. p. 41-62.
5. Gross UM, Müller-Mai C, Voigt C. Ceravital® Bioactive Glass-Ceramics. In: Hench LL, Wilson J, editors. An introduction to bioceramics. Singapore: World Scientific; 1993. p. 105-123.
6. Jarcho M. Tissue cellular and subcellular events at bone-ceramic hydroxyapatite interface. *J Bioeng* 1976;1:79-92.
7. LeGeros RZ, LeGeros JP. Dense hydroxyapatite. In: Hench LL, Wilson J, editors. An introduction to bioceramics. Singapore: World Scientific; 1993. p. 139-180.
8. Kokubo T, Shigematsu M, Nagashima Y, Tashiro M, Nakamura T, Yamamuro T, Higashi S. Apatite- and wollastonite-containing glass-ceramics for prosthetic application. *Bull Inst Chem Res. Kyoto Univ.* 1982;60:260-268.
9. Kokubo T. A/W Glass-Ceramic: Processing and properties. In: Hench LL, Wilson J, editors. An introduction to bioceramics. Singapore: World Scientific; 1993. p. 75-88.
10. Höland W, Vogel V. Machineable and phosphate glass-ceramics. In: Hench LL, Wilson J, editors. An introduction to bioceramics. Singapore: World Scientific; 1993. p. 125-137.

11. Kitsugi T, Yamamuro T, Nakamura T, Kokubo T. Bone bonding behavior of MgO-CaO-SiO₂-P₂O₅-CaF₂ glass (mother glass of A·W glass-ceramics). *J Biomed Mater Res* 1989;23:631-648.
12. Ohura K, Nakamura T, Yamamuro T, Kokubo T, Ebisawa T, Kotoura Y, Oka M. Bone-bonding ability of P₂O₅-free CaO·SiO₂ glasses. *J Biomed Mater Res* 1991;25:357-365.
13. Reck R, Störkel S, Meyer A. Bioactive glass-ceramics in middle ear surgery: An 8-year review. In: Ducheyne P, Lemons JE editors. *Bioceramics: Material characteristics versus in vivo behavior* Vol. 523. New York: New York Academy of Science; 1988. p. 100-106.
14. Yamamuro T. Replacement of the spine with bioactive glass-ceramic prostheses. In: Yamamuro T, Hench LL, Wilson J editors. *Handbook of bioactive ceramics* Vol. 1: Bioactive glasses and glass-ceramics. Boca Raton: CRC Press Inc.; 1990. p. 343-351.
15. Ono K, Yamamuro T, Nakamura T, Kokubo T. Apatite-wollastnite containing glass ceramic granule-fibrin mixture as a bone graft filler: Use with low granular density. *J Biomed Mater Res* 1990;24:11-20.
16. Hench LL, Stanley HR, Clark AE, Hall M, Wilson J. Dental applications of Bioglass[®] implants. In: Bonfield W, Hastings GW, Tanner KE editors. *Bioceramics* Vol. 4. Oxford: Butterworth-Heinemann Ltd.; 1991. p. 231-238.
17. Wilson J, Yli-Urpo A, Risto-Pekka H. Bioactive glasses: Clinical applications. In: Hench LL, Wilson J, editors. *An introduction to bioceramics*. Singapore: World Scientific; 1993. p. 63-73.
18. Yamamuro T. A/W glass-ceramic: Clinical applications. In: Hench LL, Wilson J, editors. *An introduction to bioceramics*. Singapore: World Scientific; 1993. p. 89-103.
19. Shors EC, Holmes RE. Porous hydroxyapatite. In: Hench LL, Wilson J, editors.

- An introduction to bioceramics. Singapore: World Scientific; 1993. p. 181-198.
20. Kokubo T, Miyaji F. Seramikkuseitaizairyō. In: Sato A, Ishikawa T, Sakurai Y, Nakamura A editors. Biocompatibility of biomaterials. Tokyo: Nakayamashoten; 1998. p. 39-46 [in Japanese].
 21. Kim HM, Miyaji F, Kokubo T, Nakamura T. Preparation of bioactive Ti and its alloys via simple chemical treatment. *J Biomed Mater Res* 1996;32:409-417.
 22. Kim HM, Miyaji F, Kokubo T, Nakamura T. Effect of heat treatment on apatite-forming ability of Ti metal induced by heat treatment. *J Mater Sci Mater Med* 1997;8:341-347.
 23. Yan WQ, Nakamura T, Kobayashi M, Kim HM, Miyaji F, Kokubo T. Bonding of chemically treated titanium implants to bone. *J Biomed Mater Res* 1997;37:267-275.
 24. Yan WQ, Nakamura T, Kawanabe K, Nishiguchi S, Oka M, Kokubo T. Apatite layer-coated titanium for use as bone bonding implants. *Biomaterials* 1997;18:1185-1190.
 25. Nishiguchi S, Nakamura T, Kobayashi M, Kim HM, Miyaji F, Kokubo T. The effect of heat treatment on bone-bonding ability of alkali-treated titanium. *Biomaterials* 1999;20:491-500.
 26. Nishiguchi S, Kato H, Fujita H, Kim HM, Miyaji F, Kokubo T, Nakamura T. Enhancement of bone-bonding strength of titanium alloy implants by alkali and heat treatments. *J Biomed Mater Res* 1999;48:689-696.
 27. Miyazaki T, Kim HM, Miyaji F, Kokubo T, Kato H, Nakamura T. Bioactive tantalum metal prepared by NaOH treatment. *J Biomed Mater Res* 2000;50:35-42.
 28. Kato H, Nakamura T, Nishiguchi S, Matsusue Y, Kobayashi M, Miyazaki T, Miyaji F, Kim HM, Kokubo T. Bonding of alkali- and heat-treated tantalum implants to bone. *J Biomed Mater Res: Appl Biomater* 2000;53:28-35.
 29. Miyazaki T, Kim HM, Kokubo T, Miyaji F, Kato H, Nakamura T. Effect of

- thermal treatment on apatite-forming ability of NaOH-treated tantalum metal. *J Mater Sci Mater Med* 2001;12:683-687.
30. Ohtsuki C, Iida H, Hayakawa S, Osaka A. Bioactivity of titanium treated with hydrogen peroxide solutions containing metal chlorides. *J Biomed Mater Res* 1998;35:39-47.
 31. Park JB, Lakes RS. In: *Biomaterials 2nd Ed.* New York: Plenum Press; 1992. p. 185-222.
 32. In: Chemical society of Japan editors. *Hyoujunkagakuyougijiten*. Tokyo: Maruzen; 1993. p. 478 [in Japanese].
 33. In: Ceramic society of Japan editors. *Seramikkusujiten 2nd edition*. Tokyo: Maruzen; 1997. p. 570 [in Japanese].
 34. Bonfield W. Design of bioactive ceramic-polymer composites. In: Hench LL, Wilson J, editors. *An introduction to bioceramics*. Singapore: World Scientific; 1993. p. 299-303.
 35. Kikuchi M, Itoh S, Ichinose S, Shinomiya K, Tanaka J. Self-organization mechanism in a bone-like hydroxyapatite/collagen nanocomposite synthesized *in vitro* and its biological reaction *in vivo*. *Biomaterials* 2001;22:1705-1711.
 36. Taguchi T, Muraoka Y, Matsuyama H, Kishida A, Akashi M. Apatite coating on hydrophilic polymer-grafted poly(ethylene) films using an alternate soaking process. *Biomaterials* 2001;22:53-58.
 37. Abe Y, Kokubo T, Yamamuro T. Apatite coating on ceramics, metals and polymers utilizing a biological process. *J Mater Sci Mater Med* 1990;1:233-238.
 38. Tanahashi M, Yao T, Kokubo T, Minoda M, Miyamoto T, Nakamura T, Yamamuro T. Apatite coated on organic polymers by biomimetic process: Improvement in its adhesion to substrate by NaOH treatment. *J Appl Biomater* 1994;5:339-347.
 39. Tanahashi M, Yao T, Kokubo T, Minoda M, Miyamoto T, Nakamura T, Yamamuro T. Apatite coated on organic polymers by biomimetic process: Improvement in its

- adhesion to substrate by HCl treatment. *J Mater Sci Mater Med* 1995;6:319-326.
40. Tanahashi M, Yao T, Kokubo T, Minoda M, Miyamoto T, Nakamura T, Yamamuro T. Apatite coated on organic polymers by biomimetic process: Improvement in its adhesion to substrate by glow discharge treatment. *J Biomed Mater Res* 1995;29:349-357.
 41. Hata K, Kokubo T, Nakamura T, Yamamuro T. Growth of a bonelike apatite layer on a substrate by a biomimetic process. *J Am Ceram Soc* 1995;78:1049-1053.
 42. Yokogawa Y, Pazreyes J, Mucalo MR, Toriyama M, Kawamoto Y, Suzuki T, Nishizawa K, Nagata F, Kameyama T. Growth of calcium phosphate on phosphorylated chitin fibers. *J Mater Sci Mater Med* 1997;8:407-412.
 43. Rhee SH. Hydroxyapatite coating on a collagen membrane by a biomimetic method. *J Am Ceram Soc* 1998;81:3029-3031.
 44. Oyane A, Nakanishi K, Kim HM, Miyaji F, Kokubo T, Soga N, Nakamura T. Sol-gel modification of silicone to induce apatite-forming ability. *Biomaterials* 1999;20:79-84.
 45. Oyane A, Minoda M, Miyamoto T, Takahashi R, Nakanishi K, Kim HM, Kokubo T, Nakamura T. Apatite formation on ethylene-vinyl alcohol copolymer modified with silanol group. *J Biomed Mater Res* 1999;47:367-373.
 46. Kokubo T, Ito S, Huang ZT, Hayashi T, Sakka S, Kitsugi T, Yamamuro T. Ca, P-rich layer formed on high-strength bioactive glass-ceramic A-W. *J Biomed Mater Res* 1990;24:331-343.
 47. Neo M, Nakamura T, Yamamuro T, Ohtsuki C, Kokubo T. Apatite formation on three kinds of bioactive material at an early stage *in vivo*: A comparative study by transmission electron microscopy. *J Biomed Mater Res* 1993;27:999-1006.
 48. Loty C, Sautier JM, Boulekbache H, Kokubo T, Kim HM, Forest N. *In vitro* bone formation on a bone-like apatite layer prepared by a biomimetic process on a bioactive glass-ceramic. *J Biomed Mater Res* 2000;49:423-434.

49. Ohtsuki C, Kokubo T, Neo M, Kotani S, Yamamuro T, Nakamura T, Bando Y. Bone-bonding mechanism of sintered β -3CaO·P₂O₅. *Phosphorus Res Bull* 1991;1:191-196.
50. Höland W, Vogel V, Nawmann K, Gummel J. Interface reaction between machinable bioactive glass-ceramics and bone. *J Biomed Mater Res* 1985;19:303-312.
51. Kokubo T. Surface chemistry of bioactive glass-ceramics. *J Non-Cryst Solids* 1990;120:138-151.
52. Ohtsuki C, Kushitani H, Kokubo T, Kotani S, Yamamuro T. Apatite formation on the surface of Ceravital type glass-ceramic in the body. *J Biomed Mater Res* 1991;25:1363-1370.
53. Neo M, Kotani S, Yamamuro T, Ohtsuki C, Kokubo T, Bando Y. A comparative study of ultrastructures of the interfaces between four kinds of surface-active ceramic and bone. *J Biomed Mater Res* 1992;26:1419-1432.
54. Akazawa T, Kobayashi M, Kanno T, Kodaira K. Characterization of albumin- and lysozyme- adsorption evaluated on two differently prepared apatite. *J Mater Sci* 1998;33:1927-1931.
55. Luo Q, Andrade JD. Cooperative adsorption of proteins onto hydroxyapatite. *J Colloid Interf Sci* 1998;200:104-113.
56. Okazaki J, Embery G, Hall RC, Wassell DTH, Waddington RJ, Kamada A. Adsorption of glycosaminoglycans onto hydroxyapatite using chromatography. *Biomaterials* 1999;20:309-314.
57. Kilpadi KL, Chang PL, Bellis SL. Hydroxyapatite binds more serum proteins, purified integrins, and osteoblast precursor cells than titanium or steel. *J Biomed Mater Res* 2001;57:258-267.
58. Shaferi GMSE, Moussa NA. Adsorption of some essential amino acid on hydroxyapatite. *J Colloid Interf Sci* 2001;238:160-166.

59. Combes C, Rey C. Adsorption of proteins and calcium phosphate materials bioactivity. *Biomaterials* 2002;23:2817-2823.
60. Sugiyama S, Fukuda N, Matsumoto H, Hayashi H, Shigemoto N, Hiraga, Y, Moffat JB. Interdependence of anion and cation exchanges in calcium hydroxyapatite: Pb^{2+} and Cl^- . *J Colloid Interf Sci* 1999;220:324-328.
61. Bothe JV Jr, Brown PW. Arsenic immobilization by calcium arsenate formation. *Environ Sci Technol* 1999;33:3806-3811.
62. Furuta S, Katsuki H, Komarneni S. Removal of lead ions using porous hydroxyapatite monoliths synthesized from gypsum waste. *J Ceram Soc Japan* 2000;108:315-317.
63. Mavropoulos E, Rossi AM, Costa AM, Perez CAC, Moreira JC, Saldanha M. Studies on the mechanisms of lead immobilization by hydroxyapatite. *Environ Sci Technol* 2002;36:1625-1629.
64. Ohtsuki C, Kokubo T, Takatsuka K, Yamamuro T. Compositional dependence of bioactivity of glasses in the system $CaO-SiO_2-P_2O_5$: Its *in vitro* evaluation. *J Ceram Soc Japan* 1991;99:1-6.
65. Ohtsuki C, Kokubo T, Yamamuro T. Mechanism of apatite formation on $CaO-SiO_2-P_2O_5$ glasses in a simulated body fluid. *J Non-Cryst Solids* 1992;143:84-92.
66. Li P, Ohtsuki C, Kokubo T, Nakanishi K, Soga N, Nakamura T, Yamamuro T. Apatite formation induced by silica gel in a simulated body fluid. *J Am Ceram Soc* 1992;75:2094-2097.
67. Li P, Ohtsuki C, Kokubo T, Nakanishi K, Soga N, Nakamura T, Yamamuro T. Effects of ion in aqueous media on hydroxyapatite induction by silica gel and its relevance to bioactivity of bioactive glasses and glass-ceramics. *J Appl Biomater* 1993;4:221-229.
68. Li P, Ohtsuki C, Kokubo T, Nakanishi K, Soga N, de Groot K. The role of

- hydrated silica, titania and alumina in inducing apatite on implants. *J Biomed Mater Res* 1994;28:7-15.
69. Takadama H, Kim HM, Kokubo T, Nakamura T. An X-ray photoelectron spectroscopic study of the process of apatite formation on bioactive titanium metal. *J Biomed Mater Res* 2001;55:185-193.
 70. Uchida M, Kim HM, Kokubo T, Fujibayashi S, Nakamura T. Structural dependence of apatite formation on titania gel in a simulated body fluid. *J Biomed Mater Res* 2003;64A:164-170.
 71. Uchida M, Kim HM, Miyaji F, Kokubo T, Nakamura T. Bonelike apatite formation induced on zirconia gel in a simulated body fluid and its modified solutions. *J Am Ceram Soc* 2001;84:2041-2044.
 72. Miyazaki T, Kim HM, Kokubo T, Kato H, Nakamura T. Induction and acceleration of bonelike apatite formation on tantalum oxide gel in simulated body fluid. *J Sol-gel Sci Tech* 2001;21:83-88.
 73. Miyazaki T, Kim HM, Kokubo T, Ohtsuki C, Nakamura T. Apatite-forming ability of niobium oxide gels in a simulated body fluid. *J Ceram Soc Japan* 2001;109:929-933.
 74. Tanahashi M, Matsuda T. Surface functional group dependence on apatite formation on self-assembled monolayers in a simulated body fluid. *J Biomed Mater Res* 1997;34:305-315.
 75. Miyazaki T, Ohtsuki C, Akioka Y, Tanihara M, Nakao J, Sakaguchi Y, Konagaya S. Apatite deposition on polyamide film containing carboxyl group in a biomimetic solution. *J Mater Sci Mater Med* 2003;14:569-574.
 76. In: Iwasawa Y editor. *Kagakubinran the 5th edition*. Tokyo: Maruzen; 2004. p. II-100 [in Japanese].
 77. Takadama H, Kim HM, Miyaji F, Kokubo T, Nakamura T. Mechanism of apatite formation induced by silanol groups: TEM observation. *J Ceram Soc Japan*

2000;108:118-121.

78. In: Lide DR, Frederikse HPR editors. CRC handbook of chemistry and physics. Boca Raton: CRC Press; 1995. p. 8-44 - 8-51.
79. In: Iwasawa Y editor. Kagakubinran the 5th edition. Tokyo: Maruzen; 2004. p. II-361 [in Japanese].
80. In: Iwasawa Y editor. Kagakubinran the 5th edition. Tokyo: Maruzen; 2004. p. II-344 [in Japanese].

Table 1 Typical bioactive ceramics and their components

Material	Components
Bioglass [®] [2-4]	Glass (Na ₂ O-CaO-SiO ₂ -P ₂ O ₅ system)
Ceravital [®] [5]	Crystalline apatite precipitated glass-ceramic (Na ₂ O-CaO-SiO ₂ -P ₂ O ₅ system)
Sintered hydroxyapatite ^[6,7]	Crystalline hydroxyapatite (Ca ₁₀ (PO ₄) ₆ (OH) ₂)
Glass-ceramic A-W ^[8,9]	Crystalline oxyfluoroapatite and β-wollastonite precipitated glass-ceramic (MgO-CaO-SiO ₂ -P ₂ O ₅ -CaF system)
Bioverit [®] [10]	Crystalline apatite and fluorophlogopite mica precipitated glass-ceramic (Na ₂ O-MgO-K ₂ O-CaO-(Al ₂ O ₃)-SiO ₂ -P ₂ O ₅ -F system)

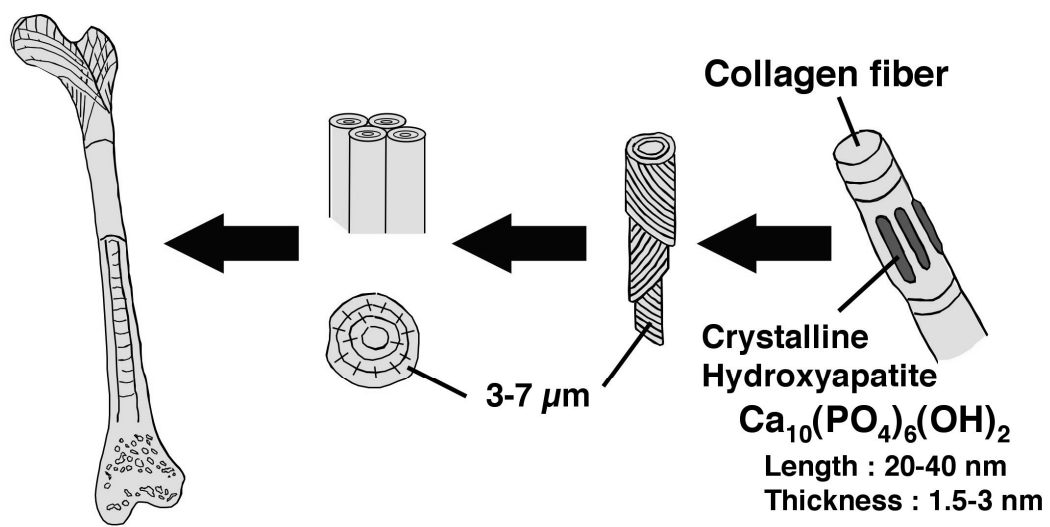


Figure 1. Structure of bone.

Table 2 Typical methods for fabrication of organic-inorganic hybrids consisting hydroxyapatite and organic polymer

Method	Reference
Mechanical mixing	[34]
Self-organization	[35]
Alternate soaking	[36]
Biomimetic coating	[37-45]

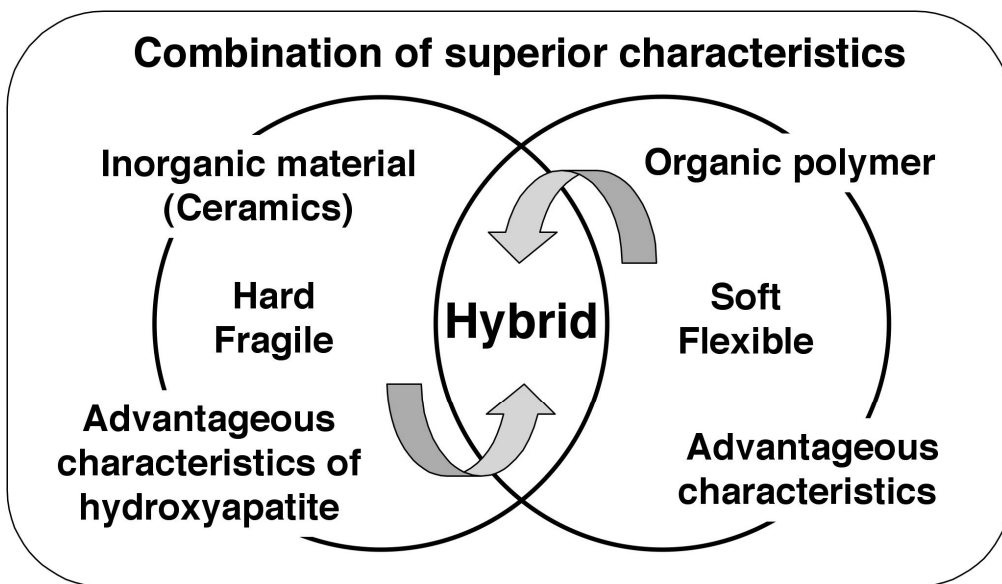


Figure 2. Concept of hybridization of hydroxyapatite and organic polymer.

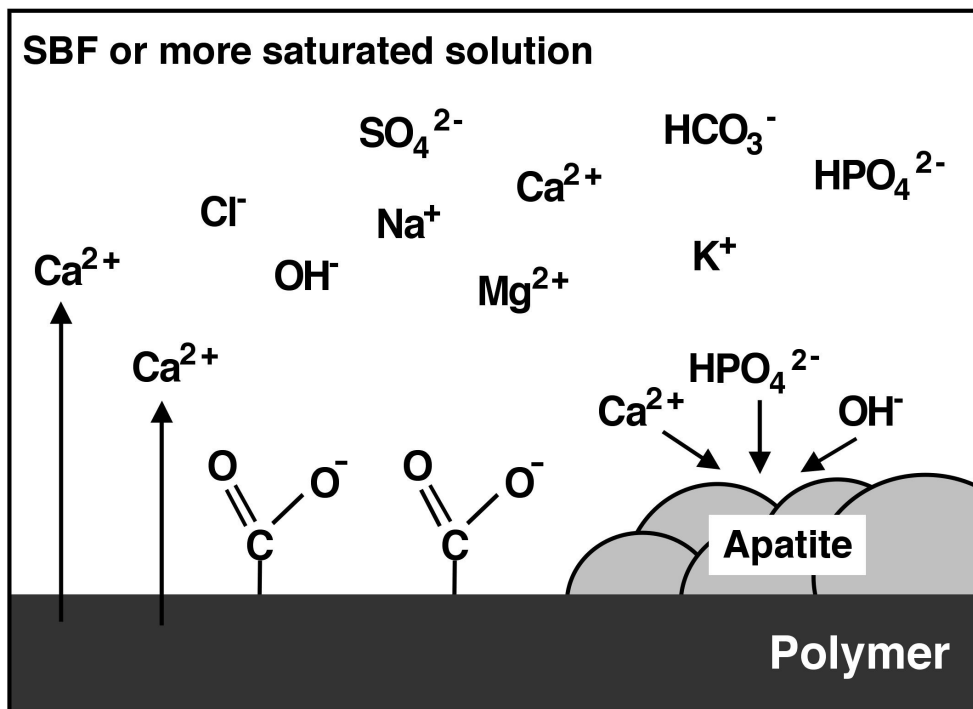


Figure 3. Apatite nucleation induced by a functional group on the surface of organic polymer and accelerated by release of calcium ions from the polymer.

Table 3 Surface charges of oxide gels and their apatite-forming ability in SBF under neutral pH conditions

Oxide gel	pH ^[76]	ζ potential / mV ^[76]	Apatite formation* ^[68]
SiO ₂ (-SiOH)	7	-102	+
TiO ₂ (-TiOH)	7	-44	+
Al ₂ O ₃ (-AlOH)	6.5	+51	-

*Apatite was formed (+), not formed (-) in SBF.

Table 4 Substances having typical functional groups and their pK_a values

Substance	pK_a [78]	Equilibrium formula
Ph-COOH*	4.19	$\text{Ph-COOH} \rightleftharpoons \text{Ph-COO}^- + \text{H}^+$
Ph-SO ₃ H*	0.70	$\text{Ph-SO}_3\text{H} \rightleftharpoons \text{Ph-SO}_3^- + \text{H}^+$
PO ₄ H ₃	2.16	$\text{PO}_4\text{H}_3 \rightleftharpoons \text{PO}_4\text{H}_2^- + \text{H}^+$
	7.21	$\text{PO}_4\text{H}_2^- \rightleftharpoons \text{PO}_4\text{H}^{2-} + \text{H}^+$
	12.32	$\text{PO}_4\text{H}^{2-} \rightleftharpoons \text{PO}_4^{3-} + \text{H}^+$
SiO ₄ H ₄	9.8	$\text{SiO}_4\text{H}_4 \rightleftharpoons \text{SiO}_4\text{H}_3^- + \text{H}^+$
	11.8	$\text{SiO}_4\text{H}_3^- \rightleftharpoons \text{SiO}_4\text{H}_2^{2-} + \text{H}^+$
	12	$\text{SiO}_4\text{H}_2^{2-} \rightleftharpoons \text{SiO}_4\text{H}^{3-} + \text{H}^+$
	12	$\text{SiO}_4\text{H}^{3-} \rightleftharpoons \text{SiO}_4^{4-} + \text{H}^+$


*Ph: 

Table 5 Equilibrium constants for formation of ion pair of calcium ion with typical anions in aqueous solution at 25°C

Anion (A^{n-})	$\log K_{as}^{*[79]}$
SO_4^{2-}	2.28
$H_2PO_4^-$	1.08
HPO_4^{2-}	2.70
$HCOO^-$	0.80
CH_3COO^-	0.77
$C_2H_5COO^-$	0.68

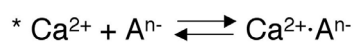


Table 6 Equilibrium constants for formation of calcium complex with typical anions

Anion	$\log K_{\text{comp}}^{[80]}$	Equilibrium formula
CO_3^{2-}	3.2	$\text{Ca}^{2+} + \text{CO}_3^{2-} \rightleftharpoons \text{CaCO}_3$
	1.0	$\text{Ca}^{2+} + \text{HCO}_3^- \rightleftharpoons \text{CaHCO}_3^+$
PO_4^{3-}	2.74	$\text{Ca}^{2+} + \text{HPO}_4^{2-} \rightleftharpoons \text{CaHPO}_4$
	1.41	$\text{Ca}^{2+} + \text{H}_2\text{PO}_4^- \rightleftharpoons \text{CaH}_2\text{PO}_4^+$
SO_4^{2-}	2.31	$\text{Ca}^{2+} + \text{SO}_4^{2-} \rightleftharpoons \text{CaSO}_4$

Chapter 1: Coating of a hydroxyapatite layer on polyamide films containing sulfonic groups

1.1. Introduction

Hydroxyapatite ($\text{Ca}_{10}(\text{PO}_4)_6(\text{OH})_2$), a type of calcium phosphate, shows high biological affinity to living bone [1,2]. Synthetic hydroxyapatite is now widely used as a substitute material for filling bony defects. Moreover, hydroxyapatite has several interesting properties, such as adsorption of proteins and virus, and exchange of ionic species in its crystal lattice [3,4]. However, the body of sintered hydroxyapatite does not have sufficiently good mechanical properties for extending its applications in medical fields. A conventional composite of hydroxyapatite and organic polymer results in reduced functionality of hydroxyapatite, because most of the particles of hydroxyapatite are normally embedded in polymer matrices. The surface of hydroxyapatite must be exposed to the surrounding environment for its valuable properties, i.e. biological properties, to be seen. The coating of hydroxyapatite onto organic polymers is therefore given much attention.

Kokubo *et al.* proposed a biomimetic process that utilizes a reaction between bioactive glass and simulated body fluid (SBF) [5,6], in order to coat a hydroxyapatite layer onto organic substrates [7,8]. This process can be used for producing a polymer substrate covered with a so-called bone-like apatite, that is carbonate-containing hydroxyapatite with small crystallites and defective structure [9]. Such a carbonate-containing hydroxyapatite shows a high biological affinity when implanted into bony defects and can achieve a tight bonding to living bone. It is therefore expected that coating of bone-like hydroxyapatite through the biomimetic method will produce organic-inorganic hybrids that can show direct bonding to living bone, in addition to specific mechanical properties arising from organic materials.

In the biomimetic process utilizing SBF, hydroxyapatite deposition on an

organic polymer can be triggered both by the existence of a specific functional group effective for induction of heterogeneous nucleation of apatite, and by an increase in concentration of calcium ions in the surrounding fluid. Therefore, in the production of a hydroxyapatite-organic polymer hybrid through such a biomimetic processing route, it is a key engineering challenge to design a substrate with heterogeneous nucleation sites for hydroxyapatite deposition. It has been reported that carboxyl (-COOH) groups play an effective role in heterogeneous nucleation of apatite in the body environment [10,11]. Miyazaki *et al.* have shown that polyamide films containing carboxyl groups have the ability to induce deposition of hydroxyapatite crystals on their surfaces in 1.5SBF that has ion concentrations 1.5 times those of SBF, when the films were incorporated with calcium chloride (CaCl₂) [12]. It is interesting to find alternative functional groups effective for hydroxyapatite formation. In this chapter, we investigated the ability of hydroxyapatite formation on polyamide films containing sulfonic (-SO₃H) groups incorporated with calcium salt by a biomimetic process. In this study, the polymer substrates were exposed to 1.5SBF for estimation of the ability of hydroxyapatite deposition, since the preliminary experiments showed that hydroxyapatite deposition was not observed on any of the samples even after soaking in SBF for 7 days. This means that the prepared films, by themselves, have lower ability of hydroxyapatite formation than the so-called bioactive material. But these findings are applicable to develop novel hybrids consisting of hydroxyapatite and organic polymers, because the modification of polymer substrates is worth on coating of hydroxyapatite through a process using 1.5SBF.

1.2. Experimental

1.2.1. Preparation of polyamide films containing sulfonic groups.

Aromatic polyamides (Figure 1-1) were prepared according to the literature method [13]. The polyamides S(0), S(0.2) and S(0.5), have 0, 20 and 50% of sulfonic

group in the polymer molecule, respectively. One gram of each polyamide powder was dissolved in 10 mL of N,N-dimethylacetamide (Wako Pure Chemical Industries Ltd., Japan), both with and without CaCl₂ (Nacalai Tesque Inc., Japan). The CaCl₂ was added to the polyamide in various mass ratios of CaCl₂/(polyamide + CaCl₂) = 0, 0.10, 0.20 and 0.40. The mixture was then stirred for 12 h to form a homogeneous viscous solution. The obtained solution was then coated onto a flat glass plate, using a bar coater. The solution coated on the glass plate was dried in a vacuum oven at 60°C under 133 Pa for 8 h. The obtained polymer films were then removed from the glass plates and cut into 10 mm × 10 mm sections. Polyamide (S(x)) films were prepared by modification with y mass% of CaCl₂ to a given total S(x) and CaCl₂, and hereafter, are denoted as S(x)Ca(y).

1.2.2. Soaking in 1.5SBF

The obtained films were then soaked in 30 mL of 1.5SBF (Na⁺ 213.0, K⁺ 7.5, Mg⁺ 2.3, Ca²⁺ 3.8, Cl⁻ 221.7, HCO₃⁻ 6.3, HPO₄²⁻ 1.5, and SO₄²⁻ 0.8 mol·m⁻³). The solution was prepared by dissolving reagent grade chemicals of NaCl, NaHCO₃, KCl, K₂HPO₄·3H₂O, MgCl₂·6H₂O, CaCl₂, and Na₂SO₄ (Nacalai Tesque Inc., Japan) in ultrapure water [7,14]. The pH of the solution was buffered at 7.40 using 75 mol·m⁻³ of tris(hydroxymethyl)aminomethane (Nacalai Tesque Inc., Japan) along with an appropriate volume of 1 kmol·m⁻³ hydrochloric acid solution. The temperature of the solution was kept at 36.5°C. After soaking for given periods, the films were taken out from the solution, and then dried at room temperature.

1.2.3. Characterization

The surfaces of the films were characterized both before and after soaking in 1.5SBF, using thin-film X-ray diffraction (TF-XRD: MXP3V, MAC Science Co., Ltd., Japan) and scanning electron microscopy (SEM: S-3500N, Hitachi, Ltd., Japan). In the

TF-XRD measurements, the angle of the incident beam was fixed at 1° against the surface of the specimen. In the SEM observations, an Au thin film was sputtered onto the surface of the specimen. Morphological observation at higher magnification was conducted for typical specimens under field emission scanning electron microscope (FE-SEM: JMS-6301F, JEOL, Japan). Composition of the surfaces of the specimens was examined by an energy dispersive X-ray microanalyzer (EDX: EMAX ENERGY EX-400, Horiba, Ltd., Japan).

1.3. Results

Figure 1-2 shows TF-XRD patterns of the surfaces of S(0.5)Ca(y) films ($y = 0, 10, 20$ and 40) before and after soaking in 1.5SBF for various periods. Peaks ascribed to apatite were observed at $2\theta = 26^\circ$ and 32° in the diffraction patterns of the S(0.5)Ca(y) films containing 20 mass% of CaCl₂ or more, after soaking for 7 days. The peak at $2\theta = 26^\circ$ was assigned to the 002 diffraction of apatite, while the one at $2\theta = 32^\circ$ was an envelope of the 211, 112 and 300 diffractions of apatite. In contrast, no peak assigned to apatite was detected for the S(0.5)Ca(y) containing 10 mass% of CaCl₂ or less. This indicates that apatite could deposit on the surface after soaking the S(0.5)Ca(y) films when the films had 20 mass% of CaCl₂ and more. Figures 1-3 and 1-4 show TF-XRD patterns of S(x)Ca(40) and S(x)Ca(20) films ($x = 0, 0.2$ and 0.5) after soaking in 1.5SBF for 7 days, respectively. Peaks assigned to apatite were detected for the films irrespective of the content of sulfonic groups when the films contained 20 mass% of CaCl₂ or more. The tendency of apatite formation estimated by detection with TF-XRD was summarized on Table 1-1. Figure 1-5 shows SEM images of the surfaces of S(x)Ca(20) and S(x)Ca(40) films ($x = 0, 0.2$ and 0.5) before and after soaking in 1.5SBF for 1, 3 and 7 days, respectively. Formation of fine particles was observed on the films S(0.2)Ca(20), S(0.2)Ca(40) and S(0.5)Ca(20) after soaking in 1.5SBF for 3 days, and S(0.5)Ca(40) for 1 day. The results of EDX (Figure 1-6) distinctly showed that the

particles consisted of calcium and phosphorus. Although TF-XRD patterns showed existence of apatite on the S(0)Ca(20) and S(0)Ca(40) films after soaking in 1.5SBF for 7 days, almost all the surfaces looked smooth under SEM observation. This is due to the phenomena that the formed layer of hydroxyapatite was easily peeled off during the operation for SEM observation. This result corresponds to adhesive strength of hydroxyapatite to polymer substrates. Adhesive strength of hydroxyapatite layer to S(0)Ca(y) films was too small to keep the hydroxyapatite layer on their surfaces, while S(0.2)Ca(y) and S(0.5)Ca(y) could show enough adhesive strength to keep the hydroxyapatite layer on their surfaces during SEM observation.

Figure 1-7 shows morphology of the deposited particles on S(0.2)Ca(40) and S(0.5)Ca(40) films, at higher magnification under FE-SEM. This morphology was very similar to that of the deposited hydroxyapatite on a substrate through biomimetic processing utilizing SBF [7]. These particles were therefore attributed to hydroxyapatite. Formation of hydroxyapatite was observed on the surface of S(0.5)Ca(40) in shorter periods after soaking in 1.5SBF than on S(0.5)Ca(20). This indicates that higher contents of CaCl₂ resulted in higher rates of hydroxyapatite formation. S(0.5)Ca(40) also showed shorter periods for the hydroxyapatite formation than S(0.2)Ca(40). Higher contents of sulfonic groups also lead to a higher rate of hydroxyapatite formation in 1.5SBF.

Figure 1-8 shows Ca/P atomic ratios of the deposited apatite on the surfaces of various kinds of films after soaking in 1.5SBF. The atomic ratios were determined by EDX analyses. Ca was not detected for each film after soaking in 1.5SBF for 6 h. This means that all the Ca²⁺ incorporated within the film were released within a few hours. The Ca/P atomic ratio of the formed layers increased with increasing soaking periods for all the film. In the case of S(0.5)Ca(40), the Ca/P ratio increased and reached to a constant value of about 1.65 after 3 days soaking.

1.4. Discussion

It is apparent from the results described above that hydroxyapatite deposition can be induced by incorporation of CaCl_2 in the aromatic polyamide. The deposition of hydroxyapatite was accelerated by the increase in concentration of sulfonic groups, because S(0.5)Ca(40) showed a higher concentration of deposited hydroxyapatite particles than S(0.2)Ca(40). The hydroxyapatite layer formed on S(0)Ca(40) was easily peeled off from the films as the hydroxyapatite layer on S(0)Ca(40) was not observed under SEM, while that formed on S(0.2)Ca(40) and S(0.5)Ca(40) was not easily peeled off under the same condition. This indicates that the sulfonic groups play an important role in not only the nucleation of the apatite but also high adhesion of the hydroxyapatite layer to the films. The higher strength means a strong interaction between the sulfonic groups and hydroxyapatite crystal. Quantitative analysis is discussed on Chapter 3 in comparison with that of polyamide films containing carboxyl groups.

It has been reported that $-\text{SiOH}$ [15], $-\text{TiOH}$ [16] groups induce hydroxyapatite formation in a biomimetic solution. Surface charges reported on oxide materials are listed on Table 3 in general introduction part [17]. From the view points of surface charges, hydroxyapatite formation can be observed on the surface with negatively charged in the biomimetic aqueous solution at about pH 7.4. Negatively charged surface may accumulate calcium ions (Ca^{2+}) in the surrounding solution to form complex between these species at initial stage inducing nucleation of apatite. Then the complexes incorporate phosphate ions to form apatite nuclei. This initial stage may govern the heterogeneous nucleation of apatite on the substrate after exposure to a solution mimicking body environment. On the other hand, previous reports proposed an interaction between Ca^{2+} and carboxyl ($-\text{COOH}$) groups on aromatic polyamide, and natural silk [12,18]. Formation of a complex, such as $-\text{COOCa}^+$ or $(-\text{COO})_2\text{Ca}$ was presumed on the initial stages on hydroxyapatite deposition. It is presumed that similar

type of complex such as $-\text{SO}_3\text{Ca}^+$ or $(-\text{SO}_3)_2\text{Ca}$ formed in the induction periods for hydroxyapatite formation. Sulfonic group dissociates to be negatively charged as $-\text{SO}_3^-$ in a physiological solution because the negative of the logarithm of the dissociation constant ($\text{p}K_a$) for sulfonic group of benzenesulfonic acid ($\text{C}_6\text{H}_5\text{SO}_3\text{H}$) is 0.70 at 25°C [19]. This value is smaller than those of benzoic acid ($\text{C}_6\text{H}_5\text{COOH}$; 4.19) at the same temperature [19]. The amount of hydroxyapatite formed on polyamide film containing 50 mol% of sulfonic groups seemed more than that containing the same percentage of carboxyl groups after soaking in 1.5SBF for 3 days, when they were incorporated with 40 mass% of CaCl_2 [20,21]. This means that rate of hydroxyapatite formation on polyamide film containing sulfonic groups is greater than that containing carboxyl groups. However, the degree of negative charge of sulfonic group is estimated to be as high as that of carboxyl group in 1.5SBF at pH7.4. The difference in rate of hydroxyapatite formation was supposed to be attributed to the number of lone electron-pairs, that is, one sulfonic group possesses seven lone pairs, while one carboxyl group has five in physiological conditions. This may have contributed to easier access of calcium ions to sulfonic groups than that to carboxyl groups. On the other hand, equilibrium constants for formation of ion pair of calcium ion with typical anions are given on Table 5 in general introduction part [22]. The constant for an anion having sulfonic group is larger than that for carboxyl group. This also indicates that it is easier for sulfonic group to associate with calcium ions in an aqueous solution around pH 7. Therefore, potential of complex formation of $-\text{SO}_3\text{Ca}^+$ and $(-\text{SO}_3)_2\text{Ca}$ may be higher than $-\text{COOCa}^+$ and $(-\text{COO})_2\text{Ca}$. These would result in high nucleation rates on the polymer substrates even under the same degree of supersaturation after Ca^{2+} release from the substrates.

After the formation of nucleation sites for hydroxyapatite, calcium phosphate with Ca/P atomic ratio below 1.6 would be formed on the surface. The calcium phosphate may be aged to result in a higher Ca/P ratio. This means that the calcium

phosphate at initial stage is formed with a high deficiency in calcium sites in crystalline hydroxyapatite. After aging, the crystalline hydroxyapatite grew to become a much stable phase with a higher Ca/P atomic ratio than at the initial stages, that is, its Ca/P ratio became near to that of the general hydroxyapatite. To control the composition and structures of the deposited hydroxyapatite, biomimetic processing provides possible way by utilizing a solution mimicking body environment and polyamide films containing different amounts of functional group or calcium salt.

1.5. Conclusions

Hydroxyapatite formation on aromatic polyamides was induced by incorporation of sulfonic groups as well as calcium chloride. This indicates that sulfonic groups are able to accelerate hydroxyapatite formation in a biomimetic solution, such as 1.5SBF. Sulfonic groups provided in a higher adhesive strength of the hydroxyapatite layer to the polymer substrates. Consequently, this study supports the idea that hydroxyapatite-polymer hybrids can be developed by modification of the polymer with sulfonic groups and calcium ions.

References

1. LeGeros RZ, LeGeros JP. Dense hydroxyapatite. In: Hench LL, Wilson J, editors. An Introduction to bioceramics. Singapore: World Scientific; 1993. p. 139-180.
2. Hench LL. Bioceramics. J Am Ceram Soc 1998;81:1705-1728.
3. Kilpadi KL, Chang PL, Bellis SL. Hydroxyapatite binds more serum proteins, purified integrins, and osteoblast precursor cells than titanium or steel. J Biomed Mater res 2001;57:258-267.
4. Combes C, Rey C. Adsorption of proteins and calcium phosphate materials bioactivity. Biomaterials 2002;23:2817-2823.
5. Kokubo T, Ito S, Huang ZT, Hayashi T, Sakka S, Kitsugi T, Yamamuro T. Ca, P-rich layer formed on high-strength bioactive glass-ceramic A-W. J Biomed Mater Res 1990;24:331-343.
6. Kokubo T, Kushitani H, Sakka S, Kitsugi T, Yamamuro T. Solutions able to reproduce *in vivo* surface-structure changes in bioactive glass-ceramic A-W. J Biomed Mater Res 1990;24:721-734
7. Tanahashi M, Yao T, Kokubo T, Minoda M, Miyamoto T, Nakamura T, Yamamuro T. Apatite coating on organic polymers by a biomimetic process. J Am Ceram Soc 1994;77:2805-2808.
8. Hata K, Ozawa N, Kokubo T, Nakamura T. Bonelike apatite formation on various kinds of ceramics and metals. J Ceram Soc Japan 2001;109:461-465.
9. Tanahashi M, Kokubo T, Nakamura T, Katsura Y, Nagano M. Ultrastructural study of an apatite layer formed by a biomimetic process and its bonding to bone. Biomaterials 1996;17:47-51.
10. Tanahashi M, Matsuda T. Surface functional group dependence on apatite formation on self-assembled monolayers in a simulated body fluid. J Biomed Mater Res 1997;34:305-315.

11. Kawashita M, Nakao M, Minoda M, Kim HM, Beppu T, Miyamoto T, Kokubo T, Nakamura T. Apatite-forming ability of carboxyl group-containing polymer gels in a simulated body fluid. *Biomaterials* 2003;24:2477-2484.
12. Miyazaki T, Ohtsuki C, Akioka Y, Tanihara M, Nakao J, Sakaguchi Y, Konagaya S. Apatite deposition on polyamide film containing carboxyl group in a biomimetic solution. *J Mater Sci Mater Med* 2003;14:569-574.
13. Konagaya S, Tokai M. Synthesis of ternary copolyamides from aromatic diamine with carboxyl or sulfonic group (3,5-diaminobenzoic acid, 2,4-diaminobenzenesulfonic acid), and iso- or terephthaloyl chloride. *J Appl Polym Sci* 2000;76:913-920.
14. Ohtsuki C, Kokubo T, Neo M, Kotani S, Yamamuro T, Nakamura T, Bando Y. Bone-bonding mechanism of sintered β -3CaO·P₂O₅. *Phosphorus Res Bull* 1991;1:191-196.
15. Takadama H, Kim HM, Kokubo T, Nakamura T. Mechanism of biomineralization of apatite on sodium silicate glass: TEM-EDX study *in vitro*. *Chem Mater* 2001;13:1108-1113.
16. Takadama H, Kim HM, Kokubo T, Nakamura T. An X-ray photoelectron spectroscopic study of the process of apatite formation on bioactive titanium metal. *J Biomed Mater Res* 2001;55:185-193.
17. In: Iwasawa Y editor. *Kagakubinran* the 5th edition. Tokyo: Maruzen; 2004. p. II-100 [in Japanese].
18. Takeuchi A, Ohtsuki C, Miyazaki T, Tanaka H, Yamazaki M, Tanihara M. Deposition of bone-like apatite on silk fiber in a solution that mimics extracellular fluid. *J Biomed Mater Res* 2003;65A 283-289.
19. In: Lide DR, Frederikse HPR editors. *CRC handbook of chemistry and physics*. Boca Raton: CRC Press; 1995. p. 8-49 - 8-51.
20. Miyazaki T, Akioka Y, Ohtsuki C, Tanihara M, Nakao J, Sakaguchi Y, Konagaya S.

- Apatite deposition on polyamide films containing carboxyl groups in body environment. In: Brown S, Clarke I, Williams P editors. Key Engineering Materials Vols. 218-220 (Bioceramics Vol. 14). Trans Tech Publications Ltd.: Switzerland; 2002. p. 133-136.
21. Akioka Y, Miyazaki T, Ohtsuki C, Tanihara M, Nakao J, Sakaguchi Y, Konagaya S. Coating of bonelike apatite on polyamide film via chemical modification with calcium chloride. In: Brown S, Clarke I, Williams P editors. Key Engineering Materials Vols. 218-220 (Bioceramics Vol. 14). Trans Tech Publications Ltd.: Switzerland; 2002. p. 137-140.
22. In: Iwasawa Y editor. Kagakubinran the 5th edition. Tokyo: Maruzen; 2004. p. II-361 [in Japanese].

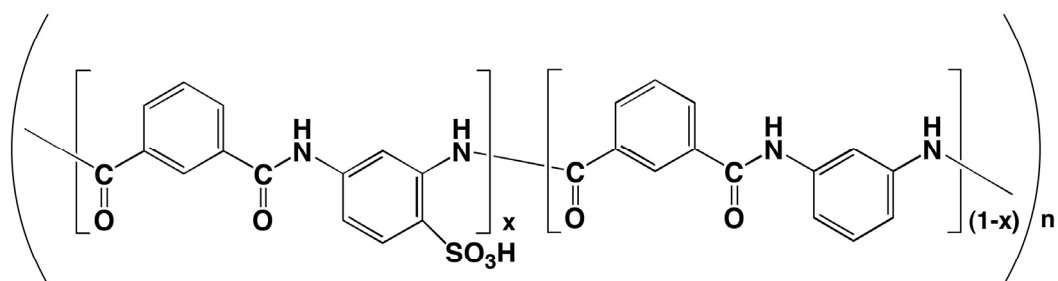


Figure 1-1. Structural formula of S(x).

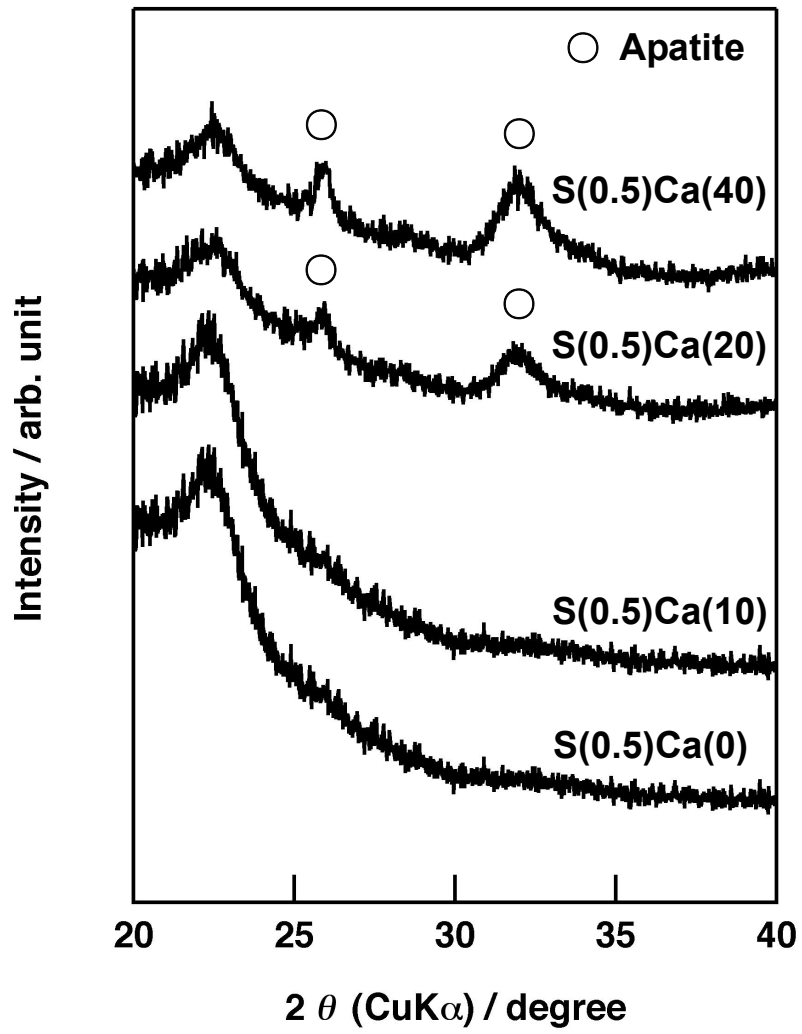


Figure 1-2. TF-XRD patterns of surfaces of S(0.5)Ca(y) films after soaking in 1.5SBF for 7 days.

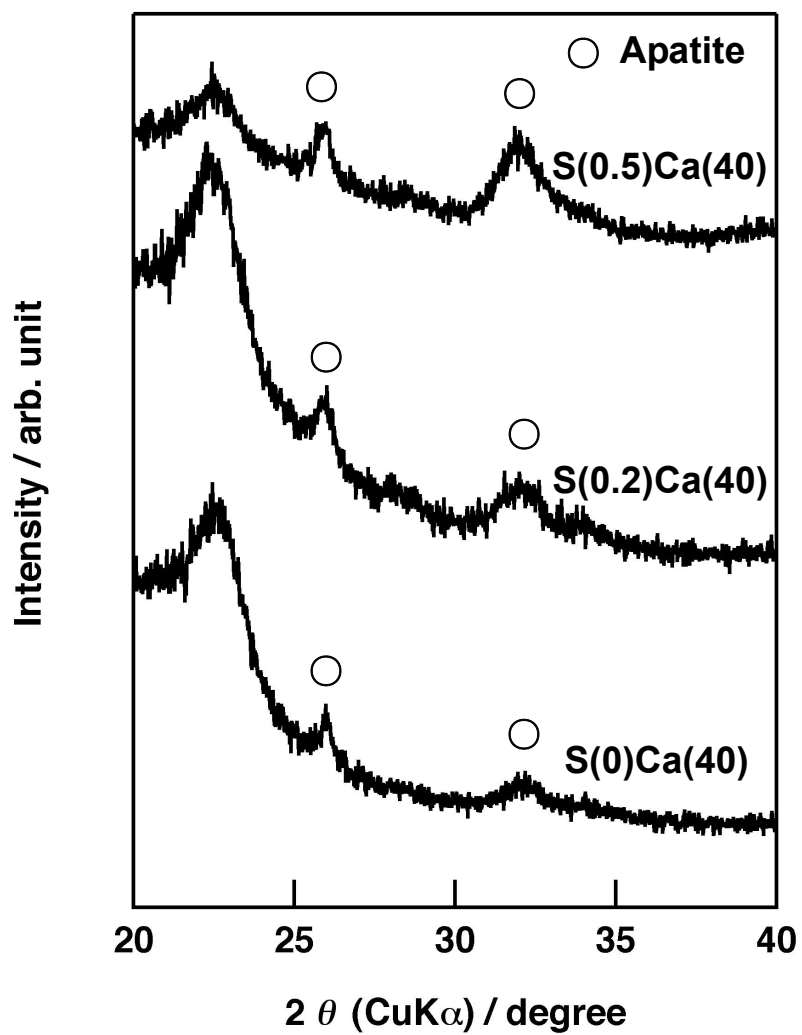


Figure 1-3. TF-XRD patterns of surfaces of S(x)Ca(40) films after soaking in 1.5SBF for 7 days.

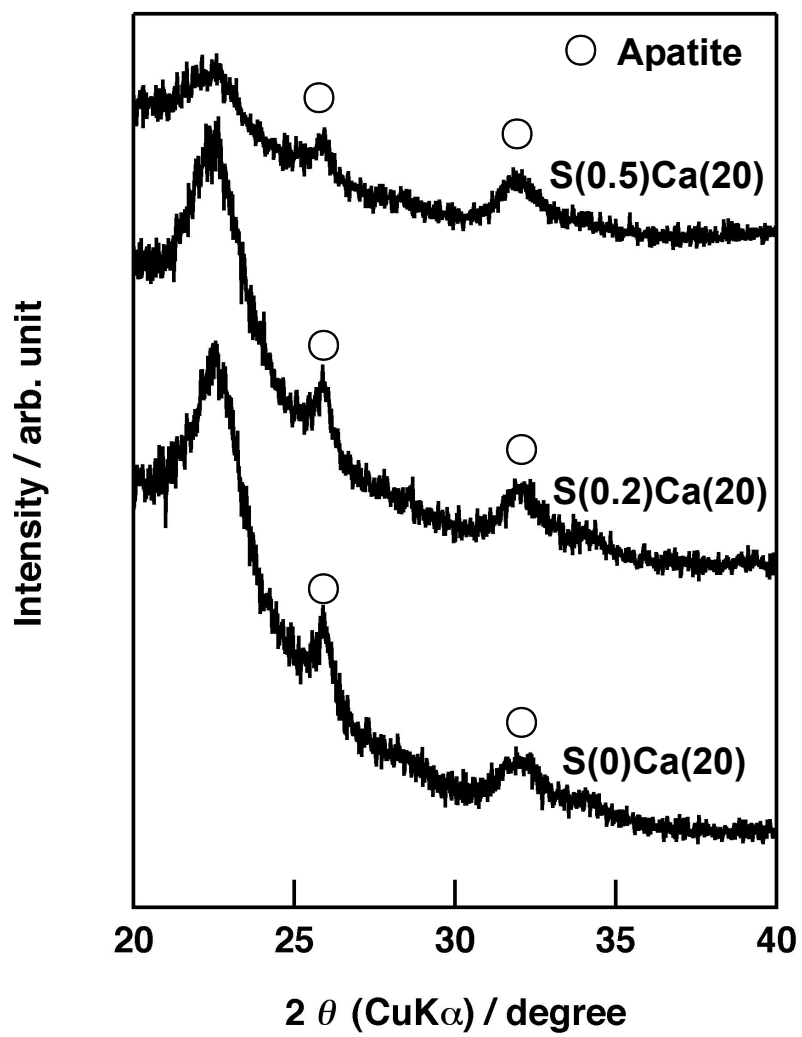


Figure 1-4. TF-XRD patterns of surfaces of S(x)Ca(20) films after soaking in 1.5SBF for 7 days.

Table 1-1 Tendency of apatite formation estimated by detection with TF-XRD

Specimen	Soaking period / day		
	1	3	7
S(0)Ca(20)	-	-	+
S(0.2)Ca(20)	-	+	+
S(0.5)Ca(20)	-	+	+
S(0)Ca(40)	-	-	+
S(0.2)Ca(40)	-	+	+
S(0.5)Ca(40)	+	+	+

Apatite was formed (+), not formed (-)

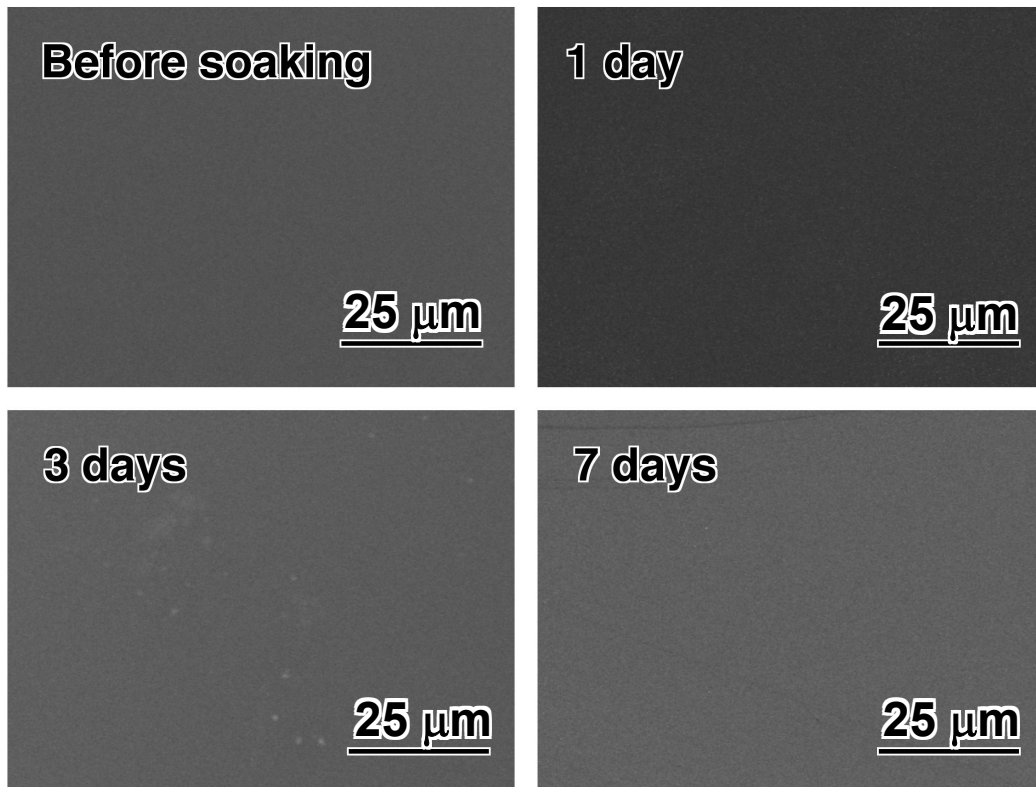


Figure 1-5(a). SEM images of surfaces of S(0)Ca(20) films before and after soaking in 1.5SBF for various periods.

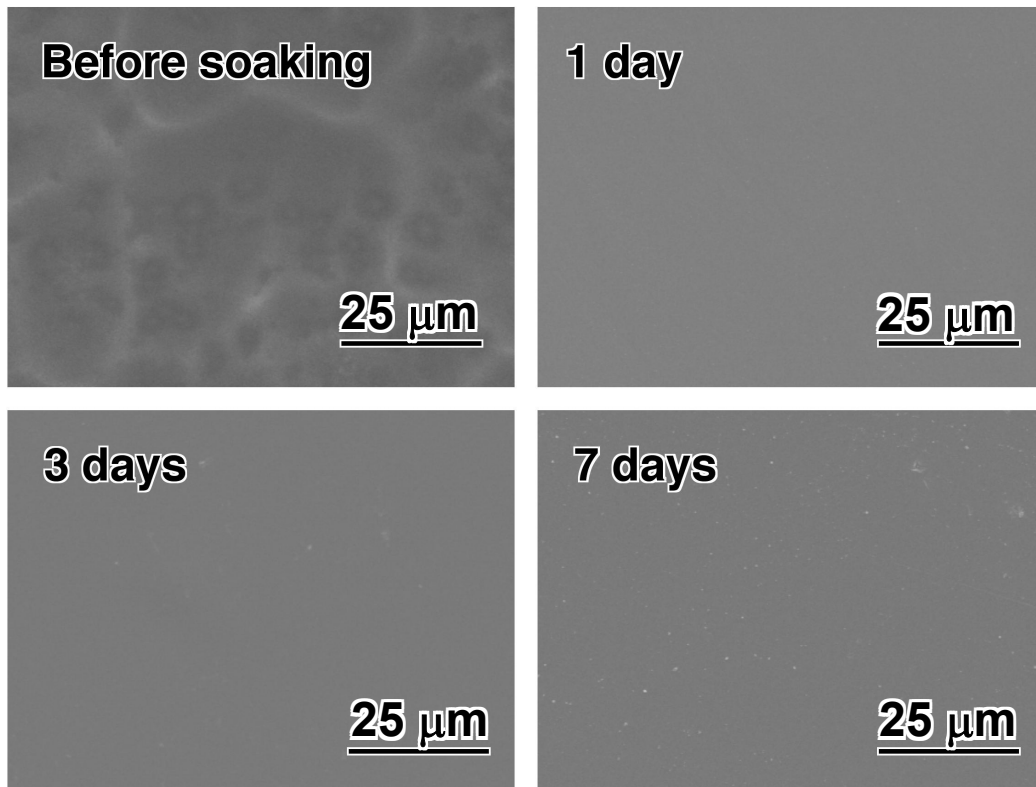


Figure 1-5(b). SEM images of surfaces of S(0)Ca(40) films before and after soaking in 1.5SBF for various periods.

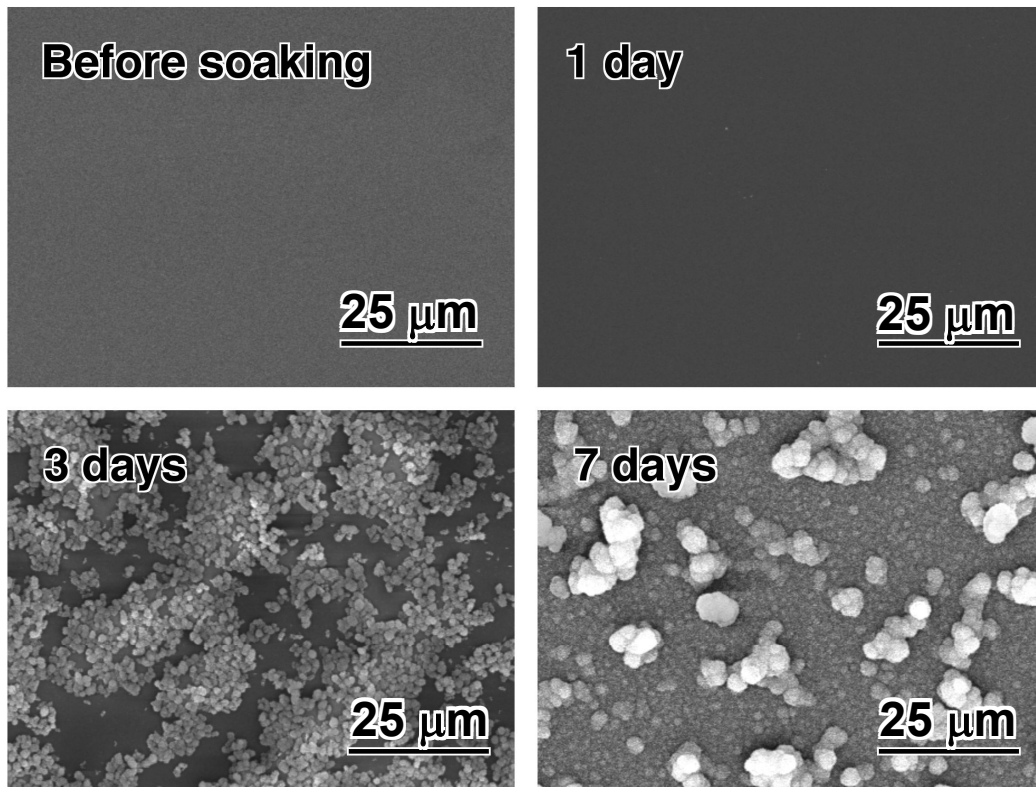


Figure 1-5(c). SEM images of surfaces of S(0.2)Ca(20) films before and after soaking in 1.5SBF for various periods.

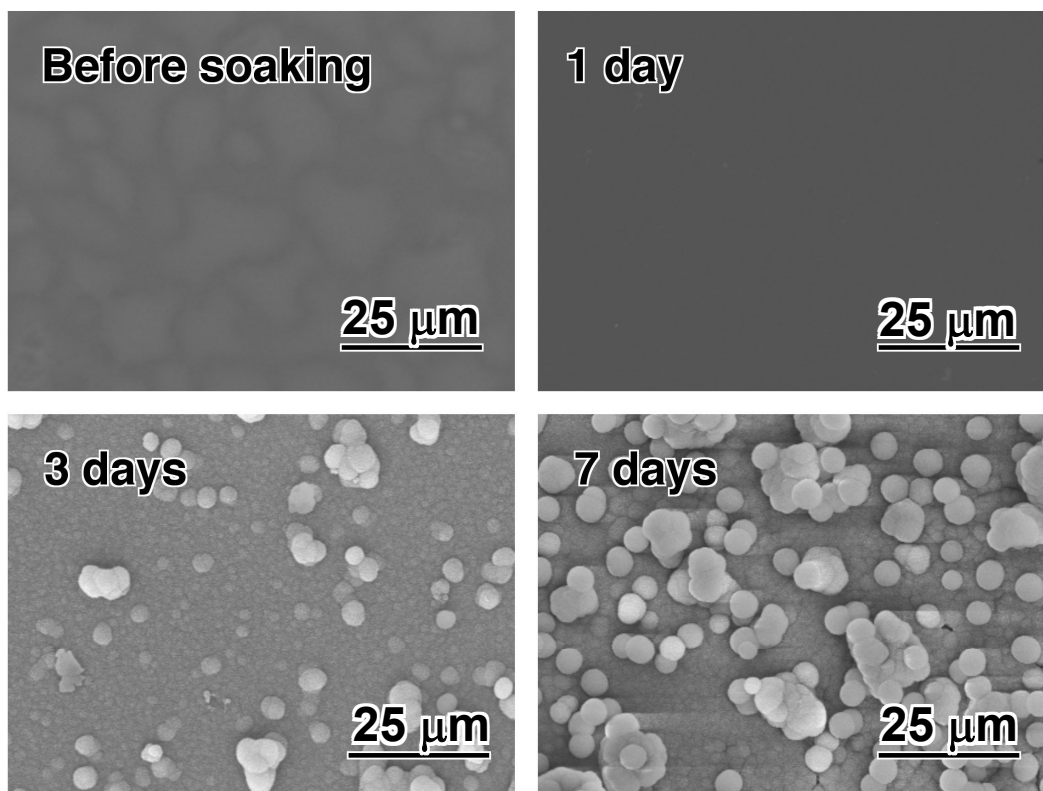


Figure 1-5(d). SEM images of surfaces of S(0.2)Ca(40) films before and after soaking in 1.5SBF for various periods.

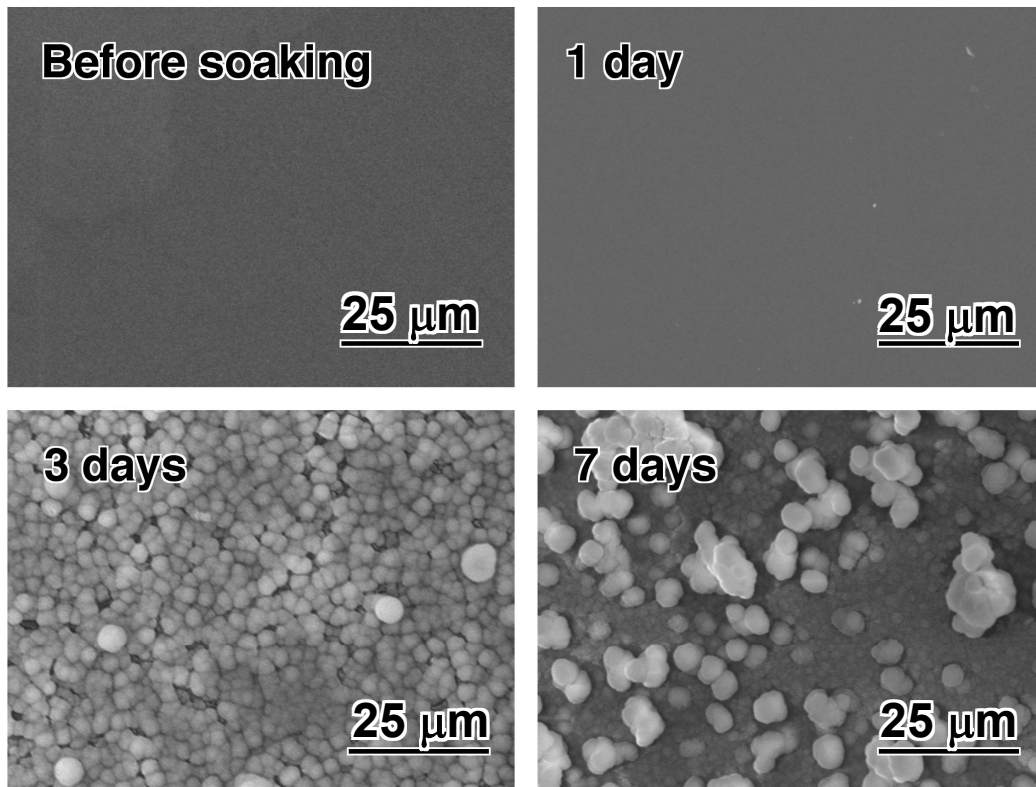


Figure 1-5(e). SEM images of surfaces of S(0.5)Ca(20) films before and after soaking in 1.5SBF for various periods.

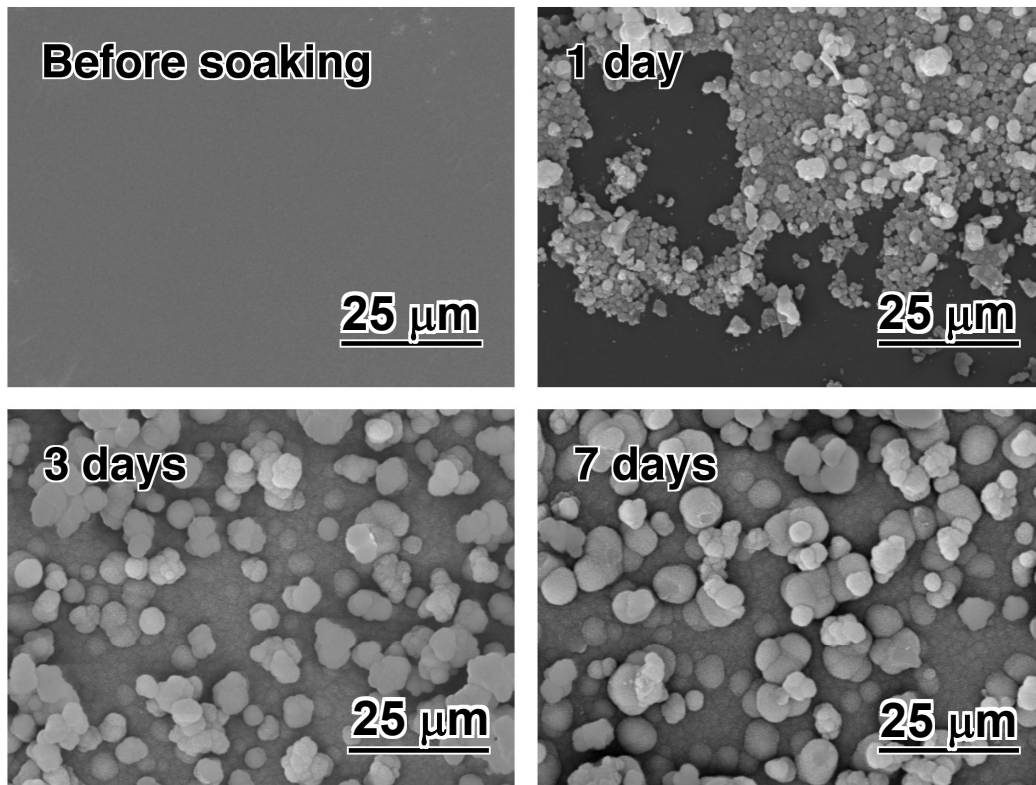


Figure 1-5(f). SEM images of surfaces of S(0.5)Ca(40) films before and after soaking in 1.5SBBF for various periods.

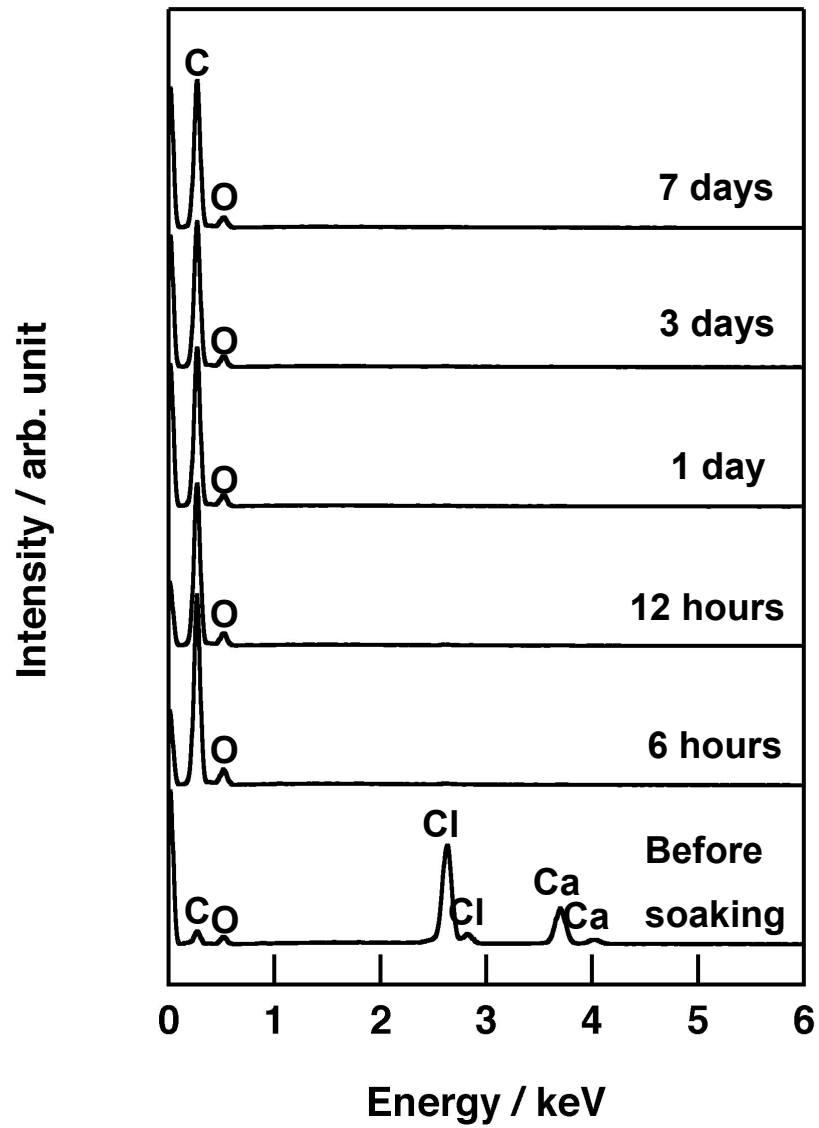


Figure 1-6(a). EDX spectra of S(0)Ca(40) films before and after soaking in 1.5SBF for various periods.

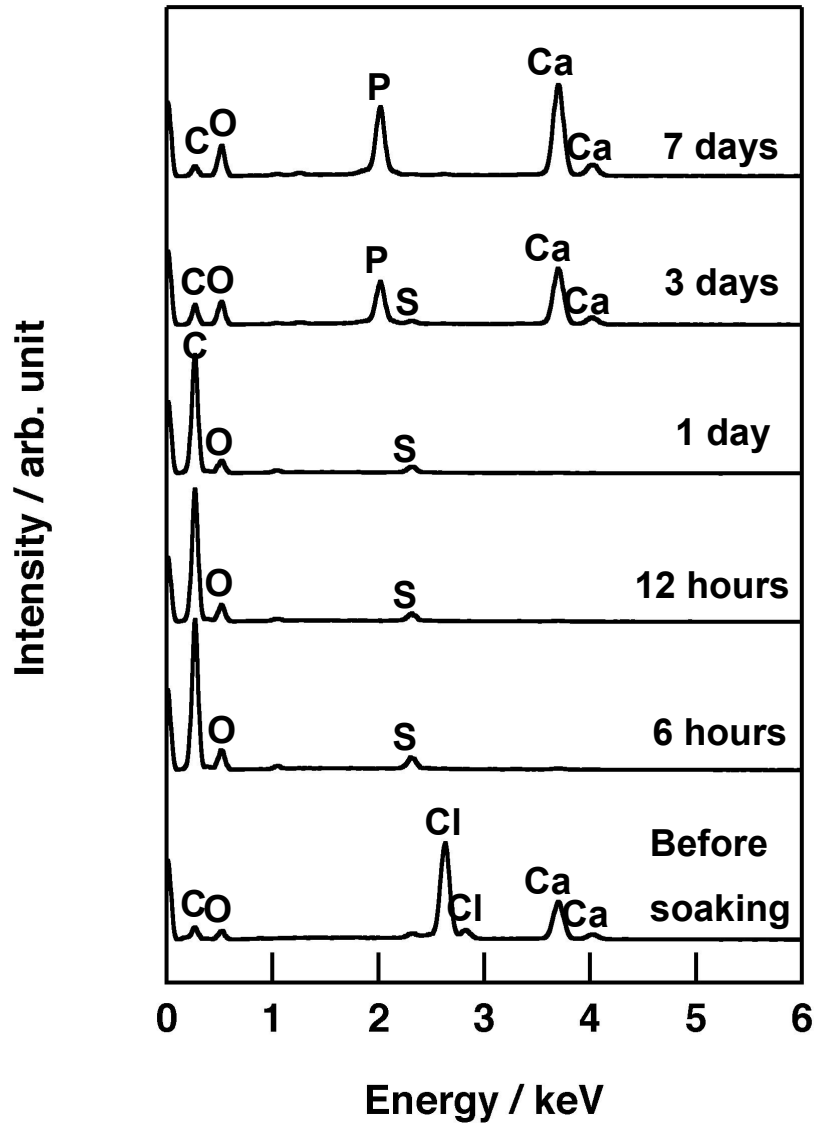


Figure 1-6(b). EDX spectra of S(0.2)Ca(40) films before and after soaking in 1.5SBF for various periods.

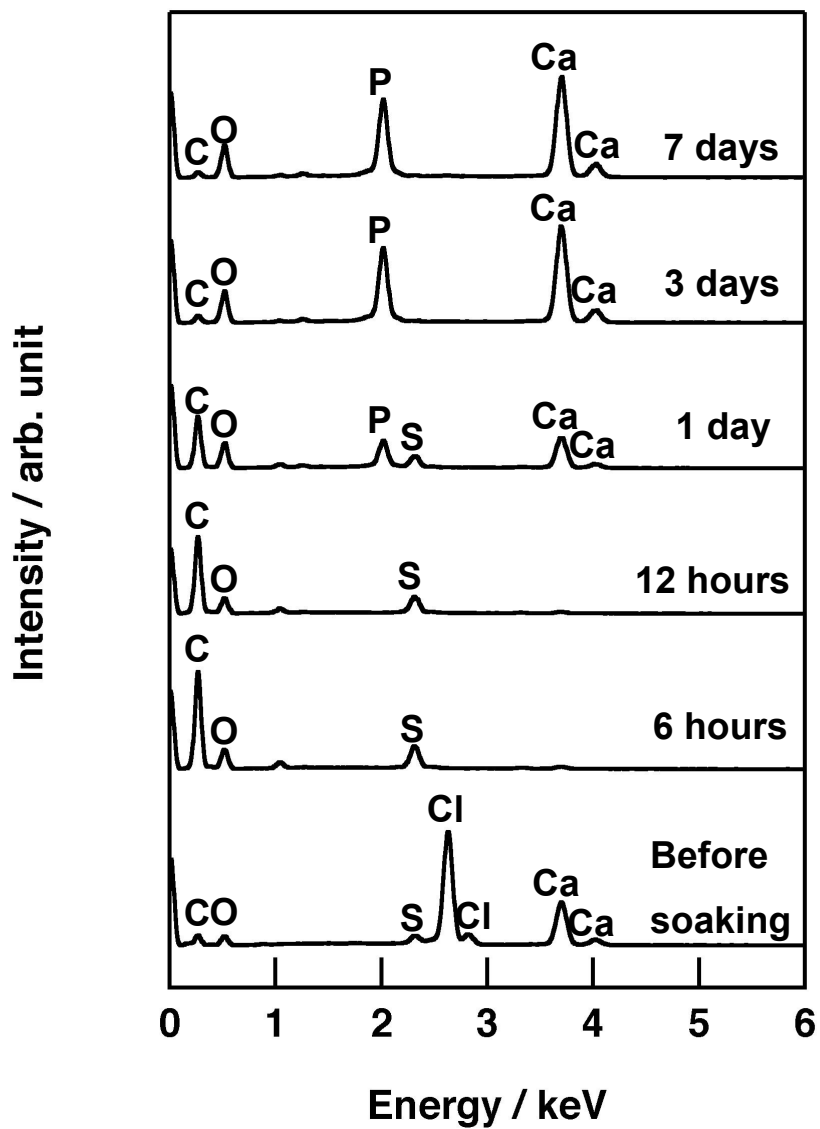


Figure 1-6(c). EDX spectra of S(0.5)Ca(40) films before and after soaking in 1.5SBF for various periods.

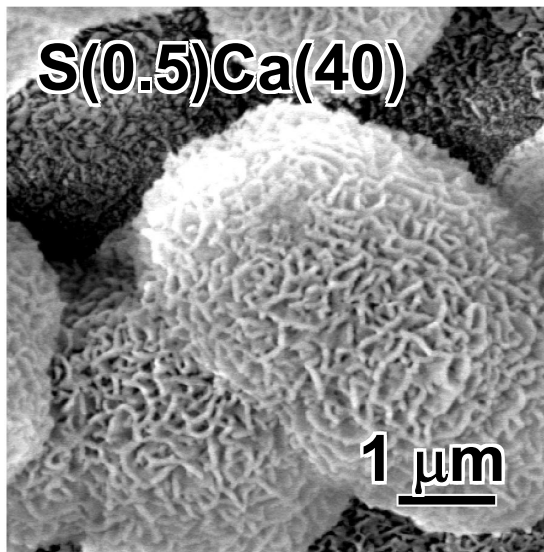
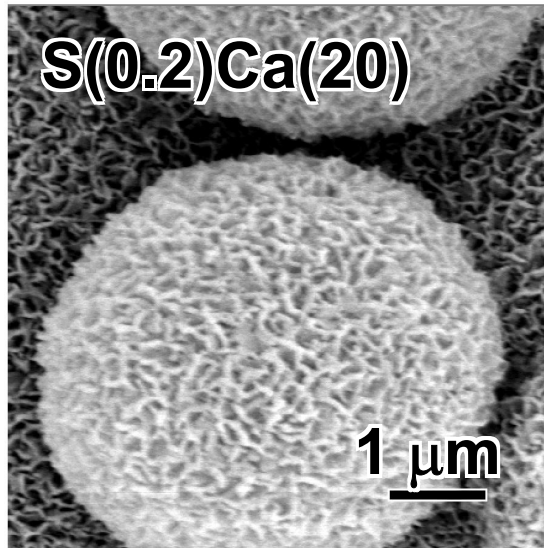


Figure 1-7. FE-SEM images of surfaces of S(0.2)Ca(40) and S(0.5)Ca(40) films after soaking in 1.5SBF for 7 days.

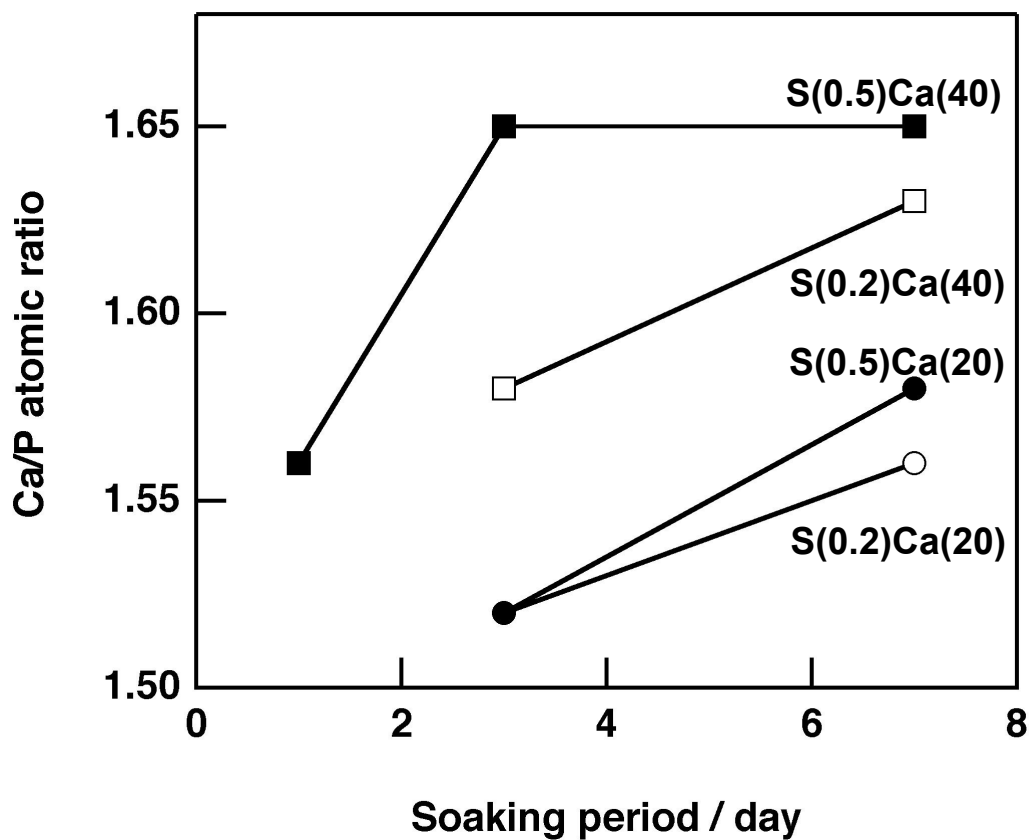


Figure 1-8. Ca/P atomic ratio of the surfaces of various kinds of films after soaking in 1.5SBF. The atomic ratio was determined by EDX analyses.

Chapter 2: Coating of a hydroxyapatite layer on polyamide films containing silanol groups

2.1. Introduction

Hydroxyapatite-polymer hybrids have attractive features as candidates for novel bone substitutes because they may show bone-bonding ability and mechanical performances derived from the organic substrate. As a method for fabrication of such a hybrid, Kokubo *et al.* proposed biomimetic process that induces hydroxyapatite formation on the surfaces of organic substrates at ambient conditions in a simulated body fluid (SBF) with ion concentrations similar to those of human extracellular fluid, or related solutions supersaturated with respect to the apatite [1,2]. In this process, apatite nucleation is induced by a local increase in concentrations of calcium and silicate ions around the surface of the substrates due to dissolution of a bioactive glass placed in the vicinity of the substrate under SBF conditions. Locally increased concentration of silicate ions produced heterogeneous nucleation sites for hydroxyapatite because heterogeneous nucleation of apatite can be triggered by specific functional groups, including -SiOH groups [3,4] and release of calcium ions (Ca^{2+}) from the materials accelerates apatite nucleation by an increase in the degree of supersaturation of the fluid with respect to apatite [5]. It was reported that carboxyl (-COOH) group is effective in apatite nucleation under biomimetic conditions [6]. Miyazaki *et al.* reported that polyamide films containing carboxyl (-COOH) groups can deposit hydroxyapatite on their surfaces after exposure to 1.5SBF with ion concentrations 1.5 times those of SBF, when they contain calcium chloride [7]. In Chapter 1, it was revealed that sulfonic groups (-SO₃H) are effective for apatite nucleation under the biomimetic condition as well. In contrast, it has been revealed that silanol groups are highly effective for induction of hydroxyapatite formation, according to reported studies of silica gels [3,4]. Recently, modification of organic polymer with

silanol groups in combination with calcium salts was attempted to achieve bioactivity and flexibility. Actually, organically modified silicates and related hybrids can acquire deposits of bone-like apatite after soaking in SBF [8-12]. Therefore, modification of aromatic polyamide with silanol groups is expected to enhance hydroxyapatite formation in a biomimetic solution. However, how modification with silanol groups influences ability of hydroxyapatite formation on the polymer substrate and adhesive strength between polymer and hydroxyapatite is not yet known. In this chapter, polyamide containing carboxyl groups was modified with silanol groups and calcium chloride. Its hydroxyapatite-forming ability was investigated in 1.5SBF and compared with polyamide containing unmodified carboxyl groups.

2.2. Experimental

2.2.1. Preparation of polyamide films containing silanol groups

One gram of aromatic polyamide containing -COOH in the polymer molecule, as shown in Figure 2-1 [13], was dissolved in 10 mL of N,N-dimethylacetamide (Wako Pure Chemical Industries Ltd., Japan). 3-aminopropyltriethoxysilane (APES: Chisso Co. Ltd., Japan), 1-ethyl-3-(3-dimethyl-aminopropyl)-carbodiimide (EDC·HCl: Peptide Institute Inc., Japan), 1-hydroxysuccinimide (HOSu: Peptide Institute Inc., Japan) and N,N-diisopropylethylamine (DIPEA: Applied Biosystems Japan Ltd., Japan) were added into the solution under the feed conditions listed in Table 2-1 to obtain polyamide Si(x). 'x' indicates the number of silicon atoms included in fed APES to two amide bonds (x = 0, 0.25 and 0.5). The structural formula is given in Figure 2-1. A 40 mass% of CaCl₂ (Nacalai Tesque Inc., Japan) against the (polyamide + CaCl₂) was then added to the solution. The solution was stirred for 24 h, and then coated on flat glass plates with a bar coater. The solution coated on the glass plate was kept for drying in a vacuum oven at 60°C under 133 Pa for 8 h. The obtained polymer films were removed from the glass plates and cut into 10 mm × 10 mm specimens.

2.2.2. Soaking in 1.5SBF

The obtained films were then soaked in 30 mL of 1.5SBF (Na^+ 213.0, K^+ 7.5, Mg^{2+} 2.3, Ca^{2+} 3.8, Cl^- 221.7, HCO_3^- 6.3, HPO_4^{2-} 1.5, and SO_4^{2-} 0.8 $\text{mol}\cdot\text{m}^{-3}$, pH 7.40) at 36.5°C for various periods. The solution was prepared by dissolving reagent grade chemicals of NaCl, NaHCO₃, KCl, K₂HPO₄·3H₂O, MgCl₂·6H₂O, CaCl₂, and Na₂SO₄ (Nacalai Tesque Inc., Japan) in ultrapure water [2,14]. The pH of the solution was buffered at 7.40 using 75 $\text{mol}\cdot\text{m}^{-3}$ of tris(hydroxymethyl)aminomethane (Nacalai Tesque Inc., Japan) along with an appropriate volume of 1 $\text{kmol}\cdot\text{m}^{-3}$ hydrochloric acid solution. The temperature of the solution was kept at 36.5°C. After soaking for given periods, the films were taken out from the solution, washed with ultrapure water, and then dried at room temperature.

2.2.3. Characterization

The surfaces of the films were characterized by scanning electron microscopy (SEM: S-3500N, Hitachi, Ltd., Japan), energy dispersive X-ray (EDX: EMAX ENERGY EX-400, Horiba, Ltd., Japan) spectroscopic analysis and thin-film X-ray diffraction (TF-XRD: MXP3V, MAC Science Co., Ltd., Japan), before and after soaking in 1.5SBF. In the SEM observations, a thin Au film was sputtered onto the surface of the specimen. In the TF-XRD measurements, the angle of the incident beam was fixed at 1° against the surface of the specimen. Morphological observation at higher magnification was conducted for typical specimens under field emission scanning electron microscope (FE-SEM: S-4800N Hitachi Ltd., Japan). The interface between Si(0) film and the hydroxyapatite formed on the film after soaking in 1.5SBF was observed using a transmission electron microscope (TEM; JEM2010, JEOL Ltd., Japan).

2.3. Results

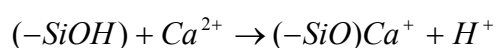
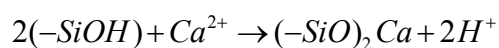
Figure 2-2 shows TF-XRD patterns of the surfaces of Si(x) (x = 0, 0.25 and 0.5) before and after soaking in 1.5SBF for various periods. Diffraction peaks assigned to apatite were detected in each specimen after soaking for 2 days. The tendency of the apatite formation on the polyamide film after exposure to 1.5SBF is summarized in Table 2-2, on the basis of the results of TF-XRD. Even when apatite was not detected by TF-XRD, the films containing silanol groups looked opaque after soaking in 1.5SBF even for 1 day. This result suggests that hydroxyapatite had been formed on the films containing silanol groups even after 1 day of soaking in 1.5SBF. Figure 2-3 shows SEM photographs of the surfaces of Si(x) (x = 0, 0.25 and 0.5) before and after soaking in 1.5SBF for various periods. Spherical particles were found to deposit on the surface for Si(0.25) and Si(0.5) within 12 h, whereas this took 2 days for Si(0). The tendency of the adhesive strength of the hydroxyapatite layer on the polyamide film to decrease with increased content of Si was suggested because the layer was easily peeled off under SEM. Figure 2-4 shows EDX spectra of the surfaces of Si(x) (x = 0, 0.25 and 0.5) before and after soaking in 1.5SBF for various periods. Peaks assigned to calcium and phosphorus were detected in the spectra of Si(0.25) and Si(0.5) within 12 h, while this took 2 days for Si(0). These data indicate that calcium phosphate (implying apatite) was formed on the surfaces of Si(0.25) and Si(0.5) within 12 h, and 2 days for Si(0). No peak assigned to apatite was detected in TF-XRD patterns of Si(0.25) and Si(0.5) after soaking 12 h despite of the existence of calcium and phosphorus. The particles initially precipitated on the film might have low crystallinity or their amount might be too small to be detected by TF-XRD. It can be seen from the SEM photographs and EDX spectra that the rate of apatite formation increases with increasing silanol group content in the polyamide films. Figure 2-5 shows morphology of the deposited particles on Si(0), Si(0.25) and Si(0.5) films after soaking in 1.5SBF for 2 days, at higher magnification under FE-SEM. This morphology was very similar to that of the deposited hydroxyapatite on a substrate through biomimetic processing utilizing SBF [2] and their

appearance is similar. This means that the bone-like apatite layer formed on the polyamide film containing silanol groups as well as carboxyl groups, and the morphology is similar independent of the kind of functional groups and silanol group content. Figure 2-6 shows the TEM image of the interface between Si(0) film and hydroxyapatite formed on the film after soaking in 1.5SBF for 7 days. It was observed that nano-sized fibers are intricately intertwined into Si(0) film, as shown in an area surrounded by a dotted frame.

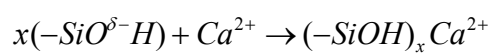
2.4. Discussion

It is apparent from the results described above that polyamide containing silanol groups showed a high capacity for hydroxyapatite formation on its surface when it contained calcium chloride, and its hydroxyapatite-forming ability appears greater than that of carboxyl groups. These results indicate that silanol groups could accelerate the hydroxyapatite formation. Substitution of carboxyl groups with silanol groups enhanced the heterogeneous nucleation on the surface of the polyamide. This means that modification with silanol groups caused increasing numbers of sites for heterogeneous nucleation of apatite on the surface of polyamide films. However, the deposited hydroxyapatite was more easily peeled off from Si(0.5) film than Si(0.25), especially the films soaked for 1 and 2 days, as seen in Figure 2-2. In contrast, hydroxyapatite deposited on Si(0) had hardly peeled off from the film. The adhesion strength between the deposited hydroxyapatite and polyamide film also depends on the types of the functional groups in the polyamide films. It is assumed that silanol groups show higher potential in induction of apatite nucleation than carboxyl groups in 1.5SBF. Almost 99% of carboxyl groups dissociate to be -COO^- , while 0.4 % of silanol groups dissociate to be $\text{-Si(OH)}_2\text{O}^-$ at pH 7.4. Almost no dissociation to $\text{-Si(OH)(O}^-)_2$, and $\text{-Si(O}^-)_3$ occurs in such a solution. From this assumption, modification of carboxyl groups with silanol groups makes access of the groups by calcium ions difficult. On the other hand, calcium

ions can be easily adsorbed to silanol groups to form Si-O-Ca bonds [15]. The electronegativity of silicon is lower than that of carbon. This may enable calcium ions to access near lone pairs of oxygen atoms in silanol groups in a dipole interaction. Moreover, one APES molecule consumes one carboxyl group and then provides three silanol groups. The modification of polyamide with APES increases the total content of functional groups. One unit of the silanol groups possesses six lone electron-pairs, while one carboxyl group has five in physiological conditions. This may also have contributed to easier access of calcium ions to the integrated silanol groups than that to carboxyl groups. Thus -SiOH groups react with calcium ions around pH 7 as shown the formulae below,



or



to form silicate complexes and then these complexes induce nuclei of apatite.

There appeared lower adhesive strength of the hydroxyapatite layer with polymer substrate containing silanol groups than that with polymer substrate containing carboxyl groups. The weak strength may be attributed to less interaction between the functional groups and Ca^{2+} ions. It is therefore assumed that the formation of $(-SiOH)_xCa^{2+}$ complex at the nucleation stage. A possible explanation is that increasing content of -SiOH causes the polyamide to swell readily in 1.5SBF and to show a high degree of shrinkage after drying, resulting in low adhesion of the film surface to hydroxyapatite. Therefore, the adhesive strength seems to be governed not only by a chemical interaction of functional groups with Ca^{2+} , but also by the mechanical property of the polyamide film itself. Actually, from the observation of the cross-section between a polyamide film containing carboxyl groups and hydroxyapatite formed on the film surface by TEM observation, the interface was found to be constructed by an

intertwining structure (see Figure 2-6). These factors are assumed to act together to form an hydroxyapatite layer with high adhesion strength against the surface of the polyamide. These findings show well that modification of organic polymers with the functional groups induces hydroxyapatite deposition, and also determines the adhesive strength of hydroxyapatite layer to the organic substrates.

2.5. Conclusions

Hydroxyapatite formation on aromatic polyamides was accelerated by modification with silanol groups. Modification of polyamide film with silanol groups accelerates the rate of apatite nucleation but decrease the adhesive strength of the formed hydroxyapatite layer with the substrates. Appropriate amount of silanol groups and calcium chloride can lead to fabrication of a new hydroxyapatite-polymer hybrid under biomimetic process using physiological solutions.

References

1. Abe Y, Kokubo T, Yamamuro T. Apatite coating on ceramics, metals and polymers utilizing a biological process. *J Mater Sci Mater Med* 1990;1:233-238.
2. Tanahashi M, Yao T, Kokubo T, Minoda M, Miyamoto T, Nakamura T, Yamamuro T. Apatite coating on organic polymers by a biomimetic process. *J Am Ceram Soc* 1994;77:2805-2808.
3. Li P, Ohtsuki C, Kokubo T, Nakanishi K, Soga N, Nakamura T, Yamamuro T. Apatite formation induced by silica gel in a simulated body fluid. *J Am Ceram Soc* 1992;75:2094-2097.
4. Li P, Ohtsuki C, Kokubo T, Nakanishi K, Soga N, Nakamura T, Yamamuro T. Effects of ion in aqueous media on hydroxyapatite induction by silica gel and its relevance to bioactivity of bioactive glasses and glass-ceramics. *J Appl Biomater* 1993;4:221-229.
5. Ohtsuki C, Kokubo T, Yamamuro T. Mechanism of apatite formation on CaO-SiO₂-P₂O₅ glasses in a simulated body fluid. *J Non-Cryst Solids* 1992;143:84-92.
6. Tanahashi M, Matsuda T. Surface functional group dependence on apatite formation on self-assembled monolayers in a simulated body fluid. *J Biomed Mater Res* 1997;34:305-315.
7. Miyazaki T, Ohtsuki C, Akioka Y, Tanihara M, Nakao J, Sakaguchi Y, Konagaya S. Apatite deposition on polyamide film containing carboxyl group in a biomimetic solution. *J Mater Sci Mater Med* 2003;14:569-574.
8. Tsuru K, Ohtsuki C, Osaka A, Iwamoto T, Mackenzie JD. Bioactivity of sol-gel derived organically modified silicates. *J Mater Sci Mater Med* 1997;8:157-161.
9. Tsuru K, Hayakawa S, Ohtsuki C, Osaka A. Bioactive gel coatings derived from vinyltrimethoxysilane. *J Sol-Gel Sci Tech* 1998;13:237-240.

10. Yabuta T, Tsuru K, Hayakawa S, Ohtsuki C, Osaka A. Synthesis of bioactive organic-inorganic hybrids with γ -methacryloxypropyltrimethoxysilane. *J Sol-Gel Sci Tech* 2000;19:745-748.
11. Kamitakahara M, Kawashita M, Miyata N, Kokubo T, Nakamura T. Bioactivity and mechanical properties of polydimethylsiloxane(PDMS)-CaO-SiO₂ hybrids with different PDMS contents. *J Sol-Gel Sci Tech* 2001;21:75-81.
12. Kamitakahara M, Kawashita M, Miyata N, Kokubo T, Nakamura T. Bioactivity and mechanical properties of polydimethylsiloxane(PDMS)-CaO-SiO₂ hybrids with different calcium contents. *J Mater Sci Mater Med* 2002;13:1015-1020.
13. Konagaya S, Tokai M. Synthesis of ternary copolyamides from aromatic diamine with carboxyl or sulfonic group (3,5-diaminobenzoic acid, 2,4-diaminobenzenesulfonic acid), and iso- or terephthaloyl chloride. *J Appl Polym Sci* 2000;76:913-920.
14. Ohtsuki C, Kokubo T, Neo M, Kotani S, Yamamuro T, Nakamura T, Bando Y. Bone-bonding mechanism of sintered β -3CaO·P₂O₅. *Phosphorus Res Bull* 1991;1:191-196.
15. Iler RK, In: *The chemistry of silica*. New York: John Wiley & Sons; 1979. p. 667.

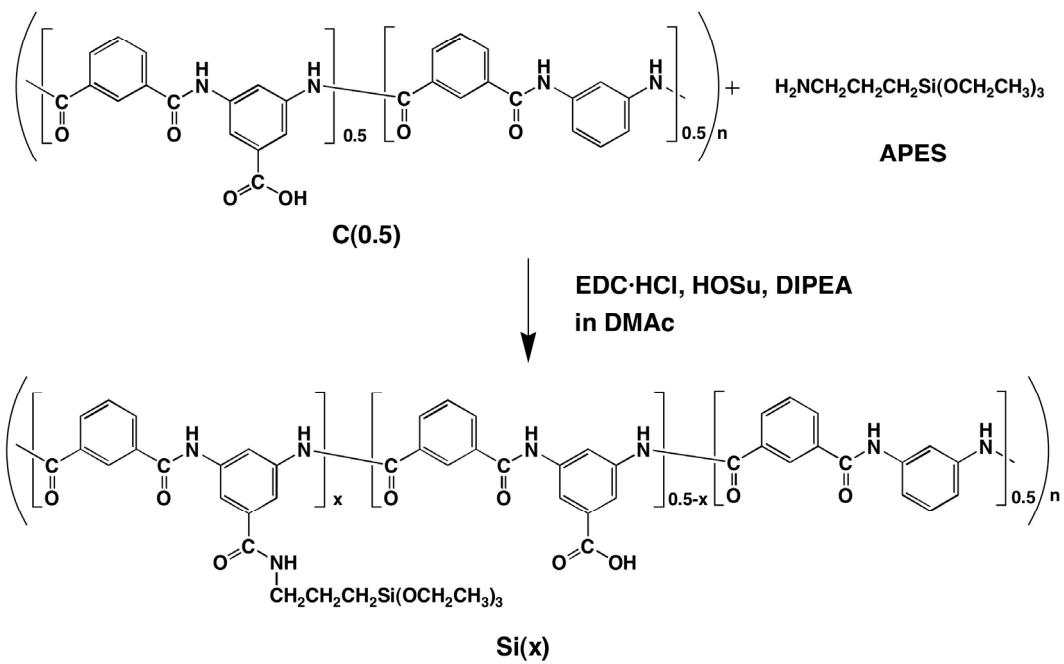


Figure 2-1. Modification of C(0.5) with APES to synthesize Si(x).

Table 2-1 Reagents used to synthesize polyamides containing -SiOH groups

Specimen	Reagent			
	APES / mL	HOSu / g	DIPEA / mL	EDC·HCl / g
Si(0)	0	0	0	0
Si(0.25)	0.24	0.26	0.4	0.4
Si(0.5)	0.46	0.26	0.4	0.4

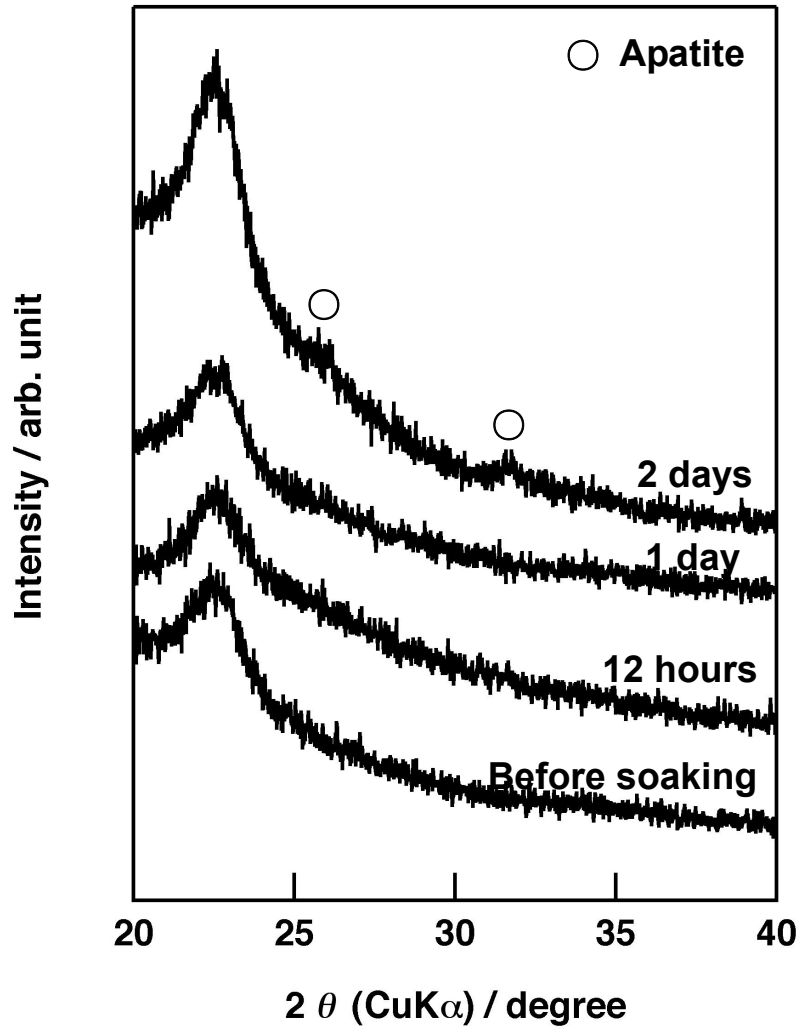


Figure 2-2(a). TF-XRD patterns of surfaces of Si(0) films before and after soaking in 1.5SBF for various periods.

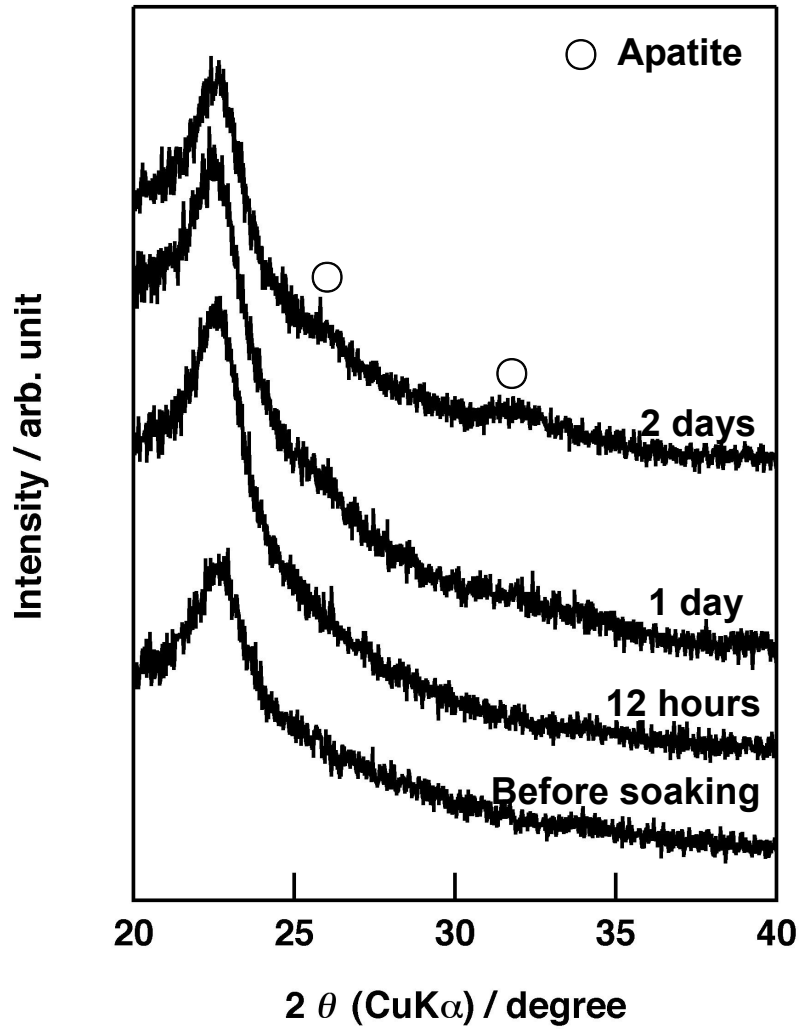


Figure 2-2(b). TF-XRD patterns of surfaces of Si(0.25) films before and after soaking in 1.5SBF for various periods.

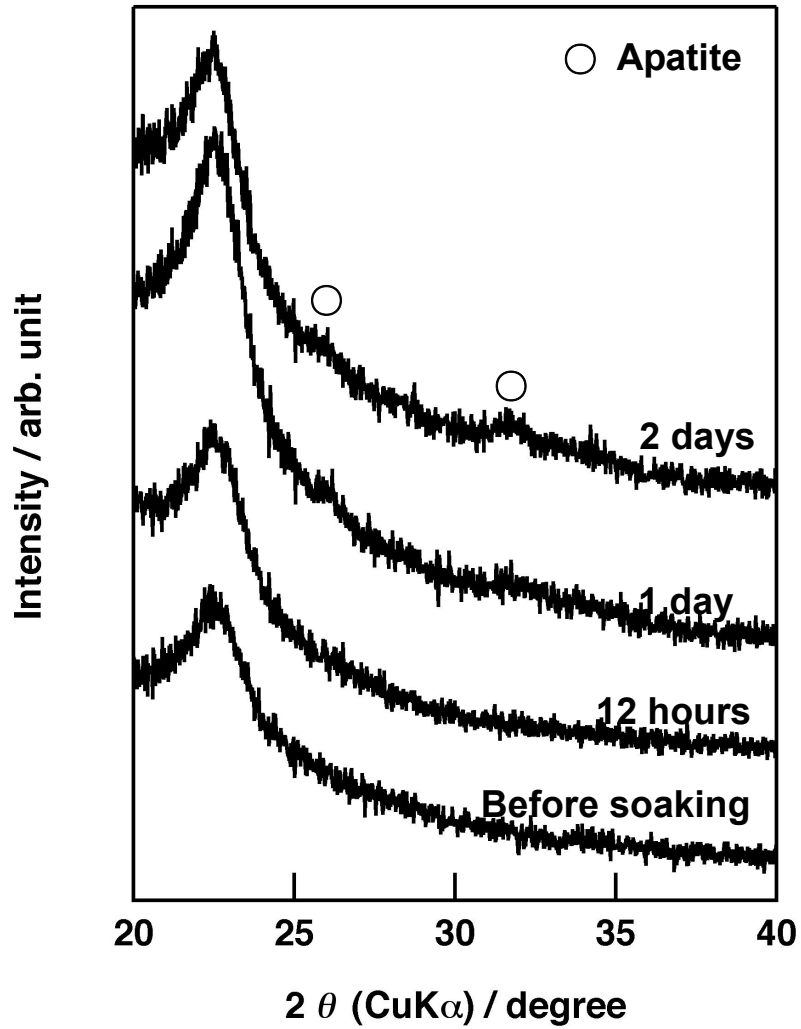


Figure 2-2(c). TF-XRD patterns of surfaces of Si(0.5) films before and after soaking in 1.5SBF for various periods.

Table 2-2 Tendency of apatite formation evaluated by TF-XRD

Specimen	Soaking period		
	12 h	1 d	2 d
Si(0)	-	-	+
Si(0.25)	-	-	+
Si(0.5)	-	-	+

Apatite was formed (+), not formed (-)

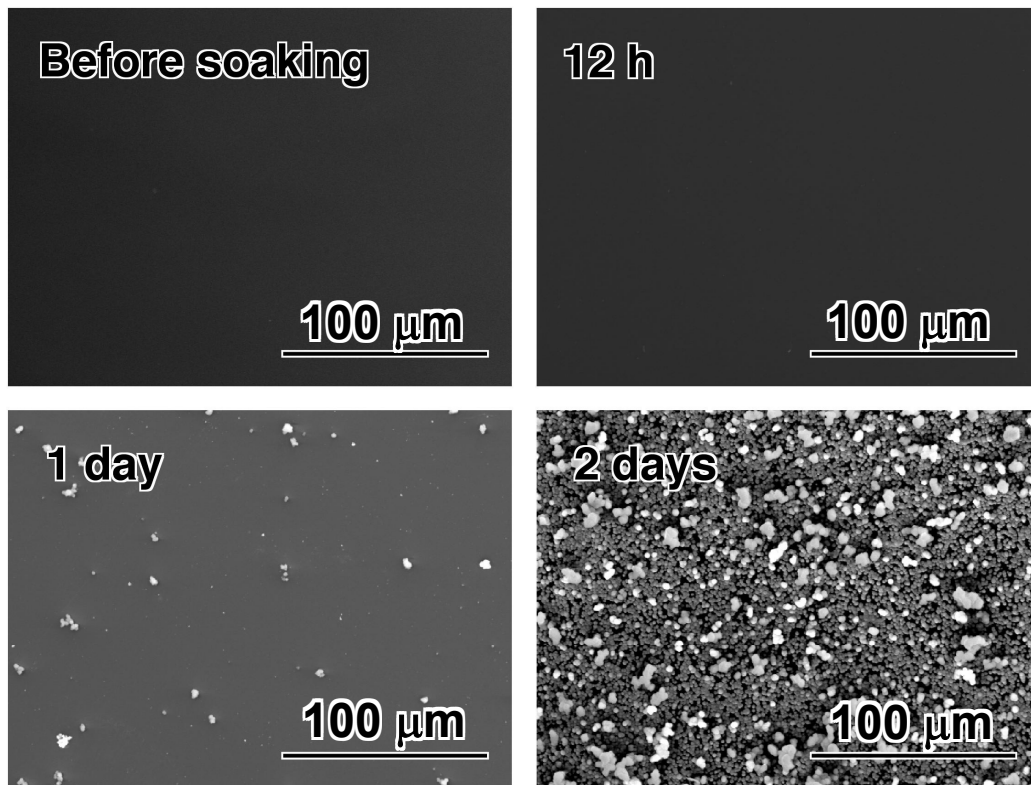


Figure 2-3(a). SEM images of surfaces of Si(0) films before and after soaking in 1.5SBF for various periods.

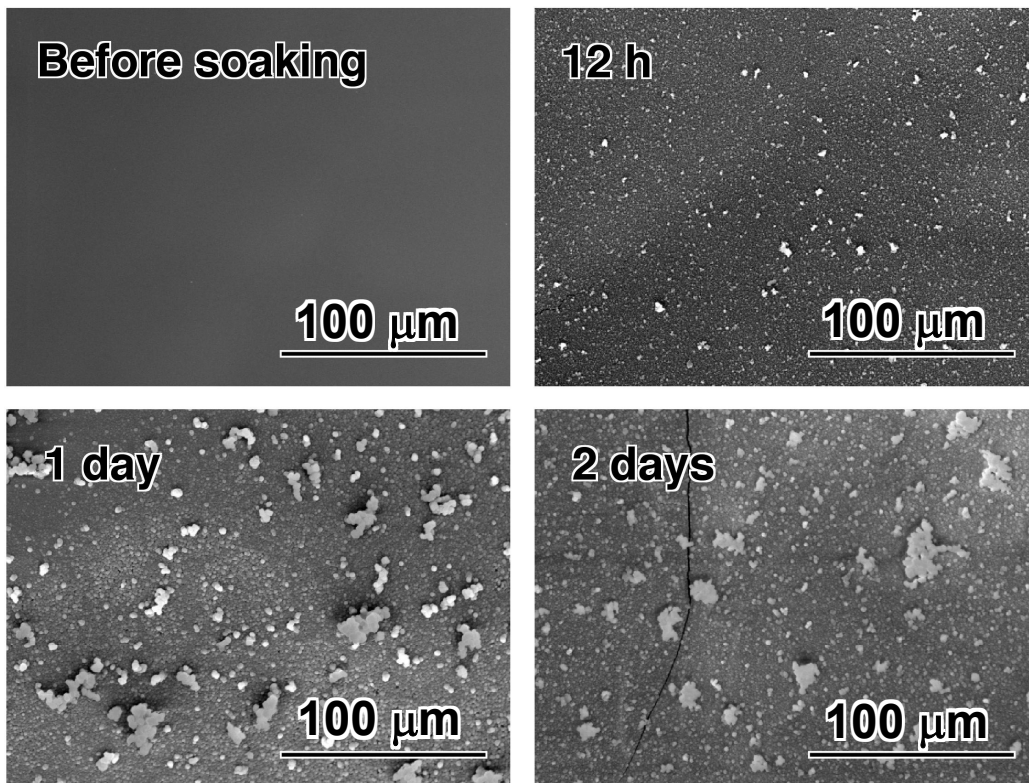


Figure 2-3(b). SEM images of surfaces of Si(0.25) films before and after soaking in 1.5SBF for various periods.

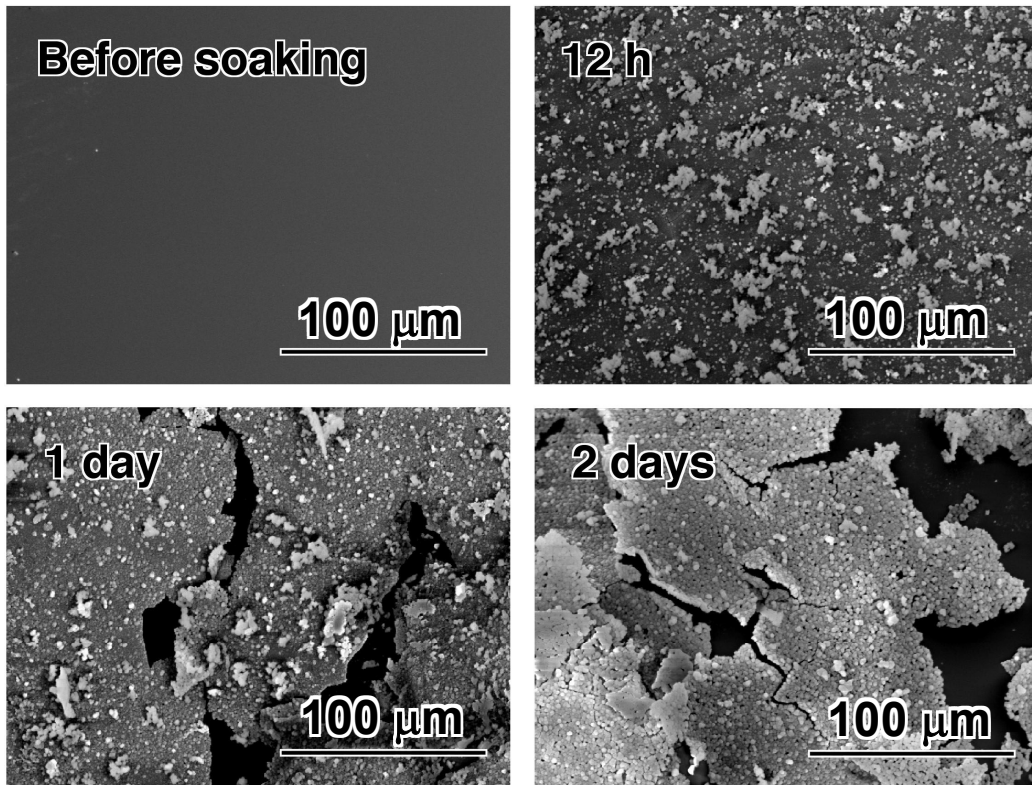


Figure 2-3(c). SEM images of surfaces of Si(0.5) films before and after soaking in 1.5SBF for various periods.

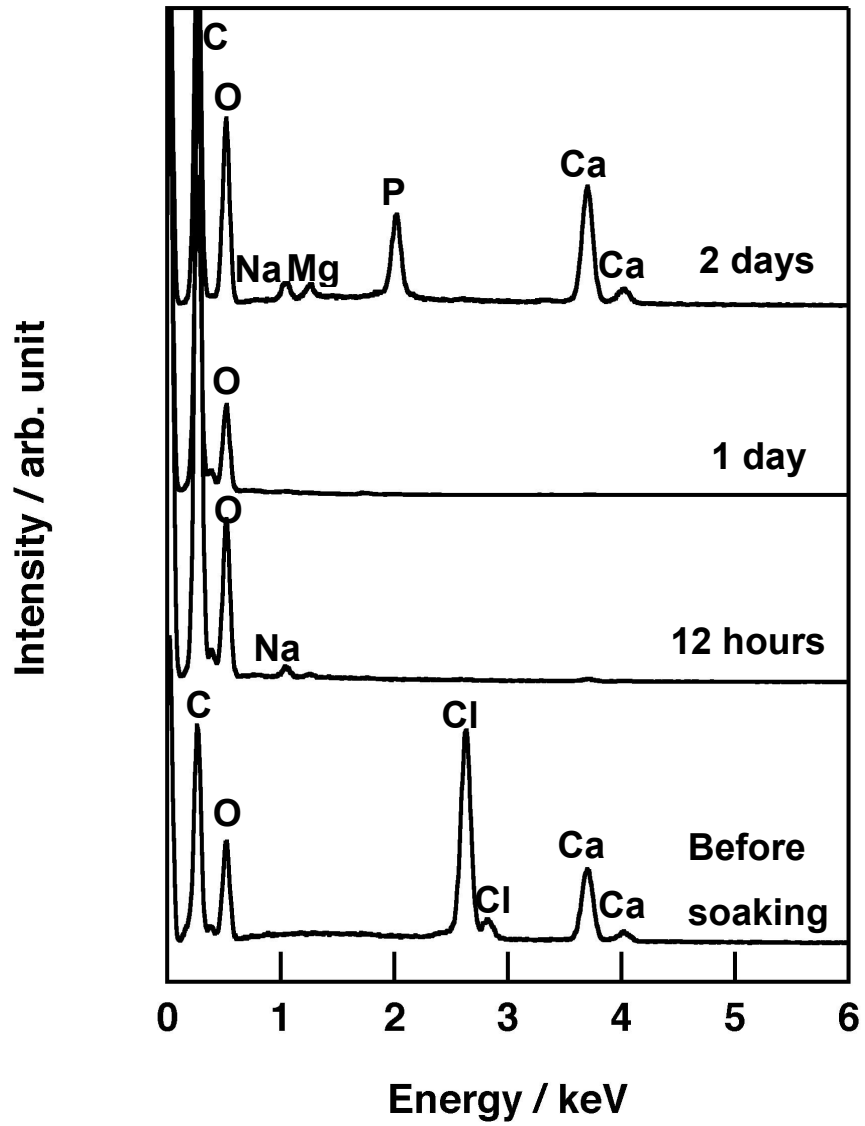


Figure 2-4(a). EDX spectra of Si(0) films before and after soaking in 1.5SBF for various periods.

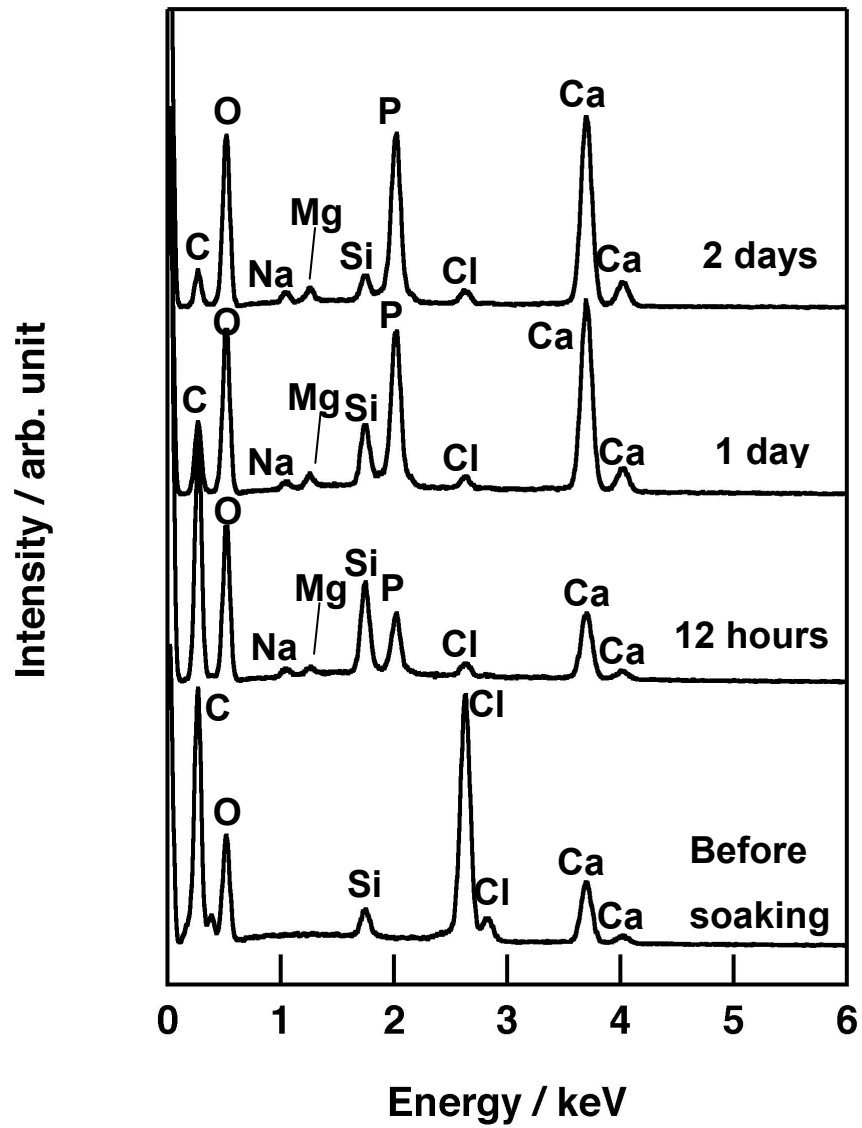


Figure 2-4(b). EDX spectra of Si(0.25) films before and after soaking in 1.5SBF for various periods.

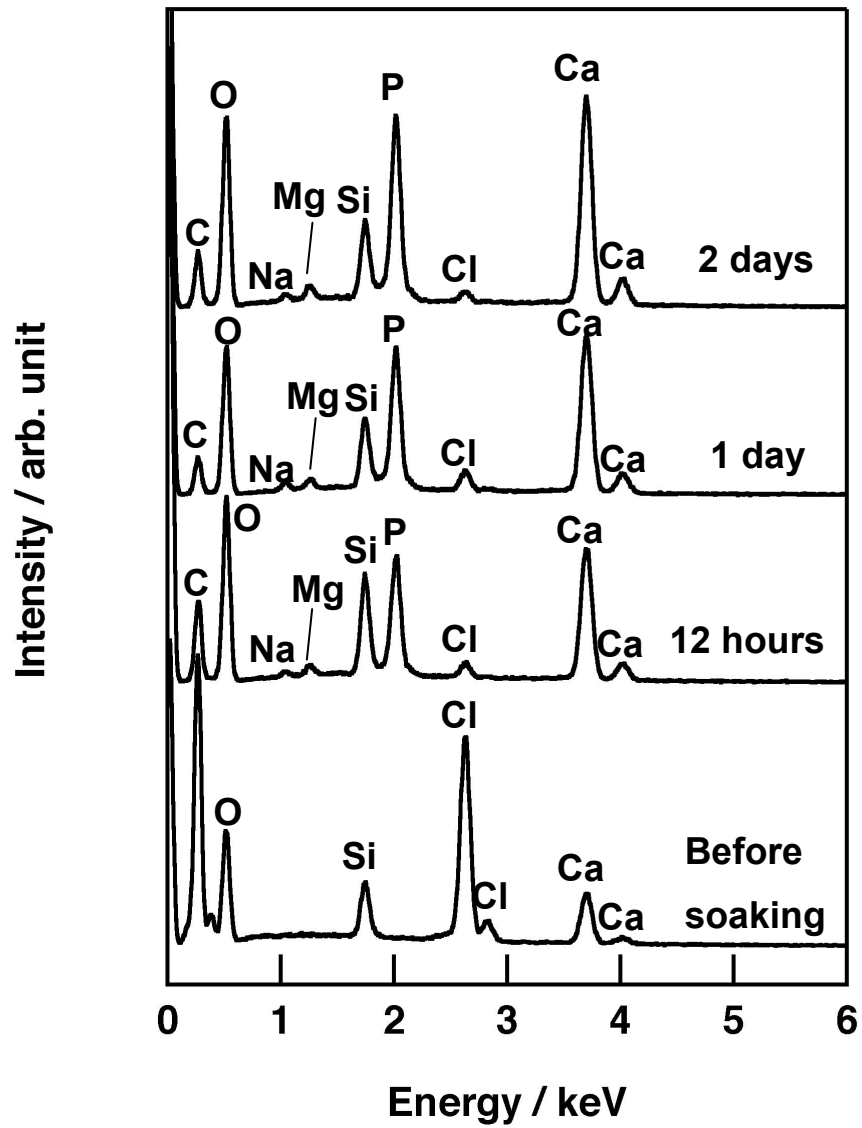


Figure 2-4(c). EDX spectra of Si(0.5) films before and after soaking in 1.5SBF for various periods.

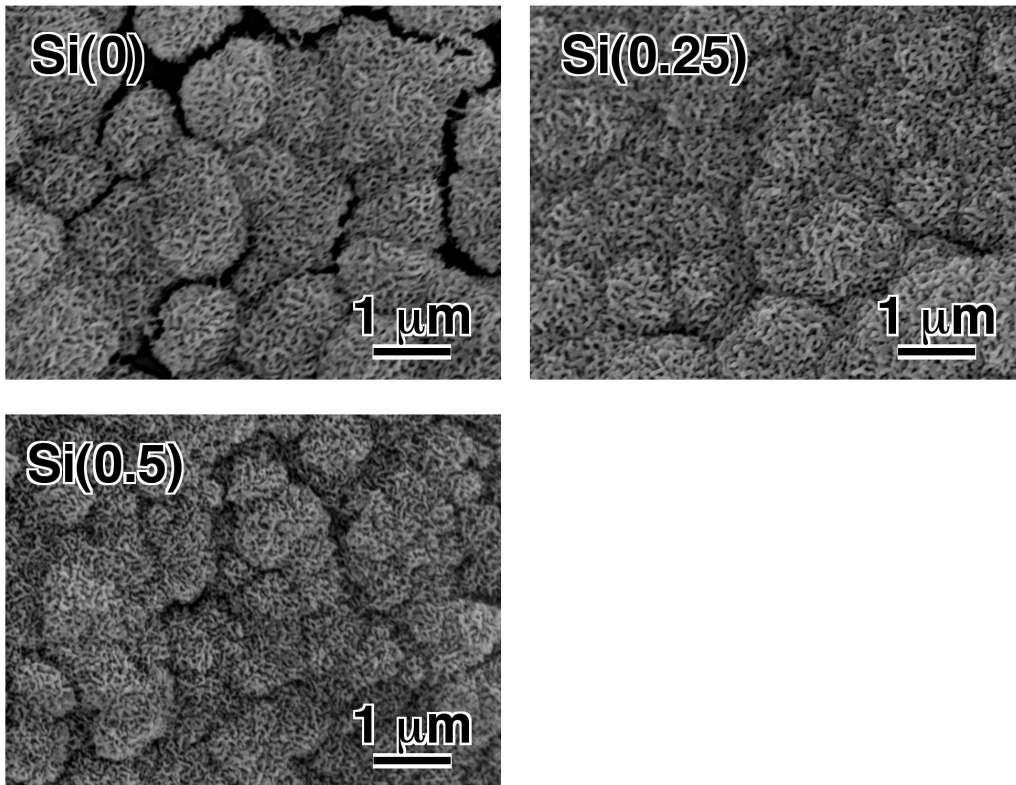


Figure 2-5. FE-SEM images of surfaces of Si(0), Si(0.25) and Si(0.5) films after soaking in 1.5SBF for 2 days.

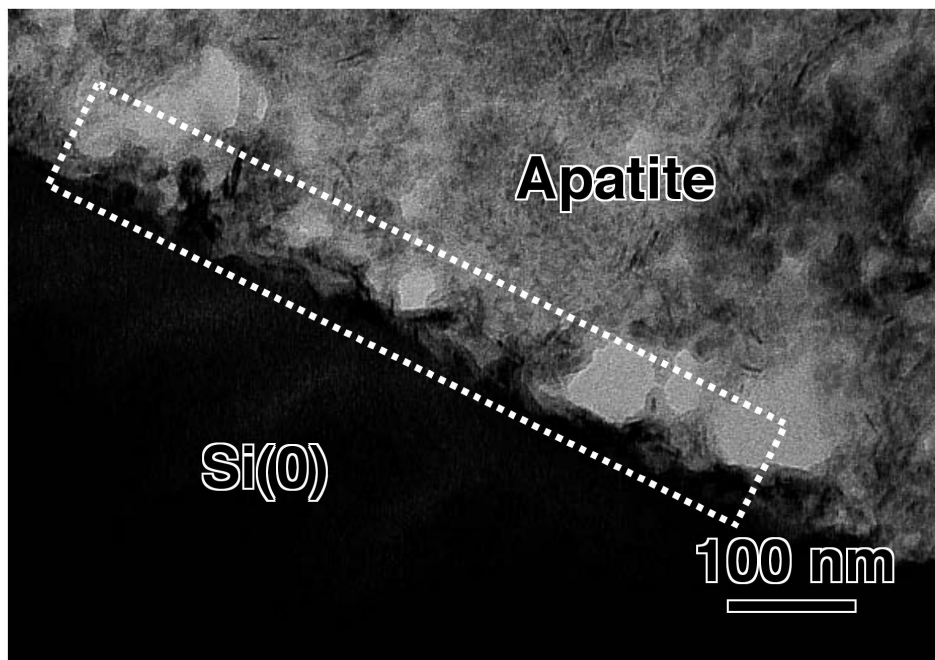


Figure 2-6. TEM image of interface between Si(0) film and apatite formed on the film after soaking in 1.5SBF for 7 days.

Chapter 3: Comparative study of induction of nucleation, crystal growth and adhesive strength of hydroxyapatite formed on polyamide films with different functional groups

3.1. Introduction

Hydroxyapatite-polymer hybrids have attractive features as a candidate for novel bone substitutes because they may show bone-bonding ability and mechanical performances derived from organic substrate. As a method for fabrication of such a hybrid, Kokubo *et al.* proposed biomimetic process that induces the hydroxyapatite formation on the surfaces of organic substrates at ambient conditions in a simulated body fluid (SBF) with ion concentrations similar to those of human extracellular fluid, or related solutions supersaturated with respect to apatite [1]. In this process, heterogeneous nucleation of apatite is triggered by specific functional groups [2-4]. This nucleation of apatite is enhanced by release of calcium ions (Ca^{2+}) from the materials, which increases degree of supersaturation of surrounding fluid with respect to apatite [5,6]. Miyazaki *et al.* reported that polyamide films containing carboxyl (-COOH) groups deposit hydroxyapatite on their surfaces after exposure to 1.5SBF with ion concentrations 1.5 times those of SBF, when they contain calcium chloride [7]. In Chapters 1 and 2, it is shown that modification of aromatic polyamide with sulfonic (-SO₃H) or silanol (-SiOH) groups also enhance heterogeneous nucleation of apatite on the polymer substrates in a solution that mimics body environment, i.e. in 1.5SBF. To understand the fundamental phenomena through an induction of hydroxyapatite formation by certain kinds of functional groups, a comparative study among these functional groups is informative. To compare the nucleation and crystal growth process of the hydroxyapatite on the polymer substrates, aromatic polyamides containing carboxyl groups or sulfonic groups are examined in this chapter because hydroxyapatite can be coated on these polyamide films with enough adhesive strength to be

experimentally evaluated. Preliminary evaluation of the adhesive strength of hydroxyapatite layer formed on some types of polyamide films showed that the adhesive strength of hydroxyapatite layer on the films modified with silanol groups and phosphate groups was not high enough to be examined on the comparison, unfortunately. Therefore, induction period of hydroxyapatite formation, the rate of crystal growth, and adhesive strength were compared using the polyamide films containing carboxyl or sulfonic groups in 1.5SBF.

3.2. Experimental

3.2.1. Preparation of polyamide film

One gram of aromatic polyamide, containing carboxyl groups (C(0.5)) or sulfonic groups (S(0.5)), as shown in Figure 3-1 [8], was dissolved in 10 mL of N,N-dimethylacetamide (Wako Pure Chemical Industries Ltd., Japan) together with 0.67 g of CaCl₂ (Nacalai Tesque Inc., Japan). The mixture was stirred for 24 h to obtain a homogenous solution. The solution was coated on a glass plate by a bar coater and dried under 133 Pa at 60°C for 8 h to obtain a film. The formed film was removed from the glass plate and cut into specimens 10 mm × 10 mm in size.

3.2.2. Soaking in 1.5SBF

The film was soaked in 30 mL of 1.5SBF (Na⁺ 213.0, K⁺ 7.5, Mg²⁺ 2.3, Ca²⁺ 3.8, Cl⁻ 221.7, HCO₃⁻ 6.3, HPO₄²⁻ 1.5, and SO₄²⁻ 0.8 mol·m⁻³, pH7.40), whose ion concentrations are 1.5 times of those of a simulated body fluid (SBF) [1,9], for various periods under shaking at 120 strokes·min⁻¹ (3 cm in stroke length) using a water bath shaker (Personal Lt-10F, TITEC, Japan) at 36.5°C. After soaking for a given period, the film was taken out from the solution and gently washed with ultrapure water.

3.2.3. Measurement of amount of hydroxyapatite formed on film and residual

components in 1.5SBF

The weight of the hydroxyapatite formed on the film was measured. This was calculated by the differences between the total weight of the film after soaking in 1.5SBF and that of the film soaked in ultrapure water for 2 h. This operation was applied to obtain the weight of pure polyamide film since CaCl_2 incorporated into the film can be removed completely by soaking it in ultrapure water for 2 h. Both the specimens after soaking in 1.5SBF and ultrapure water were dried for 24 h under ambient conditions.

The concentration of calcium (Ca) and phosphorus (P) in the solutions after soaking of the films were determined by induced coupled plasma (ICP; Optima 2000DV, PerkinElmer Japan Co., Ltd., Japan) atomic emission spectroscopy. The calibration lines were plotted with solutions diluted from a calcium standard solution (1000 ppm, Wako Pure Chemical Industries Ltd., Japan) for Ca and an aqueous solution of KH_2PO_4 (Wako Pure Chemical Industries Ltd., Japan) for P, respectively. Peaks at 317.933 nm and 213.617 nm were detected for Ca and P respectively. pH of the solutions were measured using pH meter (pH/Ion Meter, Horiba Ltd., Japan).

3.2.4. Scratch test of hydroxyapatite coating polyamide film

Films with $0.5 \text{ mg}\cdot\text{cm}^{-2}$ of hydroxyapatite were selected to examine the adhesive strength of hydroxyapatite. Firstly, a needle which had a spherical sapphire (50 μm in diameter) was equipped on a scratch testing machine (TYPE 18L, Shinto Kagaku, Co. Ltd., Japan), and touched on the surface of the film. Then load of 0.5, 1.0 or 10 g weight was applied to the needle and the specimen was moved at the speed of 60 cm/min. Morphology of the surface around the scratched area was observed by scanning electron microscope (FE-SEM: S-4800N Hitachi Ltd., Japan).

3.3. Results

3.3.1. Amount of hydroxyapatite deposited on film and concentrations of components in 1.5SBF

Figure 3-2 shows changes in weight of hydroxyapatite deposited on the film after soaking in 1.5SBF. The weight of deposited hydroxyapatite increased with increasing the soaking period for each specimen. Figure 3-3 shows pH of 1.5SBF after soaking of the film. The pH value gradually decreased with increasing soaking period and access to around 7.25 for each specimen. Figure 3-4 shows concentration of Ca after soaking of the film in 1.5SBF. The concentration increased during initial 3 h soaking for each specimen. For C(0.5), the concentration was kept to initial 12 h and then it decreased with increasing the soaking period. On the contrary, the concentration decreased with increasing the soaking period after 6 h for S(0.5). Figure 3-5 shows concentration of P after soaking of the film in 1.5SBF. For C(0.5), the concentration did not change even after soaking for 12 h and then it decreased with increasing the soaking period. On the contrary, the concentration was held during initial 3 h soaking and then it decreased with increasing the soaking period for S(0.5). These results indicate that these films released calcium ions into 1.5SBF from themselves within 6 h, and that calcium, phosphate, and hydroxyl ions were gradually consumed to form hydroxyapatite on the surface of C(0.5) film at the period between 12 h and 18 h, whereas S(0.5) film between 3 h and 6 h.

3.3.2. Adhesive strength of hydroxyapatite formed on film

Figure 3-6 shows FE-SEM images of the surfaces of C(0.5) and S(0.5) coated with hydroxyapatite around the scratched areas with different applied load. All the S(0.5) films coated with hydroxyapatite were torn from the region of polymer after given load was applied at 0.5, 1 and 10 g weight of load. On the contrary, no C(0.5) films coated with hydroxyapatite was observed to be torn and hydroxyapatite remained on the film after being scratched in the range of load between 0.5 and 10 g weight.

These results indicate that fracture toughness of S(0.5) film coated with hydroxyapatite is lower than that of C(0.5).

3.4. Discussion

3.4.1. Induction period of nucleation of apatite and its rate of crystal growth

It is clear that the induction period of nucleation of apatite for S(0.5) film is shorter than that for C(0.5) film. Regression to decreasing curves was performed for both two specimens to estimate the induction periods of apatite nucleation of them. Here the estimated induction periods for apatite nucleation were supposed to be a time at the weight of deposited hydroxyapatite equal to zero. The induction periods from the calculation were 12.5 h and 4.8 h for C(0.5) and S(0.5), respectively. This difference in the period indicates that the polyamide film containing sulfonic (-SO₃H) groups shows higher rate of apatite nucleation on the substrates than that containing carboxyl (-COOH) groups. A nucleation rate of crystals in a supersaturated solution at a temperature, T, is generally given by equation (1),

$$I = I_0 \exp\left(\frac{-\Delta G^*}{kT}\right) \exp\left(\frac{-\Delta G_m}{kT}\right) \quad (1)$$

where ΔG^* is the free energy for formation of an embryo of critical size, and ΔG_m is the activation energy for transport across the nucleus-solution interface. Among them, ΔG_m is independent of the polymer substrates. ΔG^* is given by equation (2),

$$\Delta G^* = \frac{16\gamma^3 f(\theta)}{3 \left(\frac{kT}{V_\beta} \ln \left(\frac{IAP}{K_0} \right) \right)^2} \quad (2)$$

where γ is interface energy between the nucleus and the solution, IAP is ionic activity product of the crystal in the solution, K_0 is the value of IAP at equilibrium, i.e., solubility product of the crystal, $f(\theta)$ is a function of contact angle between the nucleus and the substrate, and V_β is the molecular volume of the crystal phase. Among them, $f(\theta)$

depends upon the substrate, and IAP/K_0 , a measure of the degree of supersaturation, also depends upon the substrate when the substrate releases Ca^{2+} ions of the crystal, while others are independent of the substrates. Therefore there are two major reasons for enhancement of an induction of heterogenous nucleation of apatite on the polymer substrates. One is initial release of Ca^{2+} ions from the polymer substrates to increase the degree of supersaturation (IAP/K_0) with respect to apatite. The other is lower level of $f(\theta)$ that is generally given by equation (3),

$$f(\theta) = \frac{(2 + \cos\theta)(1 - \cos\theta)^2}{4} \quad (3)$$

Namely, $f(\theta)$ decreases with decreasing interface energy between the crystal of hydroxyapatite and substrates. Based on these parameters, S(0.5) has properties on rapid release of Ca^{2+} ions and/or a specific surface with lower interface energy against the hydroxyapatite crystals. The value of IAP can be estimated from the results of changes in Ca, P concentrations and pH (Figure 3-7) according to the method previously reported [6,10-12]. The increase in degree of the supersaturation for S(0.5) at 3 hours is as high as that for C(0.5), after the films are exposed to the 1.5SBF. Thus, the higher rate of the apatite nucleation on the surfaces of the S(0.5) can probably be attributed to lower interface energy than that of the C(0.5), due to the difference of the functional groups. Since the degree of negative charge of sulfonic group is estimated to be as high as that of carboxyl group in 1.5SBF at pH 7.4, the difference in the induction period of a nucleation of apatite between C(0.5) and S(0.5) is supposed generated by the difference in the concentration of lone electron-pairs per unit space, as discussed in Chapter 1, and/or by the difference in the equilibrium constant for formation of ion pair of calcium ion with an anionic group, as estimated and discussed in general introduction part and Chapter 1, respectively. This may have contributed to easier access of calcium ions to sulfonic groups than that to carboxyl groups. Easier association of sulfonic groups with calcium ions may lead to shortening the period for induction of nuclei of apatite than

that of carboxyl groups.

Rate of crystal growth was also compared between the polymer films containing sulfonic groups and carboxyl groups. It is reported that rate of crystal growth (R) is related to relative supersaturation (σ) of solution as shown in equation (4) [10],

$$R = k \cdot S \cdot \sigma^n \quad (4)$$

where k is the rate constant for crystal growth, S is a function of the total number of available growth sites, and n is the effective order of reaction. This relative supersaturation can be obtained from equation (5) [10],

$$\sigma = \frac{(IAP^{1/\nu} - K_{SO}^{1/\nu})}{K_{SO}^{1/\nu}} \quad .5$$

where IAP means ionic activity product of the crystal in the supersaturated solution described above, K_{SO} is the solubility product ($= 5.5 \times 10^{-118}$ for hydroxyapatite [13]), and ν is the number of ions in the molecule ($= 18$ for hydroxyapatite). IAP of hydroxyapatite can be obtained with concentrations of calcium, phosphate and hydroxyl ions [6,10-12]. From the data in Figures 3-3, 3-4 and 3-5, IAP and σ was introduced for each given period at which R was defined as tangent of weight increment curve derived from Figure 3-2. The logarithm of the rate of crystal growth (R) was plotted against the logarithm of relative supersaturation (σ) of solution in order to examine the value of n . Figure 3-8 shows the relationships between $\log R$ and $\log \sigma$ for C(0.5) and S(0.5). The $\log R$ increased with increasing $\log \sigma$ for each specimen, and this means rate of crystal growth of hydroxyapatite is dependent of supersaturation of the solution. In addition, plots for C(0.5) and S(0.5) showed similar tendency independent of the range of $\log \sigma$. This implies that the rate of crystal growth is independent on the kind of functional groups on polymer substrate. Assuming that the values of k and S are constant throughout the hydroxyapatite formation, the $\log \tilde{\sigma} \log R$ plot indicates that the value of n is varied during the hydroxyapatite formation. The value of n calculated in the range of $\log \sigma$ between 1.12 and 1.30 was 2. The effective order of reaction (n) in the range

$0 < n < 1.2$, $n \sim 2$, or $n > 2.5$ indicates that the rate of controlling process is one of adsorption and/or mass transport, surface spiral, or polynucleation, respectively [14]. Therefore, it is considered that the hydroxyapatite crystal growth is controlled by surface spiral in this range. On the other hand, the value of n was 21 when it was calculated in the range of $\log \sigma$ between 1.05 and 1.10. This indicates that polynucleation controlled the hydroxyapatite crystal growth in this range. However, it is difficult to understand the situation that the process of the crystal growth is drastically changed in the continuous system. It is considered that the actual relative supersaturation near the sample is different from the relative supersaturation calculated from the concentrations of calcium, phosphate and hydroxyl ions. At the initial stage, calcium ions are released from the sample and increase the degree of supersaturation near the sample. On the other hand, calcium, phosphate and hydroxyl ions are consumed and the degree of supersaturation near the sample decreases at the later stage. Moreover, magnesium ions in 1.5SBF might have affected the hydroxyapatite crystal growth. It is known that magnesium ions inhibit the hydroxyapatite crystal growth [15]. When calcium, phosphate and hydroxyl ions are consumed, the relative concentration of magnesium ions increases against the constituents of hydroxyapatite. In this case, the rate of constant for crystal growth (k) might decrease even in the continuous system.

Once the nuclei of apatite formed, rate of crystal growth is independent of the functional groups in the polymers, but is governed by relative supersaturation of the surrounding fluid.

3.4.2. Adhesive strength of the hydroxyapatite layer with the substrates

Adhesive strength of hydroxyapatite layer with S(0.5) film was distinctly lower than that of C(0.5). Adhesive strength is governed not only by chemical interaction between the hydroxyapatite crystals and polymer, but also by mechanical interlocking at the interface. The equilibrium constants for complex formation between

Ca^{2+} and typical anions at 25°C are listed on Table 6 in general introduction part [16]. Higher rate on complex formation with Ca^{2+} may bring higher binding of hydroxyapatite with the polymer. From this point of view, carboxyl groups show higher affinity with Ca^{2+} than sulfonic groups. On the other hand, the mechanical interlocking of the hydroxyapatite crystals with polymer substrate (Figure 2-6 in Chapter 2) gives higher strength of the adhesion. In such a case, the mechanical strength of the polymer substrates would govern the adhesive strength because breakage happens inside the substrates themselves. In the case of S(0.5), the mechanical strength of the film is considered to govern the adhesive strength of hydroxyapatite. The increase in the content of $-\text{SO}_3\text{H}$ causes the polyamide to swell easily in 1.5SBF and to show high degree of shrinkage after drying. Moreover, the molecular weight of S(0.5) is smaller than C(0.5), and this may also cause lower mechanical strength of S(0.5) than that of C(0.5). The reduced viscosities of C(0.5) and S(0.5) were 1.38 and 0.75, respectively, when the polyamides were dissolved at a concentration 0.5 g/dL in NMP at 30°C. This means that the average molecular weight of C(0.5) is larger than that of S(0.5). Therefore, S(0.5) is easily broken when a relatively high load was applied to the specimen. On the other hand, C(0.5) film shows both high chemical interaction with the hydroxyapatite crystals and enough mechanical strength, and hence achieve the high adhesive strength between the hydroxyapatite layer and substrate.

3.5. Conclusions

Induction period of nucleation of apatite was shorter for S(0.5) film than that for C(0.5). Rate of crystal growth of hydroxyapatite was not dependent on the kind of functional groups but dependent on the degree of supersaturation of the surrounding solution in which crystal is growing. Mechanical strength of polymer coated with hydroxyapatite was lower for S(0.5) than that for C(0.5) according to not only by chemical interaction but also by the mechanical property of the polyamide film itself.

References

1. Tanahashi M, Yao T, Kokubo T, Minoda M, Miyamoto T, Nakamura T, Yamamuro T. Apatite coating on organic polymers by a biomimetic process. *J Am Ceram Soc* 1994;77:2805-2808.
2. Takadama H, Kim HM, Kokubo T, Nakamura T. Mechanism of biomineralization of apatite on sodium silicate glass: TEM-EDX study *in vitro*. *Chem Mater* 2001;13:1108-1113.
3. Takadama H, Kim HM, Kokubo T, Nakamura T. An X-ray photoelectron spectroscopic study of the process of apatite formation on bioactive titanium metal. *J Biomed Mater Res* 2001;55:185-193.
4. Tanahashi M, Matsuda T. Surface functional group dependence on apatite formation on self-assembled monolayers in a simulated body fluid. *J Biomed Mater Res* 1997;34:305-315
5. Kokubo T, Kushitani H, Ohtsuki C, Sakka S, Yamamuro T. Chemical reaction of bioactive glass and glass-ceramics with a simulated body fluid. *J Mater Sci Mater Med* 1992;3:79-83.
6. Ohtsuki C, Kokubo T, Yamamuro T. Mechanism of apatite formation on CaO-SiO₂-P₂O₅ glasses in a simulated body fluid. *J Non-Cryst Solids* 1992;143:84-92.
7. Miyazaki T, Ohtsuki C, Akioka Y, Tanihara M, Nakao J, Sakaguchi Y, Konagaya S. Apatite deposition on polyamide film containing carboxyl group in a biomimetic solution. *J Mater Sci Mater Med* 2003;14:569-574.
8. Konagaya S, Tokai M. Synthesis of ternary copolyamides from aromatic diamine with carboxyl or sulfonic group (3,5-diaminobenzoic acid, 2,4-diaminobenzenesulfonic acid), and iso- or terephthaloyl chloride. *J Appl Polym Sci* 2000;76:913-920.

9. Ohtsuki C, Kokubo T, Neo M, Kotani S, Yamamuro T, Nakamura T, Bando Y. Bone-bonding mechanism of sintered β -3CaO·P₂O₅. *Phosphorus Res Bull* 1991;1:191-196.
10. Hata K, Kokubo T, Nakamura T, Yamamuro T. Growth of a bonelike apatite layer on a substrate by a biomimetic process. *J Am Ceram Soc* 1995;78:1049-1053.
11. Newman W, Newman M. In: *The chemical dynamics of bone mineral*. Chicago: University of Chicago; 1958. p. 3.
12. Nancollas GH. *In vivo* studies of calcium phosphate crystallization. In: Mann S, Webb G, Williams RJP editors. *Biom mineralization*. Germany, Weinheim: VCH Verlagsgesellschaft; 1989. p. 157-187.
13. McDonnell M, Gregory TM, Brown WE. Solubility of Ca₅(PO₄)₃OH in the system Ca(OH)₂-H₃PO₄-H₂O at 5°, 15°, 25°, and 37°C. *J Res Natl Bur Stand* 1977;81A,273-281.
14. Li P, Ohtsuki C, Kokubo T, Nakanishi K, Soga N, Nakamura T, Yamamuro T. Effects of ion in aqueous media on hydroxyapatite induction by silica gel and its relevance to bioactivity of bioactive glasses and glass-ceramics. *J Appl Biomater* 1993;4:221-229.
15. In: Iwasawa Y editor. *Kagakubinran* the 5th edition. Tokyo: Maruzen; 2004. p. II-344 [in Japanese].

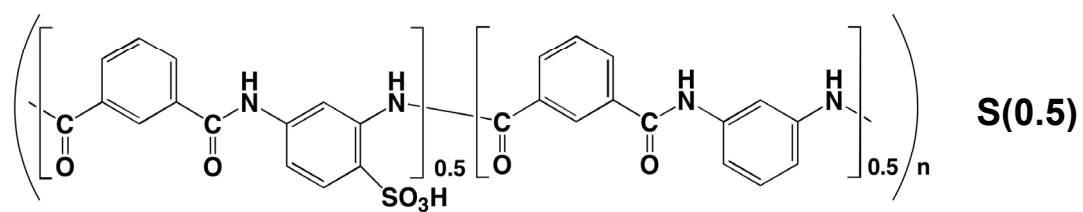
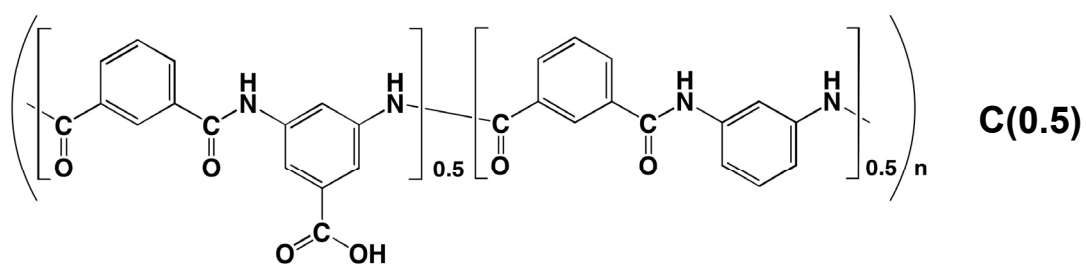


Figure 3-1. Structural formulae of C(0.5) and S(0.5).

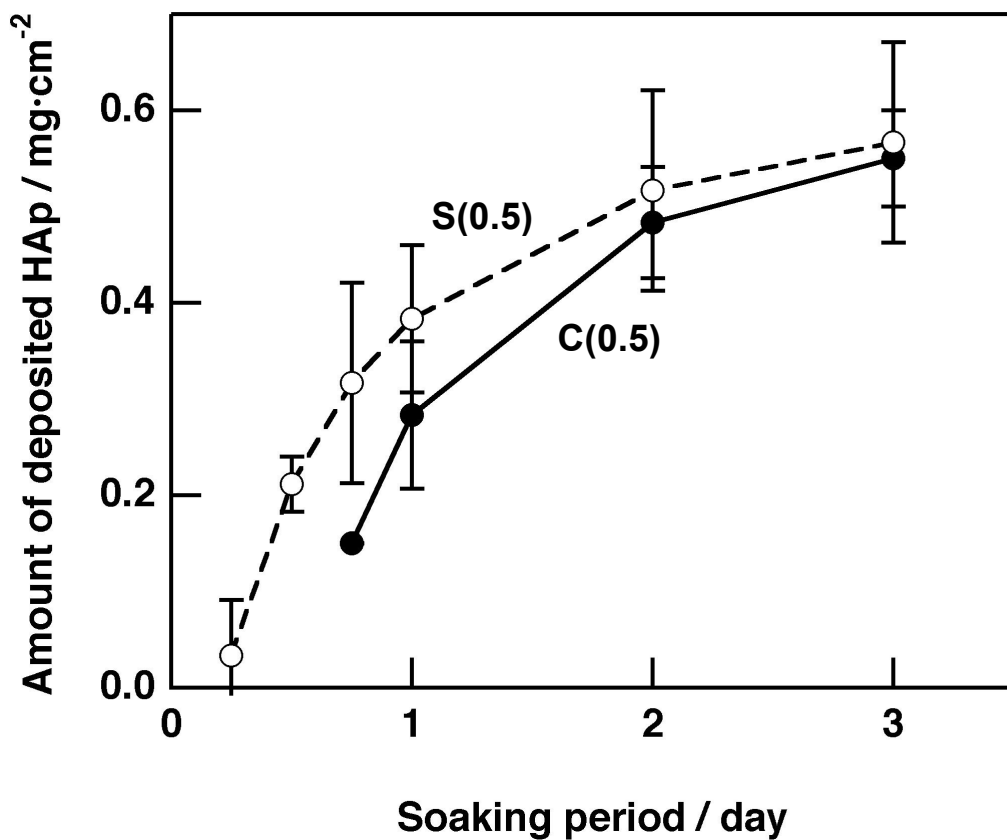


Figure 3-2. Changes in weight of apatite deposited on C(0.5) and S(0.5) films after soaking in 1.5SBF.

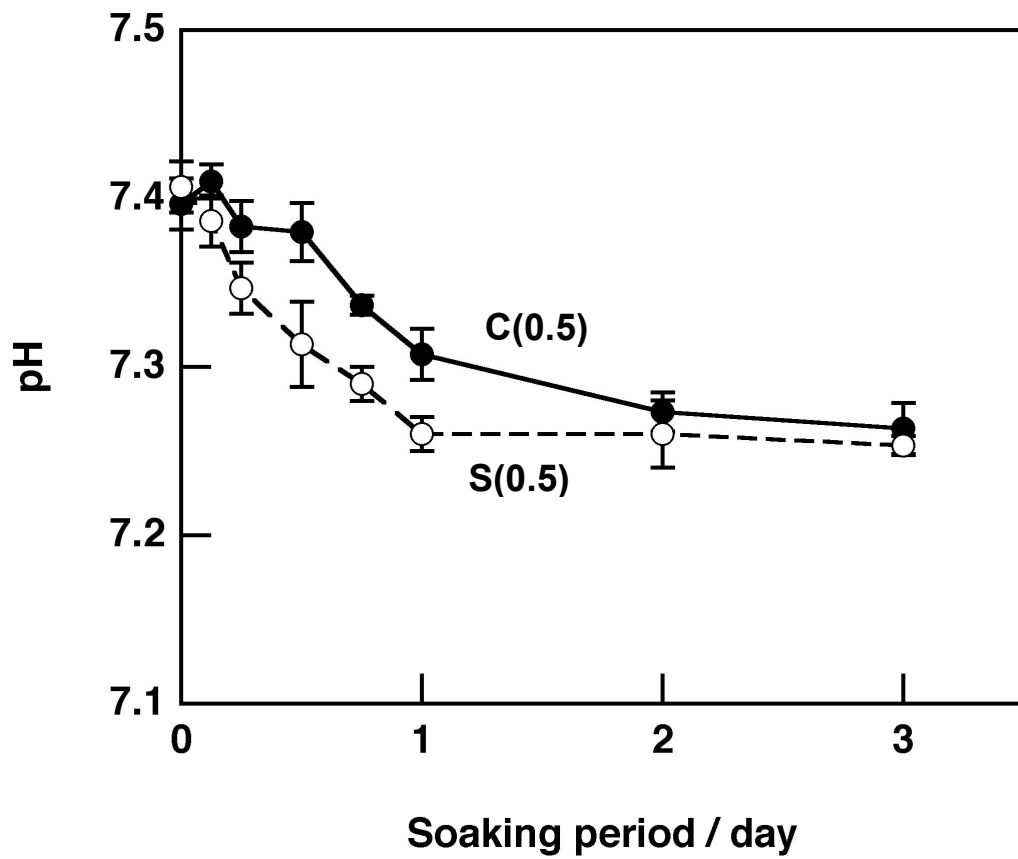


Figure 3-3. Changes in pH of 1.5SBF due to soaking of C(0.5) and S(0.5) films.

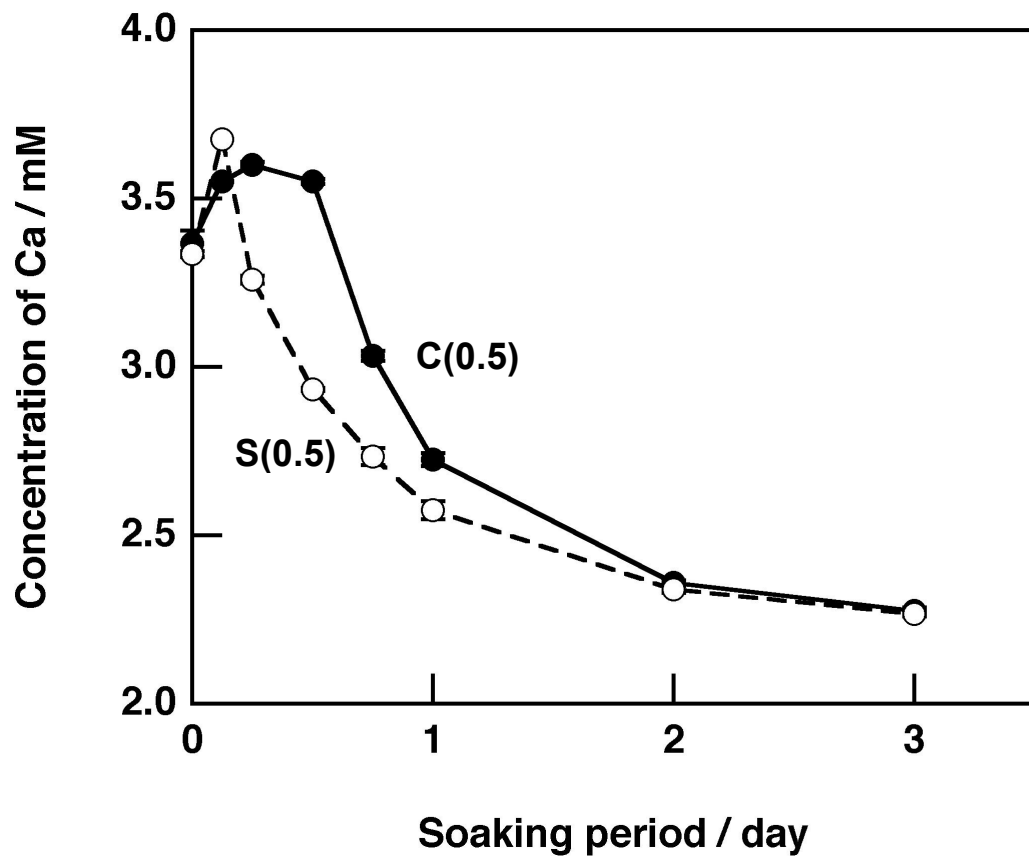


Figure 3-4. Changes in residual concentration of Ca in 1.5SBF due to soaking of C(0.5) and S(0.5) films.

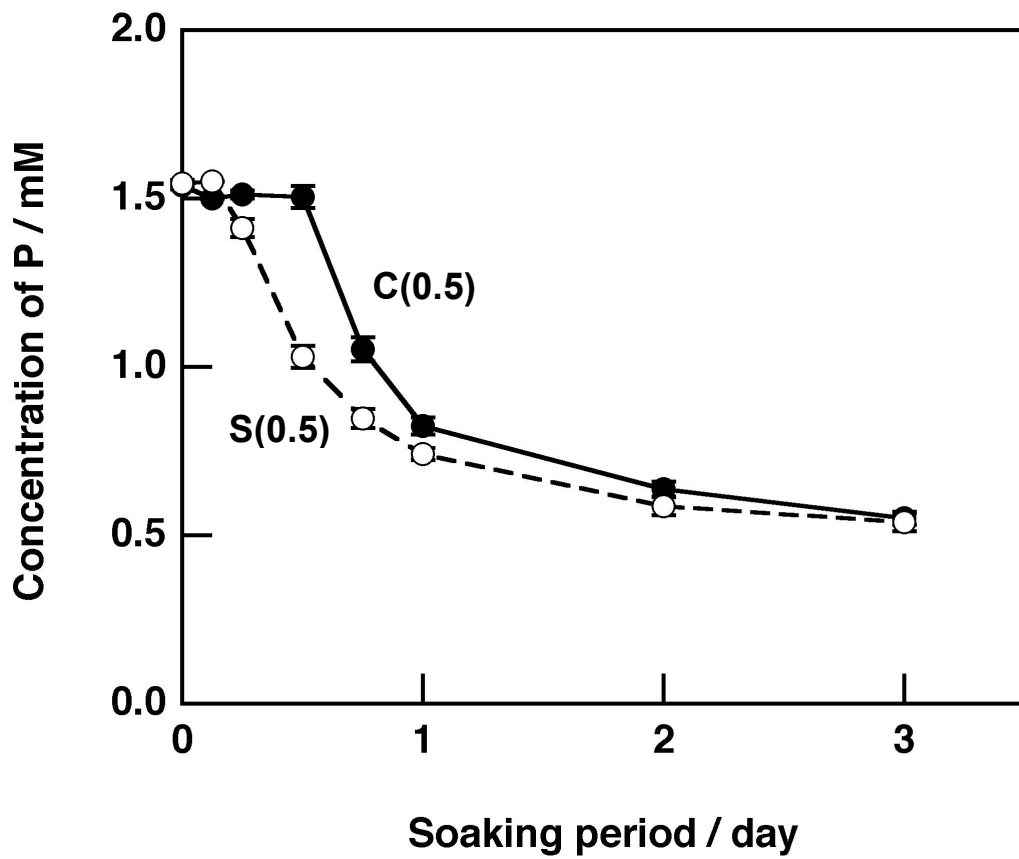


Figure 3-5. Changes in residual concentration of P in 1.5SBF due to soaking of C(0.5) and S(0.5) films.

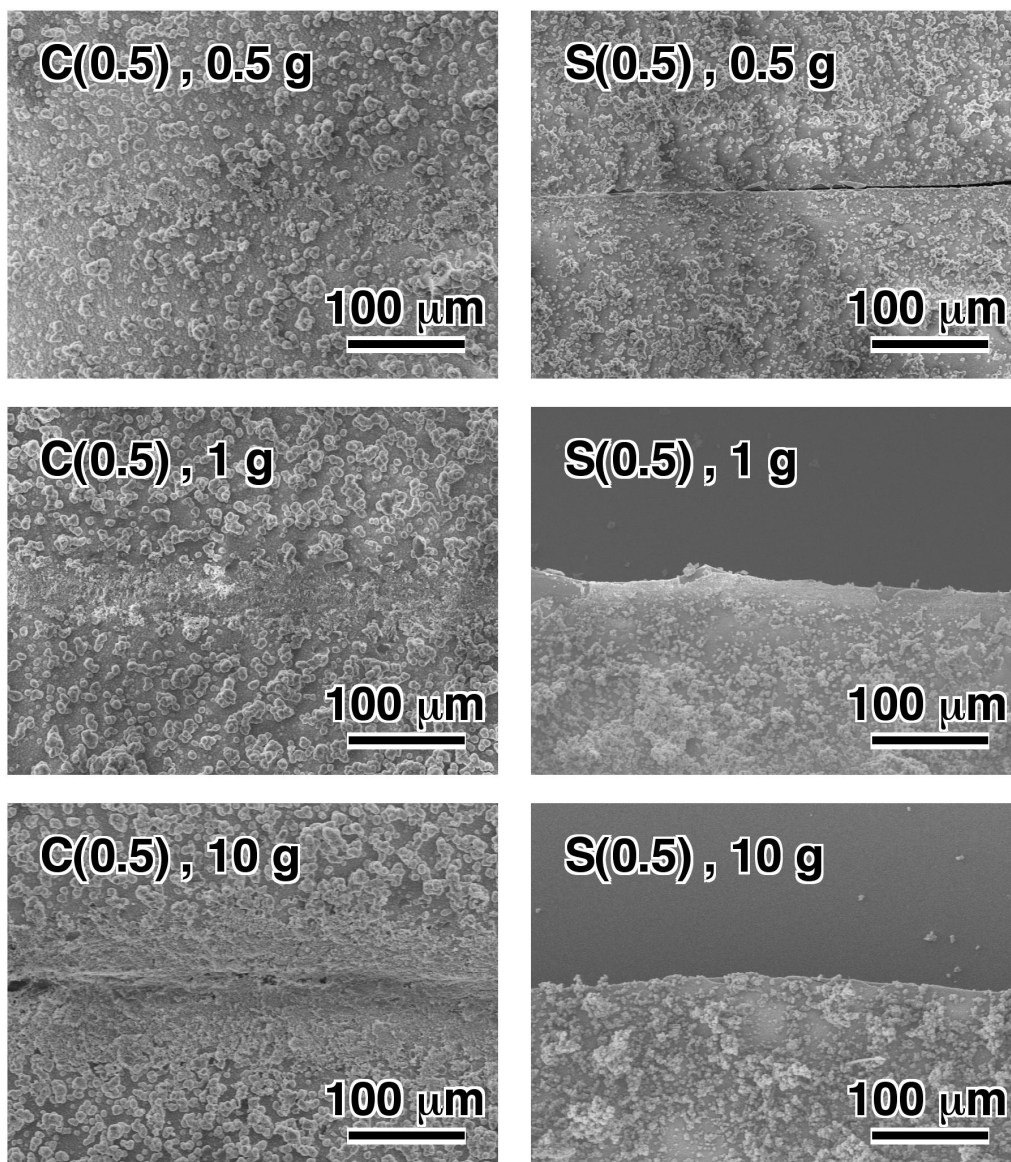


Figure 3-6. FE-SEM images of surfaces of C(0.5) and S(0.5) films around area scratched with different applied load.

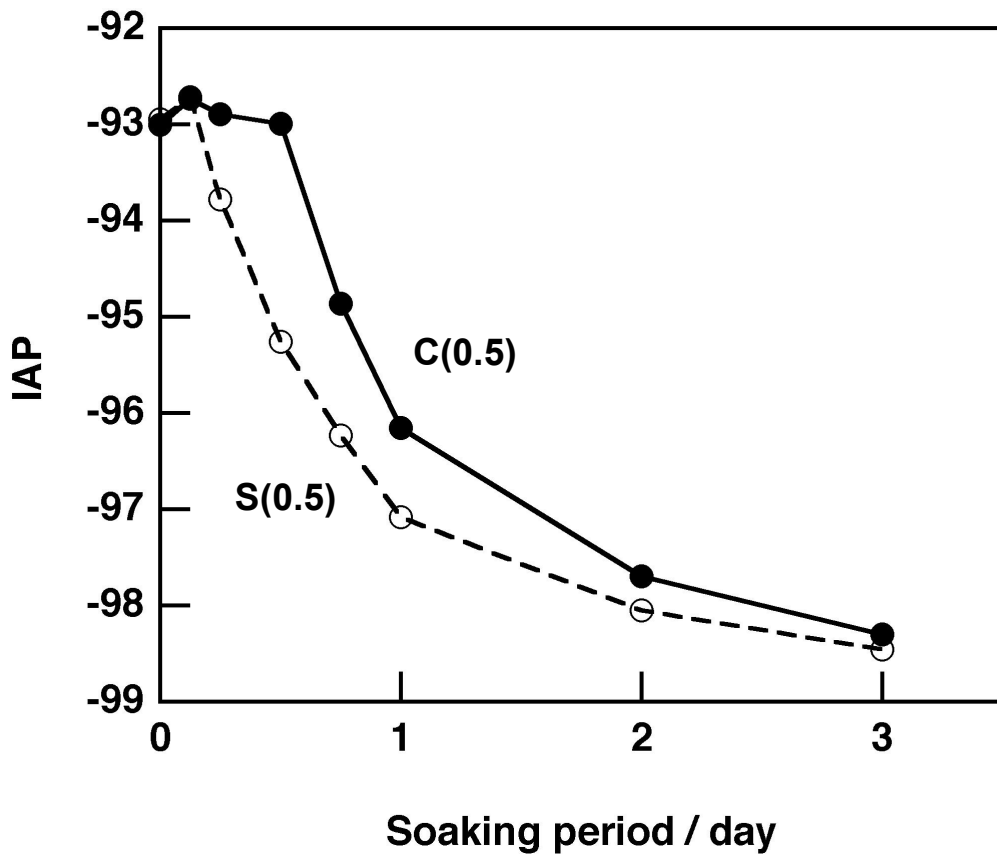


Figure 3-7. Changes in ionic activity product (*IAP*) in 1.5SBF due to soaking of C(0.5) and S(0.5) films.

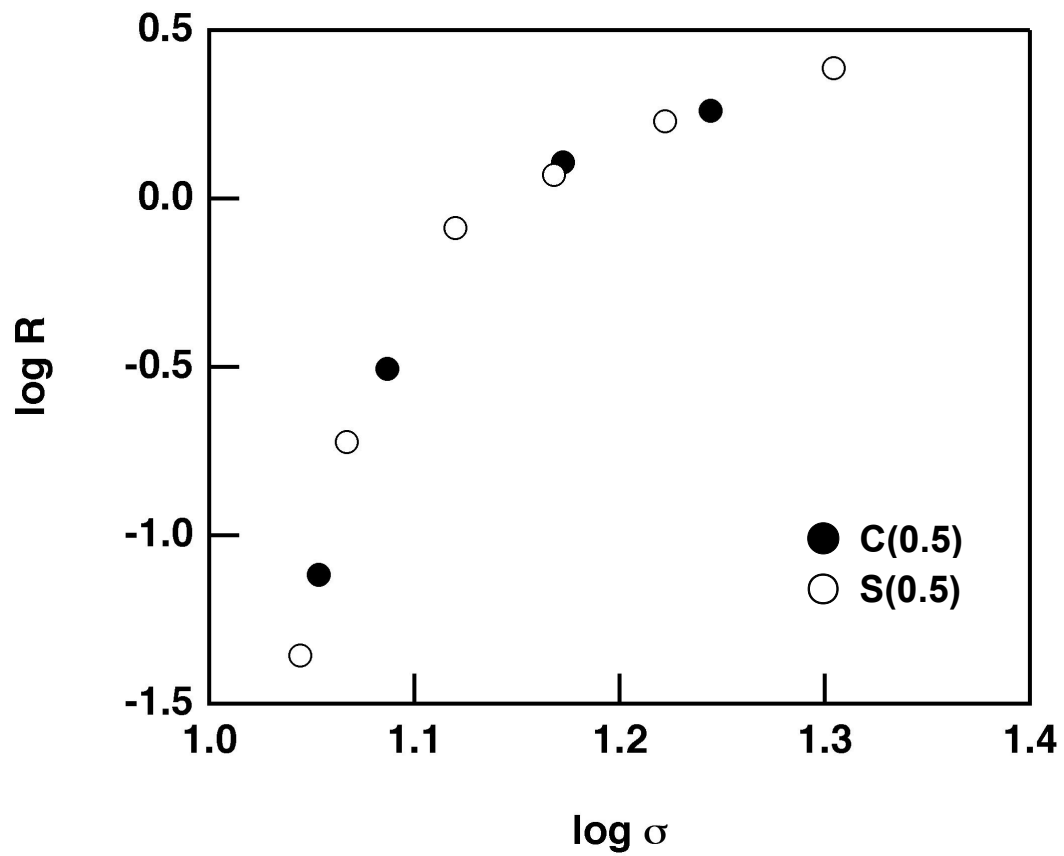


Figure 3-8. Relationships between relative supersaturation of soaking solution and rate of crystal growth of apatite.

Chapter 4: Adsorption of formaldehyde onto hydroxyapatite deposited polyamide film

4.1. Introduction

Some harmful volatile organic compounds (VOCs) have been used as a component of coating or adhesive agents for building materials [1]. Prominent among these is formaldehyde, which irritates the respiratory system and has been widely used in the past. Such harmfulness leads to a problem known as the “Sick house syndrome.” Hydroxyapatite is of considerable interest as an adsorbent for removal of harmful pollutants since it shows an ability to adsorb organic substances [2-6]. When using hydroxyapatite as a device for removal of a pollutant, such as formaldehyde, coating of hydroxyapatite is required to achieve efficient adsorption of the target organic substances from the surrounding environment. An organic polymer with hydroxyapatite coated on its surface would be a useful countermeasure against the pollutants since it can be designed in any shape without losing its activity. Some studies have been reported where biomimetic processing, using a simulated body fluid and its related solutions [7-9], was used to fabricate a coating of hydroxyapatite on an organic substrate. Miyazaki *et al.* successfully coated a hydroxyapatite layer on an aromatic polyamide film containing carboxyl groups and calcium chloride through immersion in a solution called 1.5SBF that has 1.5 times the ionic concentration of inorganic species to those of human blood plasma [10]. In this process, nano-sized hydroxyapatite particles with low crystallinity can precipitate on the polymer substrates. In Chapters 1, 2, and 3, it was revealed that hydroxyapatite layer consisting of nano-sized particles was deposited on the polyamide films containing calcium chloride after exposure to a solution mimicking body fluid (1.5SBF). From comparisons of the modification with different kinds of functional groups including carboxyl groups, sulfonic groups and silanol groups, modification of carboxyl groups can provides highest adhesive strength

among them, although the rate of hydroxyapatite formation was lowest among the three types of functional groups. Hydroxyapatite layers formed in this way may be very effective as an adsorbent of formaldehyde, but nothing has been reported. In this chapter, the capability of hydroxyapatite biomimetically deposited on a polyamide film was evaluated for the application as an adsorbent of formaldehyde.

4.2. Experimental

4.2.1. Preparation of polyamide film coated with hydroxyapatite

One gram of the aromatic polyamide, containing carboxyl groups C(50) as shown in Figure 4-1 [11], was dissolved in 10 mL of N,N-dimethylacetamide (Wako Pure Chemical Industries Ltd., Japan) together with 0.67 g of CaCl₂ (Nacalai Tesque Inc., Japan). The mixture was stirred for 24 h to obtain a homogenous solution. The solution was coated on a glass plate using a bar coater and dried under 133 Pa at 60°C for 8 h to obtain a film. The formed film was removed from the glass plate and cut into pieces 30 mm × 30 mm in size. The thickness of the obtained film was between 12 and 18 μm. The film was soaked in 270 mL of 1.5SBF (Na⁺ 213.0, K⁺ 7.5, Mg²⁺ 2.3, Ca²⁺ 3.8, Cl⁻ 221.7, HCO₃⁻ 6.3, HPO₄²⁻ 1.5, and SO₄²⁻ 0.8 mol·m⁻³), which had ion concentrations 1.5 times of those of a simulated body fluid (SBF) [7,12], for various periods under shaking at 120 strokes·min⁻¹ (3 cm in stroke length) using a water bath shaker (Personal Lt-10F, TITEC, Japan) at 36.5°C. The pH of 1.5SBF was buffered at 7.40. The 1.5SBF was renewed daily. After soaking for a given period, the film was taken out of the solution, gently washed with ultrapure water and dried in air for 24 h. The weight of the film was measured. The weight of the formed hydroxyapatite was calculated by the difference between the total weight of the film after soaking in 1.5SBF and that of the film soaked in ultrapure water for 2 h. This operation was applied to obtain the weight of pure polyamide film since CaCl₂ incorporated into the film can be removed completely by soaking it in ultrapure water for 2 h. Both the specimens after soaking in 1.5SBF and

ultrapure water were dried for 24 h under ambient conditions. The film was characterized by thin film X-ray diffraction (TF-XRD; RINT2200V/PC-LR, Rigaku Co., Japan) and scanning electron microscopy (SEM; S-3500N, Hitachi Ltd., Japan). In the SEM observations, an Au thin film was sputtered onto the surfaces of the specimens.

4.2.2. Testing the adsorption of formaldehyde

Formaldehyde gas was prepared by stirring 1 mL of 37% formaldehyde solution (Wako Pure Chemical Industries Ltd., Japan) in 500 mL of glass bottle at 23°C for 24 h. A piece of polyamide film, 30 mm × 30 mm in size and coated with hydroxyapatite, was put into a Tedlar[®] bag (SANSYO Co., Ltd., Japan). Three liters of highly pure N₂ gas (purity >99.999 vol%) and gaseous formaldehyde was then injected into the bag. The initial concentration of formaldehyde was adjusted by collecting an appropriate volume of the formaldehyde gas. After holding the specimen in the bag for 0.5, 1, 2 and 6 h, the concentration of formaldehyde in the bag was examined by a detecting tube (No. 91L, GASTEC, Japan). The ability to adsorb formaldehyde of a commercial calcined hydroxyapatite powder (Wako Pure Chemical Industries Ltd., Japan) and an activated charcoal from coconut shell (Nacalai Tesque Inc., Japan) were also tested, as comparable materials, by the method described above.

4.2.3. Morphological observation and measurement of specific surface area

Morphological observation at high magnification was carried out for typical specimens using a field emission scanning electron microscope (FE-SEM; S-4800N Hitachi Ltd., Japan). Measurement of specific surface area was carried out by automatic vapor adsorption (BELSORP-18SP FMS-LP-100, BEL JAPAN, Inc., Japan). The specific surface areas of examined specimens were determined from N₂ adsorption isotherms at 77 K under 0-0.4 relative pressure (equilibrium pressure to saturation pressure) range using the BET equation.

4.3. Results

4.3.1. Characterization of apatite deposited on polyamide film

Figures 4-2, 4-3 and 4-4 show TF-XRD patterns, SEM photographs and EDX spectra of the surfaces of polyamide films before and after soaking in 1.5SBF for 1, 2 and 3 days. Peaks at $2\theta = 26^\circ$ and 32° , which are assigned to apatite, were absent before soaking and increased in magnitude with the time of soaking (Figure 4-2). Spherical particles were observed adhering to the film surface after soaking in 1.5SBF (Figure 4-3). Peaks assigned to Ca and P were detected on the film surfaces after soaking in 1.5SBF on Figure 4-4. These results confirm that hydroxyapatite deposits on the surface of polyamide film within 1 day and it grows with increasing soaking period. Table 4-1 gives the amount of deposited hydroxyapatite per unit area after soaking in 1.5SBF for various periods. The amount of the deposited hydroxyapatite increased with increasing soaking period.

4.3.2. Removal of formaldehyde by hydroxyapatite on polyamide film

Figure 4-5 shows changes in the concentrations of residual formaldehyde after exposure to formaldehyde of various amounts of hydroxyapatite deposited on polyamides. Films with deposits of 0, 0.11, 0.28, 0.61 and $1.08 \text{ mg}\cdot\text{cm}^{-2}$ of hydroxyapatite were selected for this examination. Samples labeled as blank and 0 mg are blanks: the former was a procedural blank (nothing in the bag) and the latter had only the pure polyamide film in the bag. The concentration of residual formaldehyde decreased with increasing amount of hydroxyapatite up to the specimens with $0.61 \text{ mg}\cdot\text{cm}^{-2}$ of hydroxyapatite. The adsorption of formaldehyde on the specimen with $1.08 \text{ mg}\cdot\text{cm}^{-2}$ was similar to that with $0.61 \text{ mg}\cdot\text{cm}^{-2}$. This result indicates that the total amount of adsorbed formaldehyde and the rate of its adsorption depend on the amount of hydroxyapatite deposited on the polyamide films while they are saturated at 0.61

mg·cm⁻².

4.3.3. Comparison of hydroxyapatite deposited on polyamide film with other materials

Figure 4-6 shows changes in the concentrations of residual formaldehyde after exposure of a commercial hydroxyapatite powder and a charcoal activated from coconut shell to formaldehyde for various periods, in comparison with hydroxyapatite deposited on polyamide at 0.61 mg·cm⁻². The weight of these specimens was 20 mg. A decrease in concentration of formaldehyde was seen for every specimen, while the total amount and the rate of adsorption of formaldehyde were larger for hydroxyapatite on polyamide than those for the other specimens.

Figures 4-7 and 4-8 show changes in concentration of residual formaldehyde after exposure of hydroxyapatite deposited on polyamide at 0.61 mg·cm⁻² and the commercial hydroxyapatite powder to formaldehyde with various initial concentrations, respectively. These figures are utilized in the following. When an adsorption isotherm is categorized as a Langmuir type, the amount of adsorbate (N) is represented as a function of the equilibrium pressure of adsorbate (p) as shown below (equation (1)).

$$N = A \cdot K \cdot p / (1 + K \cdot p) \quad (1)$$

In this equation, A and K are constants which indicate the total amount of surface sites for adsorption of formaldehyde and the ratio of the rate constants of adsorption to desorption, respectively. Figure 4-9 shows relationship between equilibrium concentration and amount of adsorbed formaldehyde for hydroxyapatite deposited on polyamide at 0.61 mg·cm⁻² and the commercial hydroxyapatite powder. Every point was plotted by calculating the equilibrium pressure of formaldehyde and the total consumption of formaldehyde after exposure to formaldehyde at different initial concentrations. The equilibrium concentration was estimated by the regression of the curve of decreasing formaldehyde concentration shown in Figures 4-7 and 4-8. The amount of adsorbed formaldehyde was determined from the difference between the

initial concentration and the residual concentration estimated above, per unit weight of hydroxyapatite. Equation (1) can be rearranged into the following form (equation (2)).

$$p/N = p/A + 1/(A \cdot K) \quad (2)$$

From this Langmuir plot, the constants A and K can be obtained. Figure 4-10 shows Langmuir plot of adsorption isotherms of formaldehyde at 296 K in the two cases where hydroxyapatite deposited on polyamide at $0.61 \text{ mg}\cdot\text{cm}^{-2}$ and the commercial hydroxyapatite powder were adsorbents. The equilibrium pressure was calculated from the residual concentration of formaldehyde, which was estimated by the regression of decreasing curve of the formaldehyde concentration. Both these plots were linear. The constants A and K were obtained from the Langmuir plots, and the values are shown in Table 4-2.

Figure 4-11 shows FE-SEM photographs of the hydroxyapatite deposited on polyamide after soaking in 1.5SBF for 2 days and commercial hydroxyapatite powder at high magnification. The hydroxyapatite deposited on the polyamide film formed nano-sized particles which were observed to aggregate and form a porous network, while the commercial hydroxyapatite powder was formed of hexagonal crystal rods which grew along the c -axis to be a few micrometers in length. The commercial hydroxyapatite powder is a calcined powder with higher crystallinity determined by its powder X-ray diffraction pattern (Figure 4-12). From N_2 adsorption method, the specific surface areas of hydroxyapatite deposited on polyamide and powdered hydroxyapatite were calculated to be 226 and $7 \text{ m}^2\cdot\text{g}^{-1}$, respectively. These results show that the hydroxyapatite with larger surface areas can be formed by the biomimetic process than by calcinations. Although the activated charcoal had a much larger specific surface area ($891 \text{ m}^2\cdot\text{g}^{-1}$) than the hydroxyapatite deposited on polyamide film, it showed lower adsorption ability.

4.4. Discussion

Assuming that hydroxyapatite is composed of spherical particles, their particle sizes were calculated from the specific surface area obtained by N₂ BET method. Moreover, their crystallite sizes were also calculated from the peak width on X-ray diffraction patterns, according to Sherrer's equation. Table 4-3 summarized their particle sizes obtained from the above calculations and the FE-SEM observation. The values obtained from X-ray diffraction were quite different from the FE-SEM observation. This is because the crystal size of the calcined hydroxyapatite powder exceeds 200 nm, which is the limit size to apply Sherrer's equation. Moreover, the value of hydroxyapatite on polyamide is not reliable since Sherrer's equation is not suitable to apply to the crystal with low crystallinity. The crystallite sizes obtained from N₂ adsorption are comparable to the size of particles observed under FE-SEM at higher magnification. For calcined hydroxyapatite powder, this value is almost consistent with that calculated by N₂ adsorption examination, while the value differs eight times depending on the adsorbent for hydroxyapatite on polyamide. This difference may be attributed to existence of micropores or roughness of the surface. The higher surface area of the deposited particles on the polyamide films is attributed to nano-size hydroxyapatite particles that coagulated to form a continuous layer as seen on Figure 4-11.

The amount of formaldehyde adsorbed was larger for hydroxyapatite deposited on polyamide film than for the commercial hydroxyapatite powder, that is calcined powder. The Langmuir plots of formaldehyde at 296 K for hydroxyapatite on polyamide and calcined powder were linear, indicating that formaldehyde is adsorbed on the surface of hydroxyapatite as a monolayer within the examined range of the concentration of formaldehyde.

Both the constants A and K of hydroxyapatite on polyamide are much larger than those of calcined powder. The large A value of hydroxyapatite on polyamide is due to the large surface area. The large K value is due to high affinity to formaldehyde since

hydroxyapatite formed on polyamide shows low crystallinity and has many defects [13]. When the hydroxyapatite has many defects, its surface is so unstable that the chemical reactivity of activated sites might be enhanced, resulting in an easy reaction with an adsorbent and also in difficulty of desorption. To be specific, electrostatic or dipolar interactions between formaldehyde molecules and vacancies where calcium ions or hydroxyl ions should have existed are stronger for the hydroxyapatite with many defects than that with no defect in the structure. On the other hand, the examined activated charcoal shows less ability to adsorb formaldehyde than that of hydroxyapatite on polyamide. The activated charcoal had larger specific surface area than hydroxyapatite samples. The number of active sites for adsorption of formaldehyde should be quite smaller than that on the surface of hydroxyapatite. It is known that formaldehyde is easily adsorbed by adsorbents possessing a polar surface. In fact, it has been reported that the ability of activated carbon to adsorb formaldehyde increased with an increase in the number of amino groups on the surface of the activated carbon after amination, independent of the specific surface area [14,15]. Other studies reported that the capability of activated carbon to adsorb harmful gases is dependent on the carbonizing temperature because acidic functional groups, such as carboxyl groups, disturbing the activated site to adsorb formaldehyde are removed at appropriate temperatures [16,17]. It can be said that characteristic structures of hydroxyapatite formed biomimetically were effective for the adsorption of formaldehyde, caused not only from its small particle size but also from its low crystallinity.

The amount of adsorbed formaldehyde depended not on the thickness of the hydroxyapatite layer but on the area of the film covered by hydroxyapatite. This indicates that only the hydroxyapatite on the top surfaces can interact with formaldehyde molecules and adsorb them. When the specimens contain more than $0.61 \text{ mg}\cdot\text{cm}^{-2}$ of hydroxyapatite, the whole surfaces of the polyamide films are covered with hydroxyapatite, and therefore they have the maximum ability to remove formaldehyde.

Consequently, it was found that nano-sized hydroxyapatite layer coated biomimetically on polyamide film is expected to be a candidate for a novel and excellent adsorbent effective for removal of formaldehyde.

4.5. Conclusions

Nano-sized hydroxyapatite deposited on polyamide film using a simulated body environment showed high adsorption ability of formaldehyde. This material can become a candidate material for removing harmful VOCs such as formaldehyde.

References

1. A Guideline from the Ministry of Health, Labour and Welfare of Japan, published on February 8, 2002.
2. Luo Q, Andrade JD. Cooperative adsorption of proteins onto hydroxyapatite. *J Colloid Interf Sci* 1998;200:104-113.
3. Shaferi GMSE, Moussa NA. Adsorption of some essential amino acids on hydroxyapatite. *J Colloid Interf Sci* 2001;238:160-166.
4. Kilpadi KL, Chang PL, Bellis SL. Hydroxyapatite binds more serum proteins, purified integrins, and osteoblast precursor cells than titanium or steel. *J Biomed Mater res* 2001;57:258-267.
5. Combes C, Rey C. Adsorption of proteins and calcium phosphate materials bioactivity. *Biomaterials* 2002;23:2817-2823.
6. O. Takagi, N. Kuramoto, M. Ozawa, S. Suzuki. Adsorption/desorption of acidic and basic proteins on needle-like hydroxyapatite filter prepared by slip casting. *Ceramics International* 2004;30:139-143.
7. Tanahashi M, Yao T, Kokubo T, Minoda M, Miyamoto T, Nakamura T, Yamamuro T. Apatite coating on organic polymers by a biomimetic process. *J Am Ceram Soc* 1994;77:2805-2808.
8. Oyane A, Nakanishi K, Kim HM, Miyaji F, Kokubo T, Soga N, Nakamura T. Sol-gel modification of silicone to induce apatite-forming ability. *Biomaterials* 1999;20:79-84.
9. Takeuchi A, Ohtsuki C, Miyazaki T, Tanaka H, Yamazaki M, Tanihara M. Deposition of bone-like apatite on silk fiber in a solution that mimics extracellular fluid. *J Biomed Mater Res* 2003;65A:283-289.
10. Miyazaki T, Ohtsuki C, Akioka Y, Tanihara M, Nakao J, Sakaguchi Y, Konagaya S. Apatite deposition on polyamide film containing carboxyl group in a biomimetic

- solution. *J Mater Sci Mater Med* 2003;14:569-574.
11. Konagaya S, Tokai M. Synthesis of ternary copolyamides from aromatic diamine with carboxyl or sulfonic group (3,5-diaminobenzoic acid, 2,4-diaminobenzenesulfonic acid), and iso- or terephthaloyl chloride. *J Appl Polym Sci* 2000;76:913-920.
 12. Ohtsuki C, Kokubo T, Neo M, Kotani S, Yamamuro T, Nakamura T, Bando Y. Bone-bonding mechanism of calcined β -3CaO·P₂O₅. *Phosphorus Res Bull* 1991;1:191-196.
 13. Kokubo T, Ito S, Huang ZT, Hayashi T, Sakka S, Kitsugi T, Yamamuro T. Ca, P-rich layer formed on high-strength bioactive glass-ceramic A-W. *J Biomed Mater Res* 1990;24:331-343.
 14. Tanada S, Kawasaki N, Nakamura T, Araki M, Isomura M. Removal of formaldehyde by activated carbons containing amino groups. *J Colloid Interf Sci* 1999;214:106-108.
 15. Hirata M, Kawasaki N, Nakamura T, Bunei R, Tanada R. Removal of formaldehyde by surface-modified carbonaceous materials. *Hyoumenkagaku* 2003;24:417-422 [in Japanese].
 16. Asada T, Ishihara S, Yamane T, Toba A, Yamada A, Oikawa K. Science of bamboo charcoal: Study on carbonizing temperature of bamboo charcoal and removal capability of harmful gases. *J Health Sci* 2002;48:473-479.
 17. Rong H, Ryu Z, Zheng J, Zhang Y. Influence of heat treatment of rayon-based activated carbon fibers on the adsorption of formaldehyde. *J Colloid Interf Sci* 2003;261:207-212.

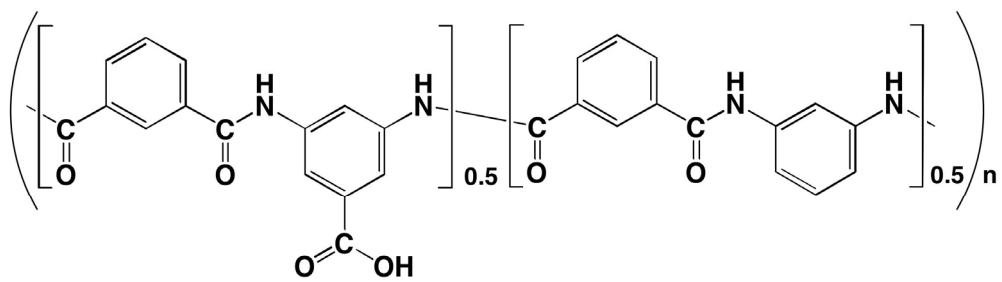


Figure 4-1. Structural formula of C(0.5).

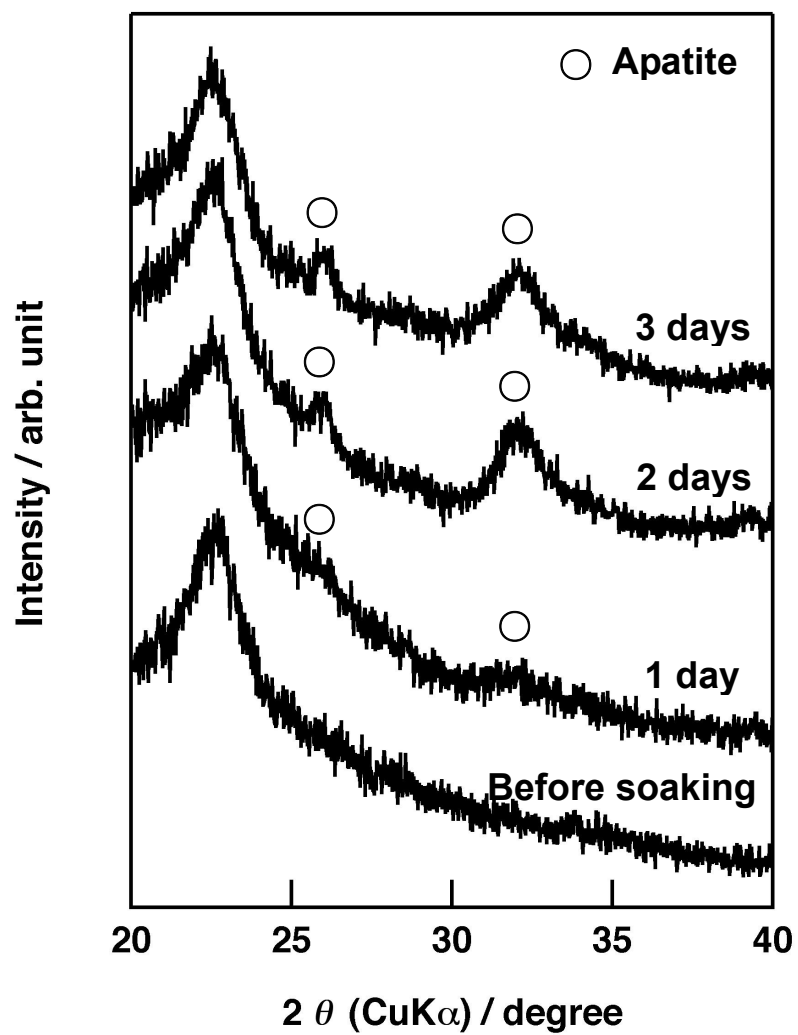


Figure 4-2. TF-XRD patterns of surfaces of C(0.5) films due to soaking in 1.5SBF for various periods.

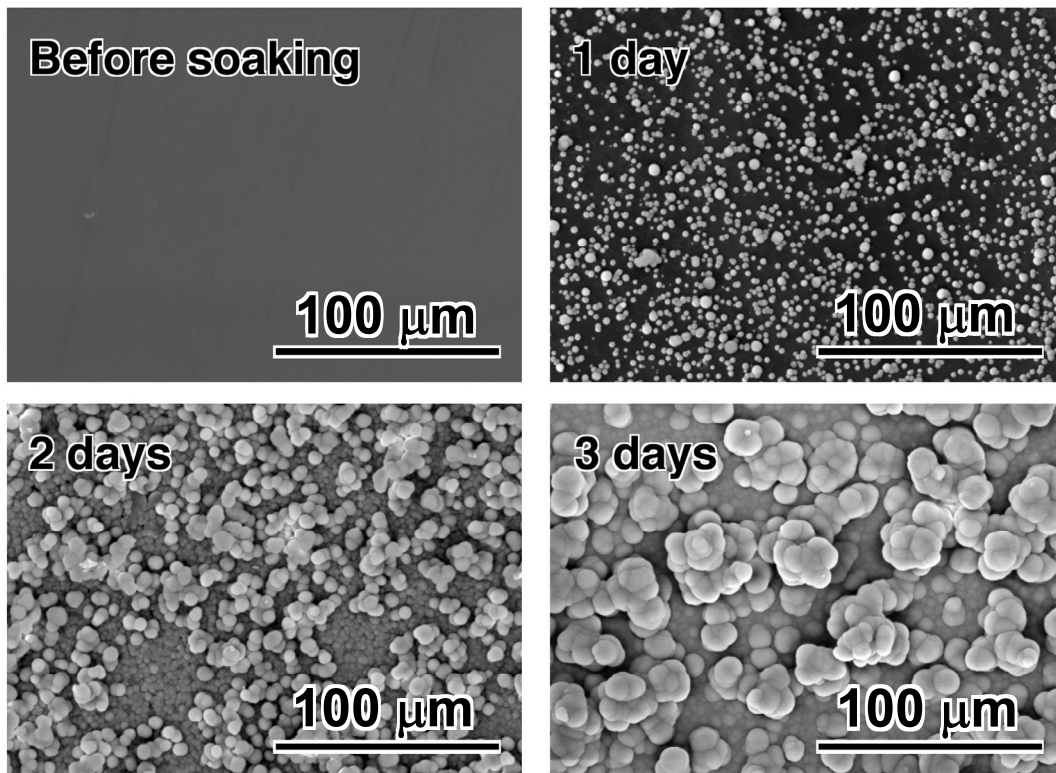


Figure 4-3. SEM images of surfaces of C(0.5) films due to soaking in 1.5SBF for various periods.

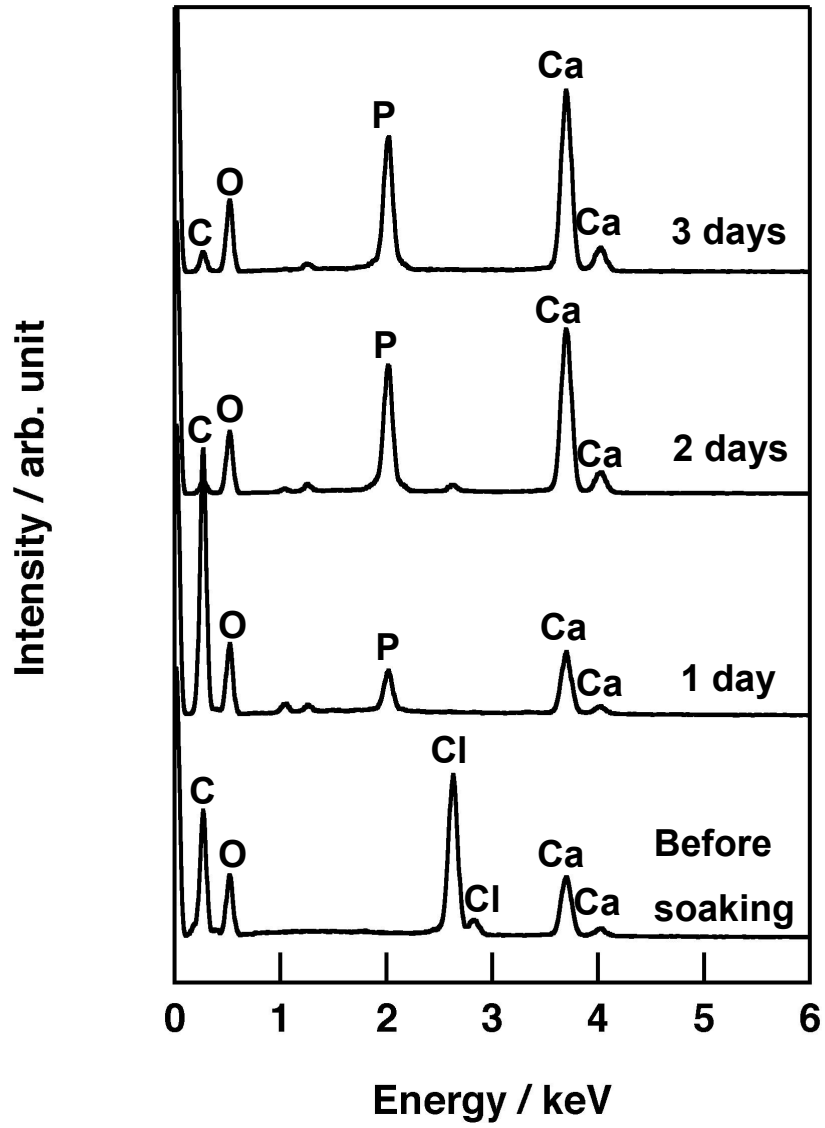


Figure 4-4. EDX spectra of surfaces of C(0.5) films due to soaking in 1.5SBF for various periods.

Table 4-1 Amount of deposited hydroxyapatite per unit area on polyamide after soaking in 1.5SBF for various periods

Soaking period / day	Weight of hydroxy-apatite / $\text{mg}\cdot\text{cm}^{-2}$
1	0.11
1.5	0.28
2	0.61
3	1.08

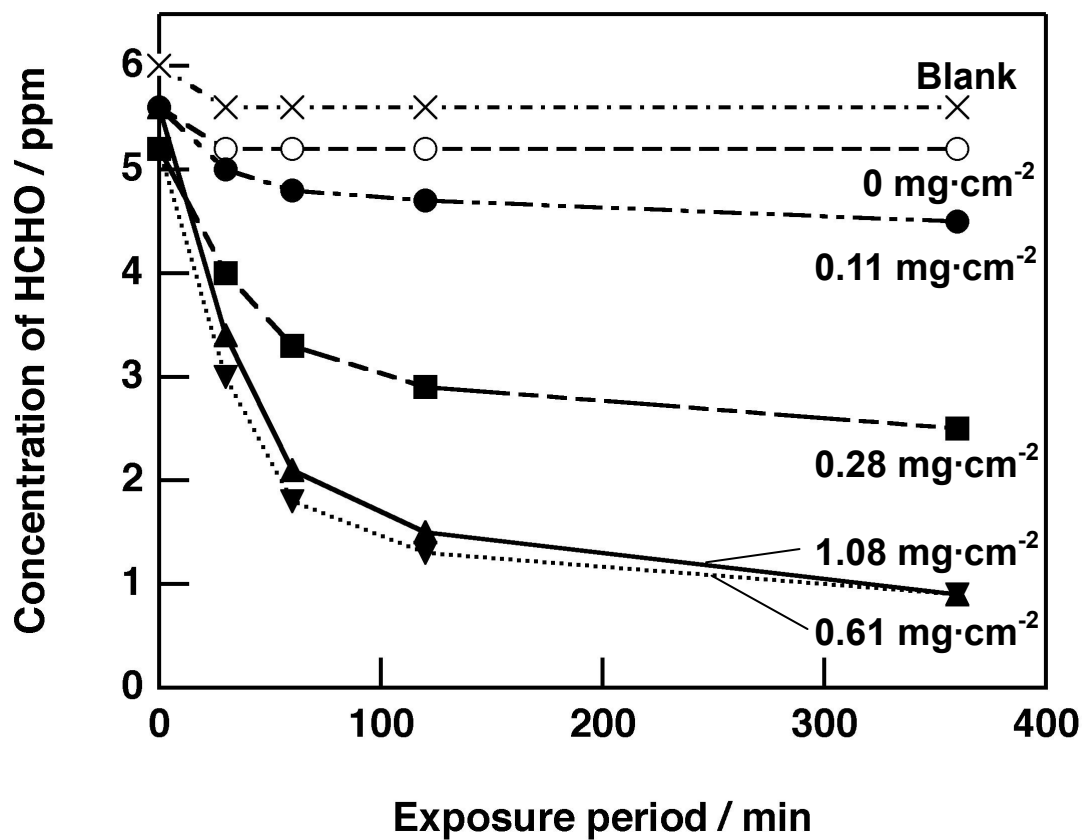


Figure 4-5. Changes in residual concentration of formaldehyde due to exposure of C(0.5) with different amounts of hydroxyapatite to formaldehyde.

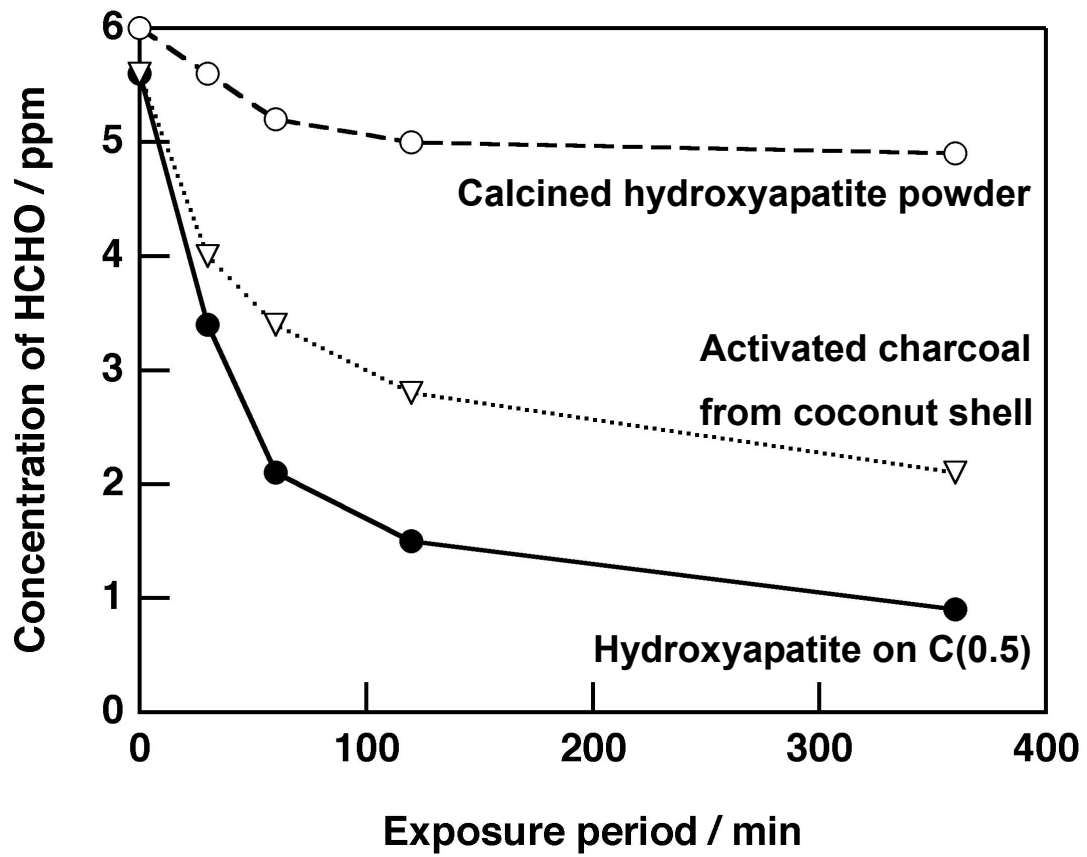


Figure 4-6. Changes in residual concentration of formaldehyde due to exposure of different kind of specimens to formaldehyde.

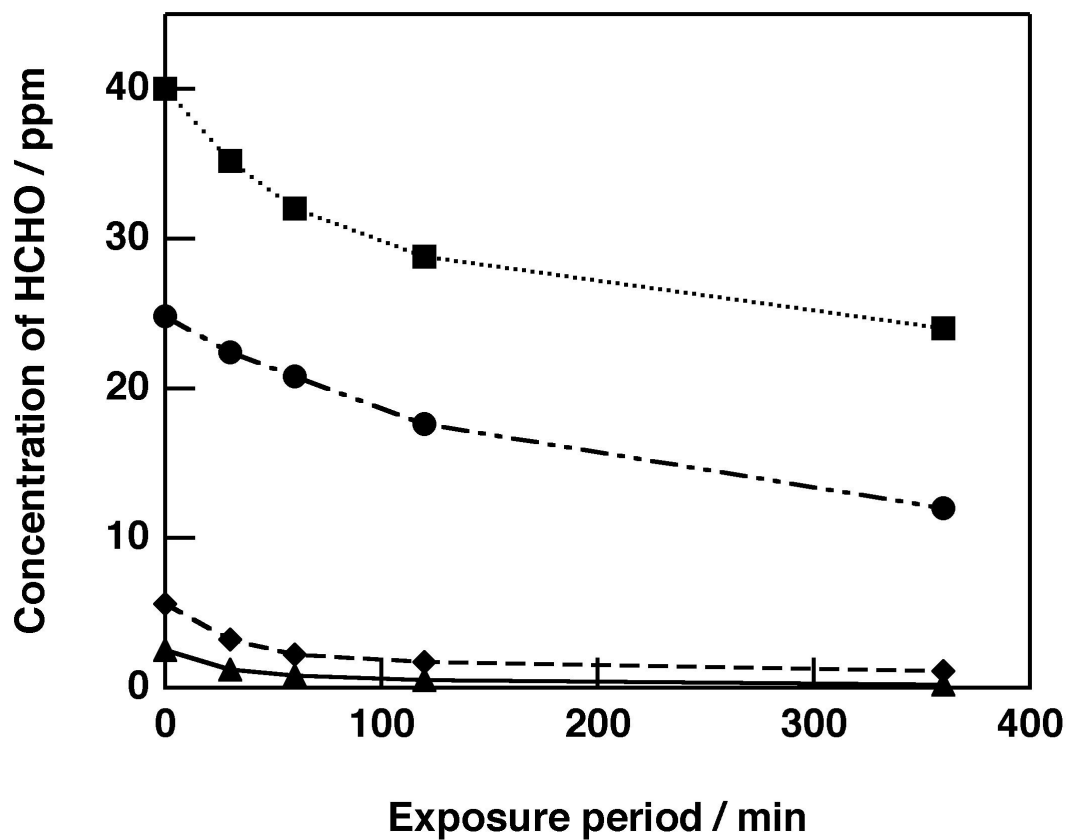


Figure 4-7. Changes in residual concentration of formaldehyde due to exposure of hydroxyapatite on C(0.5) to formaldehyde.

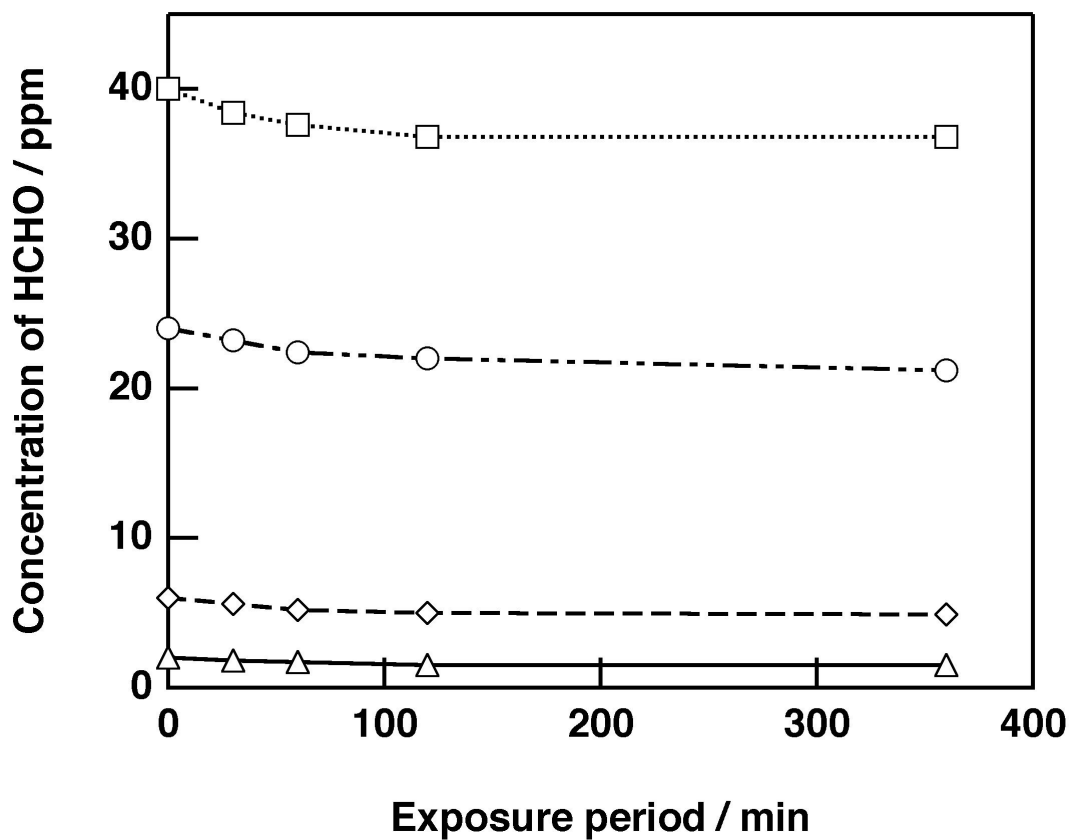


Figure 4-8. Changes in residual concentration of formaldehyde due to exposure of calcined hydroxyapatite powder to formaldehyde.

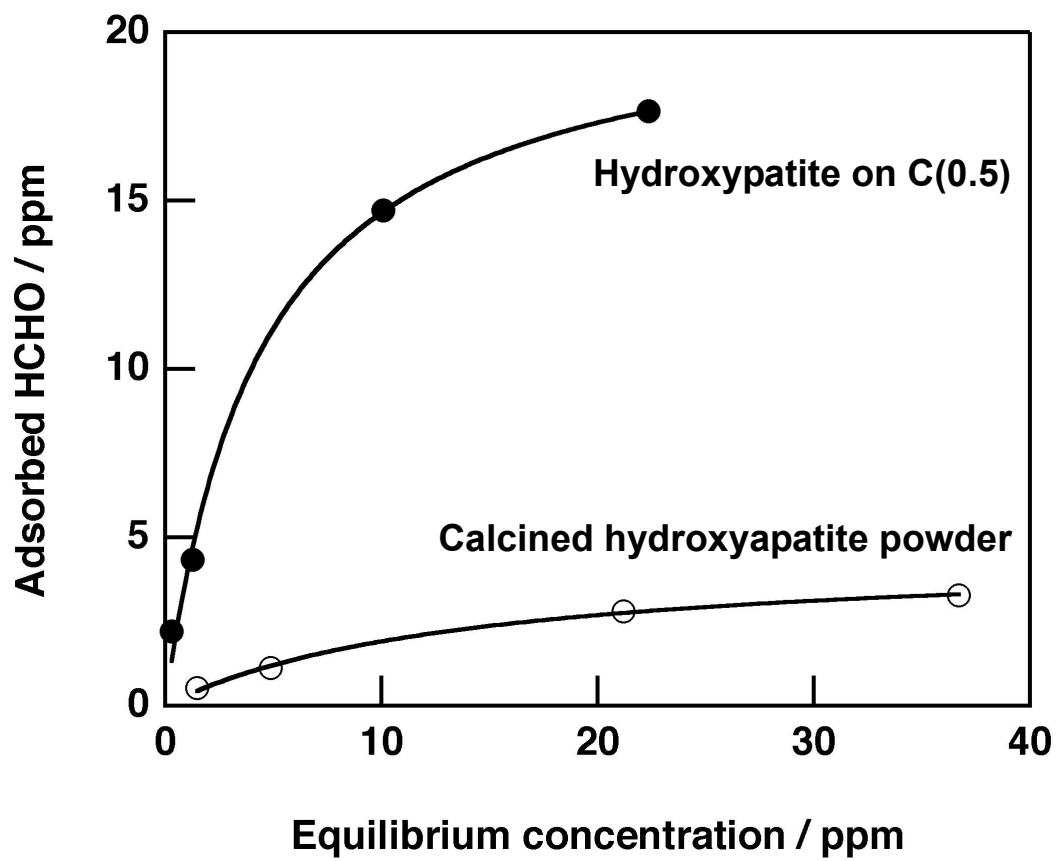


Figure 4-9. Adsorption isotherms at 296 K for apatite on C(0.5) and calcined hydroxyapatite powder.

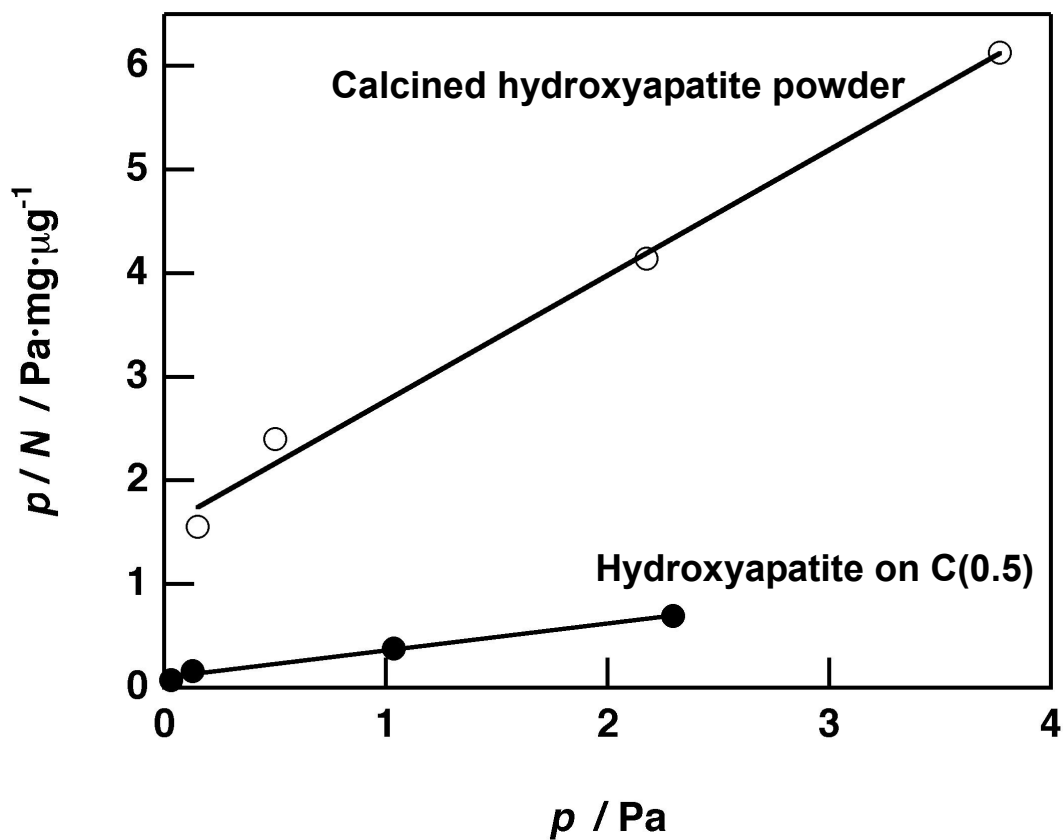


Figure 4-10. Langmuir plots at 296 K for apatite on C(0.5) and calcined hydroxyapatite powder.

Table 4-2 Langmuir constants for two kinds of hydroxyapatites

Specimen	$A / \mu\text{g}\cdot\text{mg}^{-1}$	K / Pa^{-1}
Hydroxyapatite on polyamide	3.82	2.70
Calcined hydroxyapatite	0.83	0.78

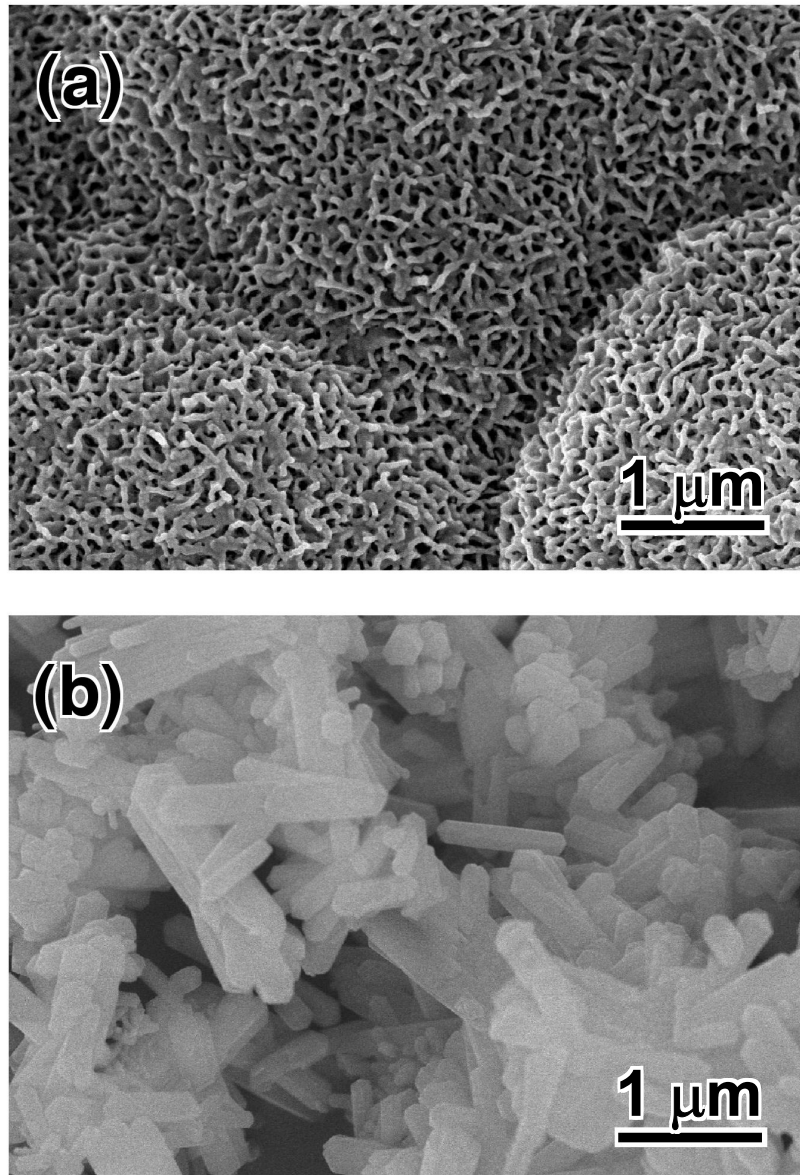


Figure 4-11. FE-SEM images of hydroxyapatite on C(0.5) (a) and calcined hydroxyapatite powder (b).

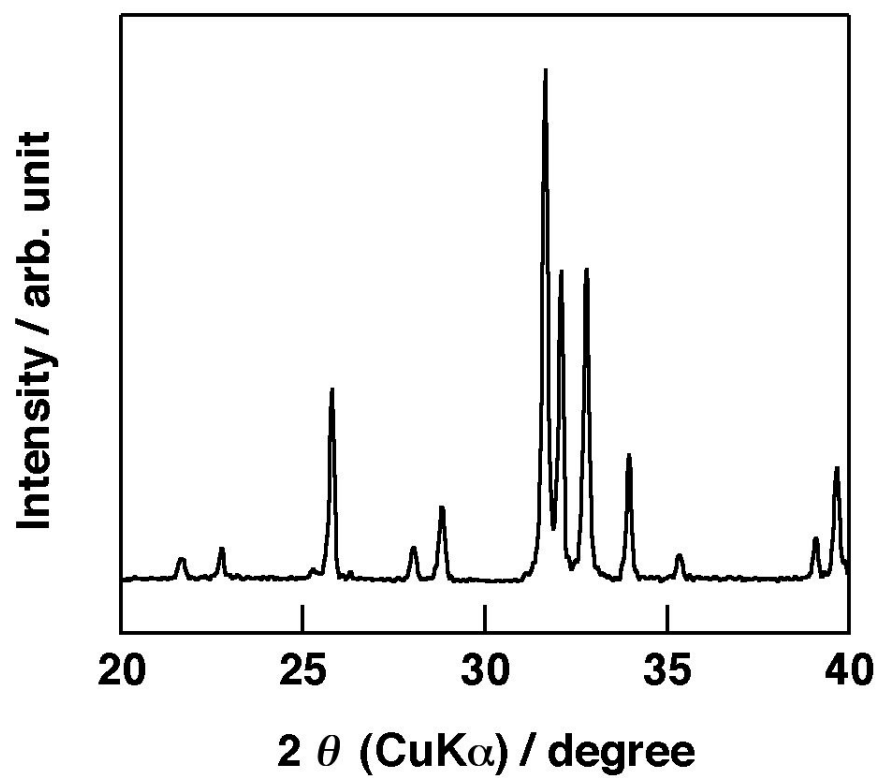


Figure 4-12. Powder XRD pattern of calcined hydroxyapatite powder.

Table 4-3 Crystallite sizes of two kinds of hydroxyapatites calculated from specific surface area obtained by BET method using N₂, X-ray diffraction (XRD) using Serrer's equation and SEM observation

Specimen	Crystallite size / nm		
	BET ^a	XRD ^a	SEM
Hydroxyapatite on polyamide	8	1	50 ^b 200 ^c
Calcined hydroxyapatite	272	50	250 ^b 1000 ^c

The size was calculated as (a) diameter of spherical particle
(b) short axis of square rod
(c) long axis of square rod

GENERAL CONCLUSION

In this study, to clarify parameters governing hydroxyapatite formation on an organic polymer, hydroxyapatite formation on the surface of polyamide film containing different kind of promising functional groups incorporated with CaCl_2 was investigated in a simulated body environment. Furthermore, the usefulness of the fabricated material was evaluated on its ability to adsorb formaldehyde.

Hydroxyapatite formation on the the polymer substrate under the biomimetic condition is governed by three steps; 1) Release of chemical species from the substrates, 2) Induction of heterogenous nucleation of apatite and 3) Crystal growth of the formed nuclei of apatite. Release of chemical species that result in increasing concentrations of Ca^{2+} , PO_4^{3-} and OH^- may enhance nucleation rate of apatite due to the assumed formula:

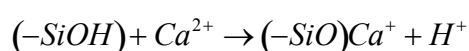
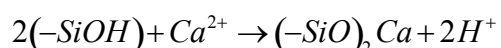


Rapid release of these species into surrounding fluid accelerate the precipitation of the hydroxyapatite. Release of calcium ions from the examined polyamide films increases the degree of the supersaturation with respect to the apatite in an especially local area around the polymer surface. This means that incorporation of the CaCl_2 has an advantage to prevent homogenous nucleation. Homogenous nucleation of the 1.5SBF may consume calcium and phosphate ions from the fluid not for the formation of a layer of hydroxyapatite on the polymer surface. To enhance the heterogenous nucleation on the surface of the polymer substrates, specific functional groups may act an important role. Once the apatite nuclei are formed, it can spontaneously grow because 1.5SBF is supersaturated with respect to apatite. Therefore, the kinds and amounts of functional groups may determine the successful coating of the polymer substrates in a solution such as 1.5SBF, that mimics body fluid. $-\text{SiOH}$, $-\text{TiOH}$ and $-\text{TaOH}$ on inorganic hydrogels are proposed to induce heterogeneous nucleation of apatite. Carboxyl and phosphate groups also show potential to induce heterogeneous nucleation when they are

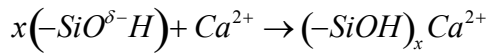
formed as self-assembled monolayer.

In Chapter 1, sulfonic ($-\text{SO}_3\text{H}$) groups in polyamide film are found as an alternative functional group effective for heterogeneous nucleation of apatite in 1.5SBF, when the film contains CaCl_2 . Polyamide films containing more than 20 mol% of $-\text{SO}_3\text{H}$ and 20 mass% of CaCl_2 formed hydroxyapatite on their surfaces after soaking in 1.5SBF within 3 days. The amount of formed hydroxyapatite and the adhesive strength between the polyamide film and formed hydroxyapatite increased with increasing content of $-\text{SO}_3\text{H}$. The morphology of the formed hydroxyapatite on the polyamide film was similar to that formed on so-called bioactive materials, that is, nano-sized hydroxyapatite was formed. This finding confirmed that negatively charged functional groups in a biomimetic condition are effective for hydroxyapatite formation.

In Chapter 2, enhancement of hydroxyapatite formation on polyamide film was found in 1.5SBF by modification of $-\text{COOH}$ with silanol ($-\text{SiOH}$) groups, when the polymer is incorporated with 40 mass% of CaCl_2 . Polyamide films modified with $-\text{SiOH}$ showed a higher ability to induce hydroxyapatite on their surfaces than the film without the modification. Increasing numbers of sites for heterogeneous nucleation were observed on the films modified with $-\text{SiOH}$, resulting in acceleration of hydroxyapatite formation. These results indicate that $-\text{SiOH}$ groups give the heterogeneous nucleation sites more effectively than carboxyl groups. It is estimated from pK_a that almost no $-\text{SiOH}$ groups dissociate in the solution around pH 7, and $-\text{SiO}^-$ is hardly formed. On the other hand, calcium ions can be easily adsorbed to silanol groups to form Si-O-Ca bonds, and calcium ions can access near lone electron-pairs of oxygen atoms in silanol groups attributed to the lower electronegativity of silicon than that of carbon. Thus $-\text{SiOH}$ group react with calcium ions at pH 7 as shown the formulae below,



or



to form silicate complexes and then these complexes induce nuclei of apatite. On the other hand, the formed hydroxyapatite layer was more easily peeled off from the film when it contained larger amounts of $-SiOH$. Increasing content of $-SiOH$, causing the polyamide to swell easily in 1.5SBF and to show high degree of shrinkage after drying, resulted in low adhesion performance of the film surface to hydroxyapatite. Therefore the adhesive strength seems to be governed mainly by the mechanical properties of the polyamide film itself.

In Chapter 3, the process of hydroxyapatite formation on the polyamide films was investigated in detail by comparison of polyamide films containing carboxyl groups ($-COOH$) and sulfonic groups ($-SO_3H$). The induction period of nucleation of apatite for polyamide film containing $-SO_3H$ was shorter than for $-COOH$, but the adhesive strength of the hydroxyapatite layer to substrate containing $-SO_3H$ was low relative to that of the substrate containing $-COOH$. Easier formation of ion pair of Ca^{2+} with $-SO_3^-$ and/or easier access of Ca^{2+} to $-SO_3^-$ attributed to the concentration of lone electron-pairs per unit space may result in fast nucleation on the substrate containing $-SO_3H$ groups. These calcium complexes may act as inductive sites at the surface of the polyamide film. $-COOH$ groups also dissociated to form $-COO^-$. This makes complexes with calcium such as $(-COO)_2Ca$ and $-COOCa^+$. Stability of ion pairs of $(-SO_3)_2Ca$ is higher than that of $(-COO)_2Ca$. Such a stable complex may accelerate the formation of apatite nuclei. Crystal growth of the formed nuclei is governed, irrespective of the polymer substrates, by the degree of supersaturation of the surrounding fluid.

In Chapter 4, the ability of adsorption of formaldehyde was examined for the hydroxyapatite layer formed on the polyamide film in 1.5SBF. Hydroxyapatite formed on polyamide had a higher ability to adsorb formaldehyde than commercially available hydroxyapatite powder. Nano-sized hydroxyapatite particles gave large amounts of sites for adsorption of formaldehyde. Defective structure of the hydroxyapatite crystals is

also expected to contribute high potential to adsorb formaldehyde molecules. This material could be a candidate for removing harmful volatile organic compounds such as formaldehyde.

It is concluded from these investigations that sulfonic and silanol groups showed potential to form hydroxyapatite on the surface of an organic polymer as well as carboxyl group when the polymer contained calcium chloride. Release of Ca^{2+} ions well affected the rate of apatite nucleation on the polymer surface due to the local increase in degree of supersaturation with respect to apatite. Functional groups contained on the polymer surface contributed to the induction of heterogeneous nucleation of an apatite, depending on the properties of formation related calcium compounds. Adhesion performance between formed hydroxyapatite and the surface of the polymer were governed not only by kinds and amounts of functional groups, but also by the mechanical strength of the polymer itself. These findings are fundamentally informative on a design and fabrication of hydroxyapatite-organic hybrids for novel bone substitutes and for functional materials such as an adsorbent of harmful organic compounds.

LIST OF PUBLICATIONS

Chapter 1

"Coating of an apatite layer on polyamide films containing sulfonic groups by a biomimetic process",

T. Kawai, C. Ohtsuki, M. Kamitakahara, T. Miyazaki, M. Tanihara, Y. Sakaguchi, S. Konagaya, 2004, *Biomaterials*, **25**, 4529-4534.

Chapter 2

"*In vitro* apatite formation on polyamide containing carboxyl groups modified with silanol groups",

T. Kawai, C. Ohtsuki, M. Kamitakahara, K. Hosoya, M. Tanihara, T. Miyazaki, Y. Sakaguchi, S. Konagaya, *J. Mater. Sci.: Mater. Med.*, submitted.

Chapter 3

"A comparative study in apatite deposition on polyamide film containing different kinds of functional groups under a biomimetic condition",

T. Kawai, C. Ohtsuki, M. Kamitakahara, M. Tanihara, T. Miyazaki, Y. Sakaguchi, S. Konagaya, *J. Ceram. Soc. Japan*, submitted.

Chapter 4

"Removal of formaldehyde by hydroxyapatite layer biomimetically deposited on polyamide film",

T. Kawai, C. Ohtsuki, M. Kamitakahara, M. Tanihara, T. Miyazaki, Y. Sakaguchi, S. Konagaya, *Environ. Sci Technol.*, submitted.

RELATED PUBLICATIONS

1. "A novel covalently crosslinked gel of alginate and silane with the ability to form bone-like apatite", K. Hosoya, C. Ohtsuki, T. Kawai, M. Kamitakahara, S. Ogata, T. Miyazaki, M. Tanihara, 2004, *J. Biomed. Mater. Res.*, **71A**, 596-601.
2. "Design of a novel bioactive calcium phosphate paste containing acetyl cellulose", T. Kawai, C. Ohtsuki, H. Inada, M. Kamitakahara, M. Tanihara, T. Miyazaki, in press, *Phosphorus Research Bulletin*, **17**, 207-212.
3. "Apatite formation on polyamide film modified with sulfonic groups", T. Kawai, C. Ohtsuki, T. Miyazaki, M. Tanihara, J. Nakao, Y. Sakaguchi, S. Konagaya, 2002, in *Proceedings of 2nd Asian BioCeramics symposium (ABC2002)*, Committee of Asian BioCeramics symposium, pp. 29-32.
4. "Apatite formation on polyamide films containing sulfonic groups by biomimetic process", T. Kawai, T. Miyazaki, C. Ohtsuki, M. Tanihara, J. Nakao, Y. Sakaguchi, S. Konagaya, 2003, *Bioceramics*, **Vol. 15 (Key Engineering Materials Vols. 240-242)**, ed. by B. Ben-Nissan, D. Sher and W. Walsh, Trans Tech Publications Ltd., Switzerland, pp. 59-62.
5. "Apatite coating on aromatic polyamide films via biomimetic mineralization", Y. Sakaguchi, S. Konagaya, C. Ohtsuki, T. Kawai, M. Tanihara, T. Miyazaki, 2003, in *Proceedings of the 8th Japan International SAMPE Symposium*, **Vol. 2**, ed. by N. Takeda, N. Hamada, S. Ogihara, A. Nakai, Society for the Advancement of Material and Process Engineering, 2003, pp. 1081-1084.

6. "Fabrication of a bioactive calcium phosphate paste with cellulose acetate", T. Kawai, C. Ohtsuki, T. Miyazaki, H. Inada, M. Kamitakahara, M. Tanihara, 2004, in *Transactions of 7th World Biomaterials Congress*, p. 997.
7. "Setting behavior and mechanical properties of bioactive paste composed of calcium phosphates and acetyl cellulose", C. Ohtsuki, T. Kawai, H. Inada, M. Kamitakahara, T. Miyazaki, M. Tanihara, 2004, in *Archives of BioCeramics Research* **Vol. 4**, ed. by B.-T. Lee, H.-Y. Song and H.-H. Lee, pp. 39-42.
8. "Bonelike[®]/PLGA hybrid materials for bone regeneration: *in vivo* evaluation", J.M. Oliveira, T. Kawai, M.A. Lopes, C. Ohtsuki, J.D. Santos, A. Afonso, 2004, in *Advanced Materials Forum II*, **Vols. 455-456**, ed. by R. Martins, E. Fortunator, I. Ferreira, C. Dias, Trans Tech Publications Inc., pp. 374-378.
9. "Effect of sulfonic group and calcium content on apatite-forming ability of polyamide films in a solution mimicking body fluid", T. Kawai, C. Ohtsuki, M. Kamitakahara, T. Miyazaki, M. Tanihara, Y. Sakaguchi, S. Konagaya, 2004, in *Bioceramics*, **Vol. 16 (Key Engineering Materials Vols. 254-256)**, ed. by M.A. Barbosa, F.J. Monteiro, R. Correia, B. Leon, Trans Tech Publications Ltd., Switzerland, pp. 525-528.
10. "*In vivo* behaviour of Bonelike[®]/PLGA hybrid: histological analysis and peripheral quantitative computed tomography (pQ-CT) evaluation", J.M. Oliveira, T. Kawai, M.A. Lopes, C. Ohtsuki, J.D. Santos, A. Afonso, 2004, *Bioceramics*, **Vol. 16 (Key Engineering Materials Vols. 254-256)**, ed. by M.A. Barbosa, F.J. Monteiro, R. Correia, B. Leon, Trans Tech Publications Ltd., Switzerland, pp. 565-568.

11. "In vitro analysis of proteins adhesion to phase pure hydroxyapatite and silicon substituted hydroxyapatite", C.M. Botelho, R.A. Brooks, T. Kawai, S. Ogata, C. Ohtsuki, S.M. Best, M.A. Lopes, J.D. Santos, N. Rushton, W. Bonfield, 2005, *Bioceramics*, **Vol. 17** (*Key Engineering Materials*, **Vols. 284-286**), ed. by P. Li, K. Zhang, C.W. Colwell, Jr., Trans Tech Publications Ltd., Switzerland, pp. 461-464.
12. "Apatite deposition on polyamide film containing silanol groups in simulated body environment", T. Kawai, C. Ohtsuki, M. Kamitakahara, M. Tanihara, T. Miyazaki, Y. Sakaguchi, S. Konagaya, 2005, *Bioceramics*, **Vol. 17** (*Key Engineering Materials*, **Vols. 284-286**), ed. by P. Li, K. Zhang, C.W. Colwell, Jr., Trans Tech Publications Ltd., Switzerland, pp. 505-508.
13. "Synthesis of biodegradable hybrid consisting of hydroxyapatite and alginate", C. Ohtsuki, K. Hosoya, T. Kawai, M. Kamitakahara, S. Ogata, T. Miyazaki, M. Tanihara, 2005, *Bioceramics*, **Vol. 17** (*Key Engineering Materials*, **Vols. 284-286**), ed. by P. Li, K. Zhang, C.W. Colwell, Jr., Trans Tech Publications Ltd., Switzerland, pp. 779-782.
14. "Induction of hydroxyapatite deposition on organic polymer under a condition mimicking body fluid", C. Ohtsuki, T. Kawai, 2002, *NEW GLASS*, **Vol. 17** [3], 17-21 [in Japanese].
15. "Control of hydroxyapatite deposition on organic polymer under biomimicking condition", C. Ohtsuki, T. Kawai, M. Kamitakahara, in press, *Phosphorus Research Bulletin*, **17**, 21-28.

ACKNOWLEDGEMENTS

The studies in the present thesis were carried out under the direction of Professor Masao Tanihara at Graduate School of Materials Science, Nara Institute of Science and Technology, Japan. The author wishes to express his sincere gratitude to Professor Masao Tanihara for his encouragement and valuable advice all through these studies.

The author expresses his sincere gratitude to Associate Professor Chikara Ohtsuki at Graduate School of Materials Science, Nara Institute of Science and Technology, Japan for his continuous support and helpful suggestion.

The author's sincere gratitude also goes to Dr. Shin-ichi Ogata, Dr. Masanobu Kamitakahara at Graduate School of Materials Science, Nara Institute of Science and Technology, Japan, and Dr. Toshiki Miyazaki at Graduate School of Life Science and Systems Engineering, Kyushu Institute of Technology, Japan for their support and helpful suggestion.

The author is sincerely grateful to Dr. Shigeji Konagaya and Dr. Yoshimitsu Sakaguchi at Toyobo Research Center Co., Ltd., Japan for their providing us polyamides used in the study of the present thesis and helpful suggestions.

The author is sincerely grateful to Professor José Domingos Santos, Dr. Maria Ascensão Lopes and all their colleagues at DEMM, Faculty of Engineering, University of Porto, Portugal for their support and helpful suggestion.

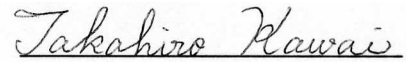
The author is sincerely grateful to Ms. Mutsumi Usui and all students in Laboratory of Biocompatible Materials Science, Graduate School of Materials Science, Nara Institute of Science and Technology, Japan for their supports and helpful suggestions.

The author is sincerely grateful to Professor Jun-ichi Kikuchi and Professor Tadashi Shiosaki at Graduate School of Materials Science, Nara Institute of Science and

Technology, Japan for their helpful advice.

Finally, the author expresses his hearty gratitude to my parents, Mr. Minoru Kawai, Ms. Sachiko Kawai, and his brother, Mr. Koji Kawai for their warm understanding and support.

March 2005

A handwritten signature in cursive script that reads "Takahiro Kawai". The signature is written in black ink on a light-colored background.

Takahiro Kawai